Dissertation
submitted to the
Combined Faculties for the Natural Sciences and for Mathematics
of the Ruperto-Carola University of Heidelberg, Germany
for the degree of
Doctor of Natural Sciences

presented by

Diplom-Physikerin Lisa Kastner
born in: Munich, Germany
Oral examination: 14th June 2016

The ubiquitin E3 ligase Rtt101 affects the replication stress response and replicative senescence through Mrc1/Claspin

Referees: Prof. Dr. Christine Clayton

Dr. Brian Luke

Summary

The budding yeast protein Rtt101 serves as a scaffold for the assembly of a variety of ubiquitin E3 ligase complexes. Both Rtt101 and its human counterpart CUL4 have been implicated in the maintenance of genomic integrity. In the absence of *RTT101*, cells are highly sensitive to the genotoxic agents MMS and CPT, which cause DNA damage that results in replication fork stalling in the ensuing S-phase of the cell cycle. The established roles and substrates of Rtt101 can only partially explain the striking drug sensitivity.

In a genetic screen using *Saccharomyces cerevisiae* as a model organism we identified Mrc1 as a key suppressor of *rtt101* drug sensitivity. Amongst others, Mrc1 contributes to the activation of the intra S-phase checkpoint in response to replicative stress and couples the DNA helicase to the leading strand DNA polymerase ε.

The rescue of *rtt101* cells by *MRC1* deletion depended on the presence of the Rad52 protein, the central player of the budding yeast homologous recombination machinery. By employing separation of function alleles we determined that the loss of Mrc1's checkpoint function was not sufficient to alleviate *rtt101* drug sensitivity. Instead, the replicative function of Mrc1 seemed to be toxic for *rtt101* cells. Our data suggested that Rtt101 does not target Mrc1 for proteolysis.

We propose that the ubiquitination of Mrc1 (or an unknown factor regulating Mrc1) by Rtt101 modulates the replisome at the stalled fork, possibly inducing the uncoupling of the helicase from the polymerase. This could allow the production of ssDNA that might trigger replication fork repair or restart by a homologous recombination-based pathway.

Telomeres, particularly short telomeres, are difficult to replicate regions of the genome. Telomere shortening during replicative senescence is a natural process in human somatic cells that can be mimicked in budding yeast by deletion of the catalytic subunit of telomerase, Est2.

Rtt101 had been reported to prevent premature senescence. Our experiments showed that Rtt101 does not exert its protective function by influencing telomere length. Nor did the accumulation of spontaneous DNA damage that has been reported for *rtt101* cells contribute to the acceleration of senescence. Deletion of *RTT101* further compromised the viability of senescing *rad52 est2* cells suggesting that the crucial action of Rtt101 at shortening telomeres does not involve a homologous recombination event. Surprisingly, *mrc1 est2* cells also senesced fast

and were epistatic with *rtt101 est2* cells. This indicates that during senescence Rtt101 and Mrc1 protect shortening telomeres through a common mechanism. This is in contrast to the situation at stalled replication forks after treatment with MMS or CPT. We speculate that Rtt101 and Mrc1 act in concert to prevent precocious senescence signalling by delaying the creation of subtelomeric ssDNA.

Taken together, our results provide insights into how the Rtt101, and perhaps human CUL4, E3 ligase functions to promote genome stability in the face of replication stress and telomere shortening.

Zusammenfassung

Das Protein der Bäckerhefe Rtt101 dient als Gerüst für den Aufbau verschiedener Ubiquitin-E3-Ligase-Komplexe. Rtt101 und CUL4, sein Gegenstück in menschlichen Zellen, tragen zum Erhalt der Unversehrtheit des Genoms bei. In Abwesenheit von Rtt101 reagieren Zellen hochempfindlich auf die genotoxischen Substanzen MMS und CPT. Diese verursachen DNA-Schäden, die in der darauffolgenden S-Phase die Replikationsgabel zum Stillstand bringen. Die bekannten Funktionen und Substrate der Rtt101-basierten Ubiquitin-E3-Ligase-Komplexe können die auffällige Empfindlichkeit gegenüber genotoxischen Substanzen nur teilweise erklären.

In einem genetischen Screen mit dem Modellorganismus *Saccharomyces cerevisiae* identifizierten wir Mrc1 als entscheidenden Faktor für die Unterdrückung der Empfindlichkeit von *rtt101*-Zellen. Mrc1 trägt unter anderem zur Aktivierung des Intra-S-Phase-Checkpoints als Reaktion auf Replikationsstress bei und koppelt die DNA-Helikase an die den Leitstrang synthetisierende Polymerase ε.

Für die Rettung der *rtt101*-Zellen durch die Deletion von *MRC1* war das Protein Rad52 nötig, das ein zentraler Bestandteil der homologen Rekombinations-maschinerie ist. Mithilfe von funktionsspezifischen Allelen konnten wir zeigen, dass der Verlust von Mrc1's Checkpoint-Funktion nicht ausreichend war, um die Empfindlichkeit von *rtt101*-Zellen zu mindern. Stattdessen schien die Replikationsfunktion von Mrc1 für *rtt101*-Zellen schädlich zu sein.

Unsere Daten legten nahe, dass Rtt101 nicht zur Proteolyse von Mrc1 beiträgt. Wir schlagen vor, dass die Ubiquitinierung von Mrc1 (oder eines noch unbekannten, Mrc1 regulierenden Faktors) durch Rtt101 das Replisom an der blockierten Replikationsgabel moduliert und möglicherweise die Helikase von der Polymerase entkoppelt. Dies würde zur Produktion einzelsträngiger DNA führen, was wiederum die Reparatur oder den Neustart der Replikationsgabel durch homologe Rekombination einleiten könnte.

Telomere, insbesondere kurze Telomere, lassen sich nur schwer replizieren. Die Verkürzung der Telomere während der replikativen Seneszenz ist ein natürlicher Prozess in somatischen, menschlichen Zellen, der in Bäckerhefe durch die Deletion der katalytischen Untereinheit der Telomerase, Est2, imitiert werden kann.

Es war bekannt, dass Rtt101 vorzeitige Seneszenz verhindert. Unsere Experimente zeigten, dass Rtt101 seine Schutzfunktion nicht durch Beeinflussung der Telomerlänge ausübt. Auch die Häufung spontaner DNA-Schäden, die in *rtt101*-

Zellen stattfindet, beschleunigt die Seneszenz nicht. Die Deletion von *RTT101* setzte die Lebensfähigkeit von seneszenten *rad52 est2*-Zellen weiter herab. Dies impliziert, dass die Funktion von Rtt101 an sich verkürzenden Telomeren nicht auf homologer Rekombination beruht. Überraschenderweise wurden auch *mrc1 est2*-Zellen vorzeitig seneszent und waren epistatisch mit *rtt101 est2*-Zellen. Dies zeigt an, dass Rtt101 und Mrc1 sich verkürzende Telomere seneszenter Zellen durch einen gemeinsamen Mechanismus schützen. Dies unterscheidet sich von der Situation an blockierten Replikationsgabeln nach der Behandlung mit MMS oder CPT. Wir spekulieren, dass Rtt101 und Mrc1 zusammenarbeiten, um die vorzeitige Signalisierung von Seneszenz zu verhindern, indem sie die Entstehung von subtelomerischer, einzelsträngiger DNA verzögern.

Zusammengenommen bieten unsere Ergebnisse Einblicke, wie die Rtt101 E3-Ligase, und vielleicht auch CUL4 in menschlichen Zellen, zur Stabilität des Genoms im Angesicht von Replikationsstress und Telomerverkürzung beiträgt.

1 Introduction

1.1 Cells need to maintain genomic integrity in the face of endogenous and exogenous threats

The maintenance of genomic stability is crucial for all organisms as mutations and genomic rearrangements can be the cause for a variety of pathological disorders or cell death. Threats to genomic integrity arise from DNA damage inflicted either by endogenous influences such as reactive metabolites or by exogenous DNA damaging factors like ionizing radiation, UV light or genotoxic agents. In addition, the replication of DNA during the S-phase of the cell cycle is a phase of particular vulnerability of the genome. Cells must be able to cope with various types of obstacles, which slow down or stall replication forks, and might lead to replication fork break down and double strand break (DSB) formation that can trigger genomic rearrangements. These obstacles include transcribing RNA polymerases, tightly bound non-histone protein-DNA complexes, natural replication slow zones and bulky DNA lesions (Branzei and Foiani 2009).

In order to meet these challenges cells have developed an impressive array of mechanisms to survey, control and repair their genetic material. The cellular reactions to the different kinds of aberrant DNA structures that may arise during S-phase or as a consequence of direct DNA lesions are conserved from yeast to humans. Since this study was done using budding yeast as a model organism, the following paragraphs will focus on the checkpoint and DNA damage response mechanisms of *S. cerevisiae* and point out parallel mechanisms of particular relevance to this study in human cells.

1.2 DNA damage and stalled replication forks activate checkpoint signalling

The concept of "checkpoints" was first introduced by Hartwell and Weinert and describes “controls that ensure the order of cell cycle events” (Hartwell and Weinert 1989). Several checkpoints ensure that eukaryotic cells do not progress in the cell cycle in unfavourable conditions. At the G1 checkpoint (cell growth checkpoint) external and internal conditions are checked to allow or prevent cell cycle entry. The intra S-phase checkpoint delays replication if DNA damage or abnormal replication

intermediates are sensed in S-phase. The G2/M (or DNA damage checkpoint) prevents the initiation of mitosis unless DNA damage is repaired. The metaphase checkpoint (spindle checkpoint) blocks the separation of the duplicated chromosomes until each chromosome is attached to the spindle. In the following paragraphs the pathways triggered by the DNA damage checkpoint and the intra S-phase checkpoint will be discussed.

The two key players of the *S. cerevisiae* DNA damage checkpoint are the phosphatidylinositol 3-kinase-related kinases (PIKKS) Mec1 (ATR in humans) and Tel1 (ATM in humans). Activation of these two checkpoint proteins triggers the phosphorylation and activation of the two major effector kinases Rad53 (CHK2 in humans) and Chk1 (CHK1 in humans) via the mediators Rad9 (MDC1 and 53BP1 in humans) and Mrc1 (Claspin in humans).

Tel1 responds mainly to DSBs, while Mec1 is activated by a variety of different lesions that trigger the generation of ssDNA as well as DSBs. DSBs are characterized by exposed DNA ends that can be bound by the MRX (Mre11-Rad50-Xrs2) complex and the Ku70/80 heterodimer (Martin, Laroche et al. 1999, Lisby, Barlow et al. 2004, Wu, Topper et al. 2008). The MRX complex recruits Tel1/Mec1, which phosphorylates histone H2A forming P-H2A in the regions flanking the DSB. In higher eukaryotes it is the histone variant H2AX that is phosphorylated to form γH2AX. P-H2A or γH2AX is a hallmark of damaged DNA (Rogakou, Pilch et al. 1998, Redon, Pilch et al. 2003). It recruits numerous chromatin remodelling complexes to the site of damage and promotes binding of the mediator Rad9 to methylated histone H3 ($H3K79^{Me}$), which recruits and activates the effector kinase Rad53 (Lisby, Barlow et al. 2004, Toh, O'Shaughnessy et al. 2006).

Sae2 and the MRX complex initiate DSB resection, whereby the MRX complex additionally recruits Dna2, Exo1 and the Sgs1 helicase for continued and more extensive resection. Exposed ssDNA is quickly covered by RPA and becomes a signal for the recruitment of a number of checkpoint and repair proteins including the Mec1-Ddc2, the Rad24-RFC complex (RFC-like complex) and Ddc1-Mec3-Rad17 complex (9-1-1 or PCNA-like complex). The Mec1-Ddc2 complex binds DNA via the Ddc2 component (Rouse and Jackson 2002). This allows Mec1 to phosphorylate nearby targets, which often overlap with those of Tel1, like histone H2A. Mec1 also phosphorylates the mediator Rad9, which recruits the effector kinase Rad53 for subsequent phosphorylation and activation by Mec1. The presence of both the RFC-

like and the PCNA-like complexes are required for efficient phosphorylation of Rad53 by Mec1 (de la Torre-Ruiz, Green et al. 1998).

The generation of ssDNA and the subsequent activation of Mec1 is also common to the processing of lesions other than DSBs such as NER (Nucleotide Excision Repair) of UV-induced DNA photoproducts or BER (Base Excision Repair) and explains the more prominent role of Mec1 over Tel1 in checkpoint signalling in *S. cerevisiae*.

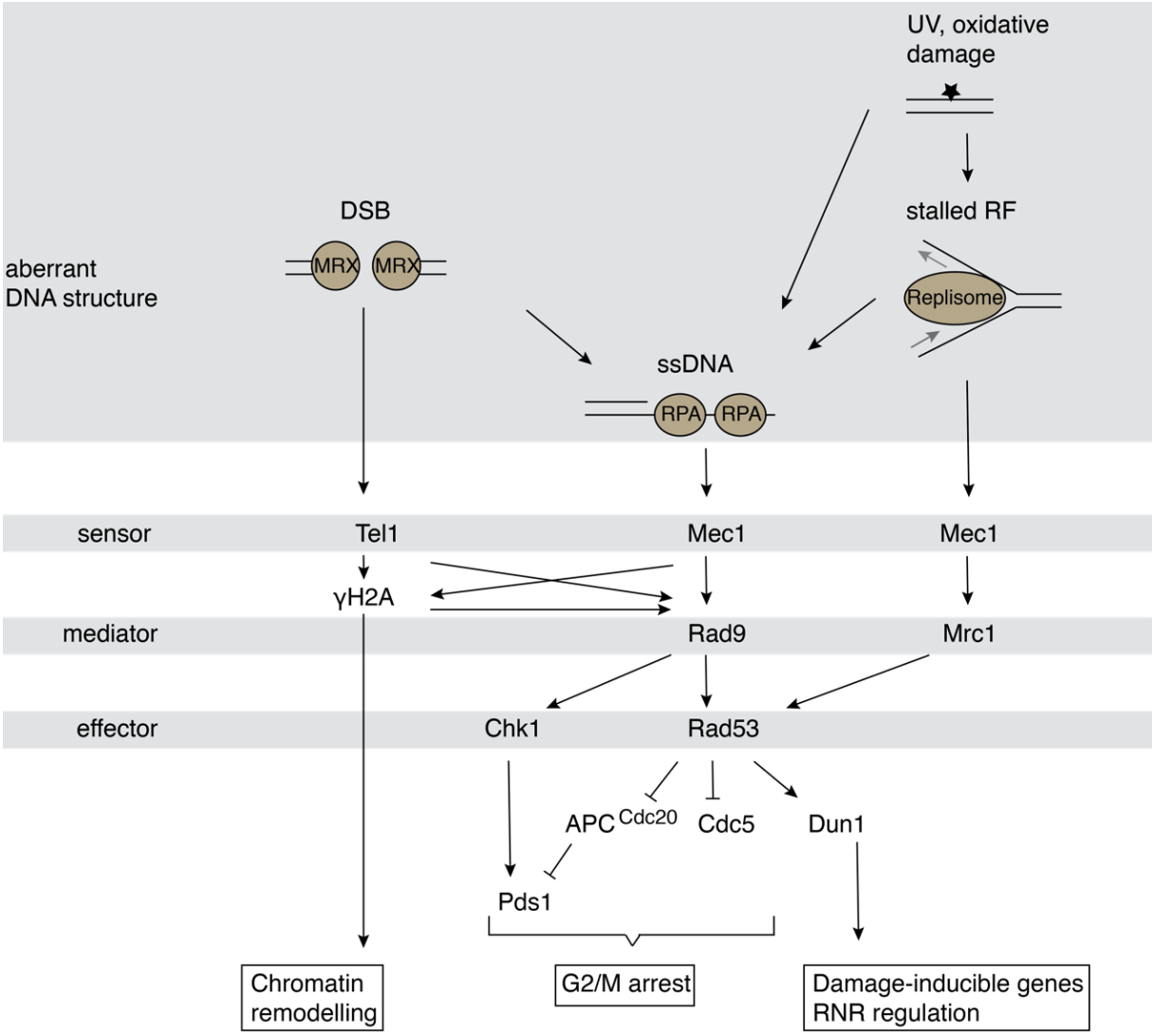

Figure 1 Simplified overview of the checkpoint response to DNA damage and stalled replication forks in *Saccharomyces cerevisiae*. This figure was adapted from Harrison and Haber 2006, and Lisby and Rothstein 2009. The processes are explained in detail in the text.

Endogenous and exogenous replication stress results in replication fork stalling and elicits signalling activities, which also result in Mec1 dependent Rad53 activation. The main contribution to Rad53 phosphorylation in S-phase is mediated by Mrc1 (Mediator of the Replication Checkpoint) (Alcasabas, Osborn et al. 2001, Osborn and

Elledge 2003). However, the significance of the two mediators Rad9 and Mrc1 in replication stress varies depending on the precise kind of replication stress inflicted on the cell.

Activated Rad53 mediates cell cycle arrest and transcriptional induction of repair proteins via its three main targets Cdc20, Cdc5 and Dun1. Inhibition of the interaction of APC^{Cdc20} (Anaphase Promoting Complex) with Pds1 (Securin in human) by Rad53 prevents Pds1 degradation, which is required for the entry into mitosis (Agarwal, Tang et al. 2003). Pds1 stabilization is also promoted by its hyperphosphorylation as a consequence of DNA damage, which depends on Mec1, Rad9 and Chk1, another Mec1 target. In addition, Rad53 also inhibits Cdc5 in order to inhibit mitotic exit and allow time for damage repair (Cheng, Hunke et al. 1998, Sanchez 1999).

DNA damage induces a transcriptional response that is regulated by the Dun1 kinase and ensures that the elevated need for dNTPs during repair is met by transcriptional induction of ribonucleotide reductase (RNR) genes (Zhou and Elledge 1993, Zhao, Chabes et al. 2001, Zhao and Rothstein 2002).

While the pathways resulting in checkpoint activation have been studied in detail, far less is known about how cells resume the cell cycle after successful repair. During this process called recovery, the checkpoint needs to be deactivated. In *S. cerevisiae* dephosphorylation of Rad53 by the phosphatases Pph3 and Ptc2 combined with degradation of Mrc1 by the SCF^{Dia2} ubiquitin E3 ligase are proposed to contribute to checkpoint downregulation after MMS-induced damage in S-phase (O'Neill, Szyjka et al. 2007, Fong, Arumugam et al. 2013). Likewise, the human homologue of Mrc1, Claspin, is degraded in an SCF-$^{\beta TrCP}$-dependent manner during recovery from replication stress (Mailand, Bekker-Jensen et al. 2006, Peschiaroli, Dorrello et al. 2006).

The processes described under 1.2 are examined from different points of view in the reviews listed here (Rouse and Jackson 2002, Harrison and Haber 2006, Lisby and Rothstein 2009, Branzei and Foiani 2010), which served as a basis for section 1.2.

1.3 The rescue of stalled replication forks is crucial to maintain genome stability

The assembly of the replisome occurs in a stepwise process that is tightly regulated. The minichromosome maintenance (MCM) helicase complex (Mcm2-7) is loaded onto origins of replication in G1 with the help of ORC/Cdc6/Cdt1 to form the pre-

replicative complex (preRC). The addition of the MCM-associated factors Cdc45 and the GINS complex in S-phase triggers the formation of the active replisome. The S-phase replisome is complemented with DNA polymerase α-primase, which initiates each new Okazaki fragment of the lagging strand, DNA polymerase δ and DNA polymerase ε, which synthesize the lagging and leading strand, respectively. Accessory proteins involved in mediating DNA synthesis are replication factor C (RFC) and proliferating cell nuclear antigen (PCNA) (Branzei and Foiani 2010).

At least two factors have been identified that couple the two main catalytic activities of DNA unwinding and DNA synthesis. Ctf4 interacts with the CMG helicase (Cdc45-MCM-GINS) and polymerase α-primase and Mrc1 binds subunits of the CMG helicase and polymerase ε (Lou, Komata et al. 2008, Gambus, van Deursen et al. 2009, Komata, Bando et al. 2009, Tanaka, Katou et al. 2009). A wealth of additional regulatory proteins contributes to form the fully functional replisome.

Replication fork stalling occurs frequently under normal growth conditions due to tightly bound protein DNA complexes, collisions of the DNA replication machinery with transcribing RNA polymerases or DNA lesions. Since the formation of new pre-replicative complexes is restricted to G1, the breakdown of a replication fork by dissociation of essential replisome components from the stalled fork during S-phase is considered an irreversible event (Labib 2000). Replication fork stalling can lead to replication fork breakdown, which results in gapped molecules representing hemireplicated DNA. The exposition of long stretches of ssDNA and four-branched structures due to reversed forks are highly recombinogenic and may lead to gross chromosomal rearrangements and the appearance of DSBs due to nucleolytic cleavage of aberrant recombination intermediates (Takeuchi, Horiuchi et al. 2003, Ahn, Osman et al. 2005, Lambert, Watson et al. 2005, Branzei and Foiani 2009). Thus, the stabilization of stalled forks and their controlled restart becomes an issue of utmost importance in the maintenance of genome stability.

Mrc1, Tof1 and Csm3 form a heterotrimeric complex that is part of the replisome during normal fork progression as well as upon HU-induced fork stalling. In both situations it contributes to the stabilization of the replisome by preventing the uncoupling of replication proteins from the replicated DNA (Katou, Kanoh et al. 2003, Bando, Katou et al. 2009).

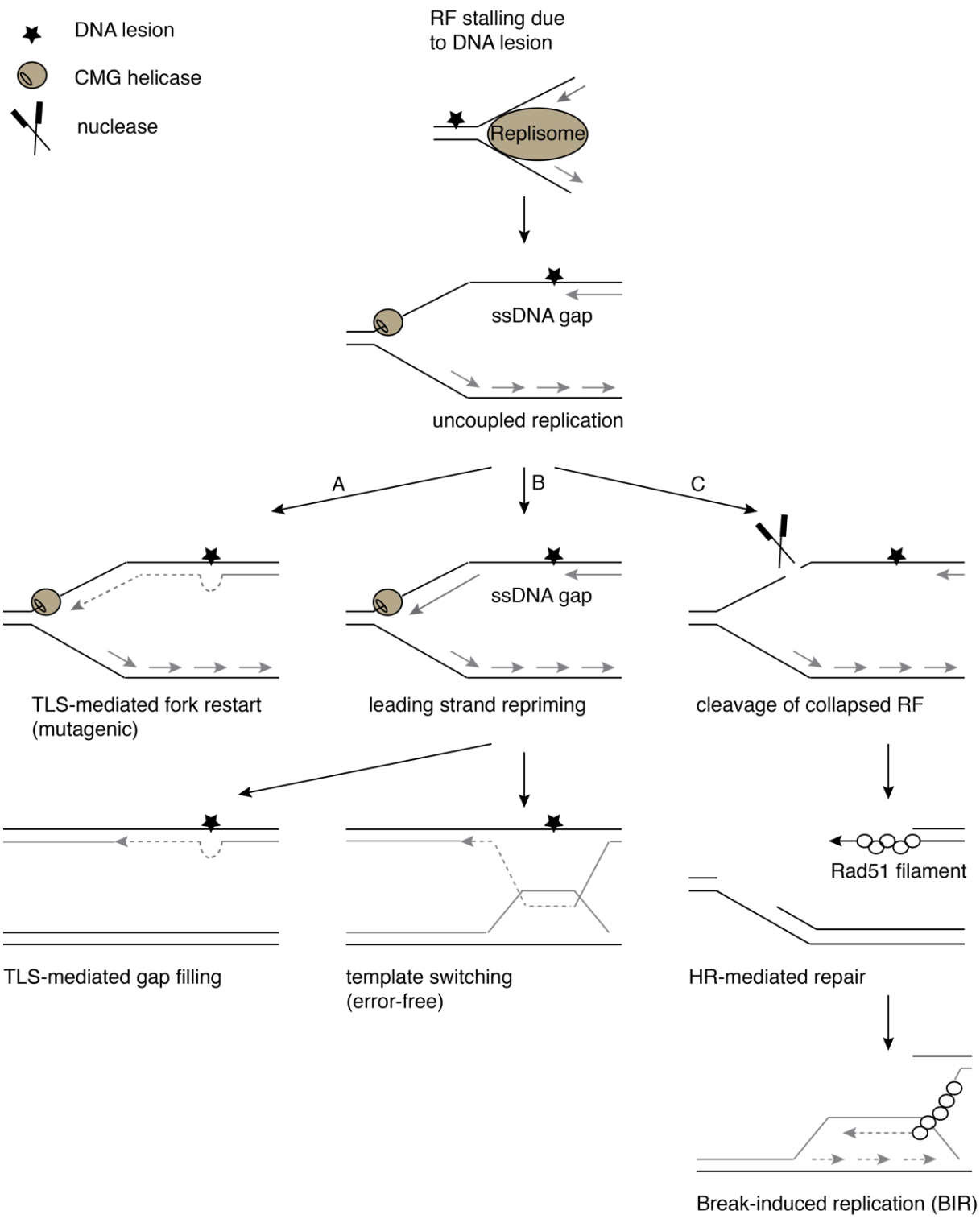

Figure 2 Mechanisms for resumption of replication after replication fork arrest due to a DNA lesion on the leading strand. Template unwinding seems to occur beyond the site of damage and is uncoupled from leading strand synthesis creating a ssDNA gap. Bypass of the damage can occur via different pathways. (A) Transient recruitment of a TLS polymerase is a mutagenic mechanism that depends on PCNA modification. (B) Repriming on the leading strand leaves a ssDNA gap that can be filled postreplicatively by TLS or by an error-free recombination-mediated mechanism (template switching). (C) RF cleavage creates one-ended DSBs that can be repaired by break-induced replication (BIR) using the sister chromatid as a template. Adapted from (Yeeles, Poli et al. 2013)

Mrc1 and to a lesser extent Tof1 are also required for the full activation of the checkpoint response (Alcasabas, Osborn et al. 2001, Foss 2001, Osborn and Elledge 2003), which ensures repair and replication fork restart by a number of different mechanisms including translesion synthesis (TLS), template switching and break-induced replication (BIR).

Continuous synthesis through DNA lesions is possible through the recruitment of lesion-bypass DNA polymerases, which temporarily replace the replicative polymerases and mediate a process called translesion synthesis (TLS). TLS is an error-prone mechanism.

Recruitment of lesion-bypass polymerases depends on the ubiquitination of PCNA by the Rad6-Rad18 heterodimer (Moldovan, Pfander et al. 2007). Repriming on the leading strand leaves ssDNA gaps that can be filled by postreplicative TLS or by error-free recombination-dependent template switching.

Failed replication fork restart and nucleolytic cleavage of aberrant recombination intermediates that are formed in this process can give rise to one-ended DSBs. Break-induced replication and sister chromatid recombination are homology-mediated recombination mechanisms that depend on Rad52 (Cortes-Ledesma, Tous et al. 2007). It is noteworthy that all of these mechanisms require the controlled decoupling of the DNA unwinding activity from the DNA synthesis activity of the replisome and therefore the physical separation of the CMG helicase complex from polymerase ε (in the case of leading strand damage) as shown in Figure 2. Alternatively, fork regression can also precede template switching and HR-mediated fork restart. The causes, consequences and possible repair and restart mechanisms of stalled replication forks are reviewed in (Branzei and Foiani 2009, Branzei and Foiani 2010, Yeeles, Poli et al. 2013). These reviews served as a basis for section 1.3.

Despite the efforts and the progress that have been made in understanding the regulation of replication and the mechanisms available to counteract replication fork breakdown and to promote genome stability during replication stress there is still a lot to learn about the role of many proteins that, when mutated, cause replication defects. The budding yeast proteins Rtt101 and Rtt107 have both been shown to be involved in replication fork restart. In response to DNA damage Rtt107 is phosphorylated by Mec1 and is thought to function as a scaffold recruiting repair proteins to the site of damage, including the endonuclease Slx4 and the SMC5/6

complex (Ohouo, Bastos de Oliveira et al. 2010, Leung, Lee et al. 2011). Rtt101 is a member of the cullin family of proteins and assembles ubiquitin E3 ligase complexes. Rtt101 is required for efficient resumption of replication after MMS treatment (Luke, Versini et al. 2006). Rtt101 and Rtt107 likely localize to chromatin as a complex upon replication fork stalling, where they might promote recovery by sister-chromatid recombination (Duro, Vaisica et al. 2008, Roberts, Zaidi et al. 2008). The molecular mechanism, however, remains elusive.

1.4 Endogenous and exogenous factors cause a variety of DNA lesions

DNA lesions occur frequently in the absence of external damaging agents. Metabolites such as reactive oxygen species (ROS) can damage the DNA in many ways, producing base modifications, abasic sites or non-conventional single-strand breaks. DNA integrity can also suffer from spontaneous hydrolysis resulting in deamination of bases and abasic sites. (Lindahl 1993, Waris and Ahsan 2006).

Exogenous threats to the genome include UV light, ionizing radiation and chemical agents. UV light generates pyrimidine dimers as the most common lesion, while ionizing radiation creates DSBs as the most toxic of its DNA lesions.

Methylmethane sulfonate (MMS) adds methyl groups to DNA bases. It has been used for decades as a "radiomimetic" drug. DSBs, however, do not seem to be a direct consequence of MMS treatment, but result from repair/replication intermediates that lead to strand breaks by aberrant processing or replication fork collapse (reviewed in Wyatt and Pittman 2006).

Topoisomerases are specialized DNA nucleases that relieve torsional stress, which arises during DNA replication, transcription or chromatin remodelling, by inducing and resealing DNA breaks. Top1 travels with the replication fork and removes positive supercoiling ahead of the fork by introducing a single-strand break (nick). The anticancer drug camptothecin (CPT) stabilizes the otherwise transient DNA-enzyme intermediate called cleavage complex and prevents religation. Collisions of the replication machinery with this stabilized protein-DNA complex cause DNA lesions and DSBs (Pommier 2006).

Hydroxyurea (HU) is a widely used drug to induce replication stress. It reversibly inhibits ribonucleotide reductase (RNR). In response to diminished cellular nucleotide pools replication is slowed down and replication forks stall (Alvino, Collingwood et al.

2007). Zeocin is a glycopeptide antibiotic, whose deleterious effects arise from the generation of both DSBs and single-stranded nicks (Povirk 1996, Burger 1998).
Since HU treatment interferes with normal replication it activates the S-phase checkpoint, while DSB induction by Zeocin triggers the DNA damage checkpoint. Both MMS and CPT cause DNA damage that is exacerbated by DNA replication and thus have the capability of activating both the DNA damage and the S-phase checkpoint depending on the drug concentration and the cell cycle stage of cells treated.

1.5 Telomeres protect the ends of linear chromosomes from being recognized as DNA damage

Telomeres are the nucleoprotein structures at the end of linear chromosomes. Telomeres protect the natural chromosome ends from being recognized as DNA damage due to their similarity with DSBs. Thus, one of the main functions of telomeres is to solve the so-called "end protection problem". The other main function is to solve the "end replication problem", which will be discussed in the next section.
The mechanisms telomeres employ to meet these challenges depend on the repetitive telomeric DNA sequence, the proteins localizing to telomeres and the structure of telomeric DNA. These main telomeric features are conserved from yeast to human (Blackburn, Greider et al. 2006).
Budding yeast telomeres consist of double-stranded, non-nucleosomal $TG_{1\text{-}3}$ repeats and a single-stranded 3' G-rich overhang. Wild type yeast telomeres are roughly 275-375 bp long. The overhang comprises about 12-15 nucleotides and increases to up to 30 nt in late S-phase, when telomeres are replicated and subsequently processed (Wellinger, Wolf et al. 1993, Soudet, Jolivet et al. 2014).
It has been shown that human telomeres, which are about 10-15 kb long ending in a G-strand overhang of about 50-200 nt, can fold back and invade the ds telomeric DNA forming a t-loop (Griffith, Comeau et al. 1999). Budding yeast telomeres are thought to maintain a similar structure with the tip of the telomere being tethered to the subtelomeric region by protein-protein interactions. Telomere looping likely contributes to the protection of telomeres by inhibiting homologous recombination and telomere-fusions by NHEJ (Poschke, Dees et al. 2012).

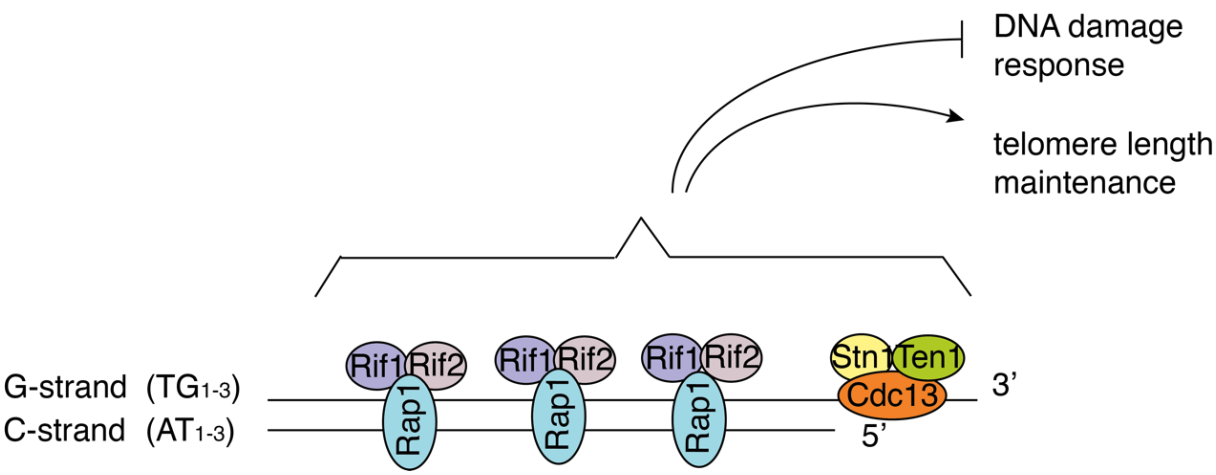

Figure 3 Simplified telomere structure in *S. cerevisiae*. Telomeric dsDNA is bound by Rap1, which recruits Rif1 and Rif2. The Rap1/Rif1/Rif2 complex is crucial for telomere protection and length homeostasis. The Rap1 binding proteins Sir2, Sir3 and Sir4, which contribute to the heterochromatic structure of telomeric and subtelomeric DNA, are not shown. The single-stranded overhang is bound by Cdc13, which recruits Stn1 and Ten1 forming the CST complex. The CST complex also takes part in the protection of telomeres and the regulation of telomere length. Telomere looping is not shown in this figure.

The region adjacent to the telomere is called the subtelomere and contributes to telomere function. Subtelomeres are characterized by low gene density and possess specialized subtelomeric repetitive elements. All budding yeast subtelomeres harbour a so-called X element, while about half of the 32 chromosome ends additionally possess between one and four copies of a sequence termed the Y' element (Walmsley, Chan et al. 1984).

Telomeres recruit a specialized set of proteins. In humans, a subset of these proteins has been termed the Shelterin complex, consisting of TRF1, TRF2, TIN2, RAP1, TPP1 and POT1 (de Lange 2005). *S. cerevisiae* is equipped with a "shelterin-like" complex consisting of Rap1, Rif1 and Rif2. Rap1 binds to the double-stranded part of yeast telomeres and recruits Rif1 and Rif2. The single-stranded overhang is bound by Cdc13, which interacts with Stn1 and Ten1, which together form the CST complex. Together, these proteins perform a variety of functions that help maintain telomeric integrity.

The essential protein Rap1 plays a crucial role in the suppression of checkpoint activation by telomeres, in the establishment of silent chromatin in the subtelomeric region and in telomere length homeostasis. Rap1 counteracts the recruitment of the MRX complex to telomeres, prevents telomere fusions by NHEJ and inhibits Tel1 binding to telomeres through Rif1 and Rif2 (Pardo and Marcand 2005, Hirano, Fukunaga et al. 2009). Rap1 also recruits the silent information regulators Sir2, Sir3

and Sir4 to telomeres, which spread into the subtelomeric region and establish a heterochromatic state by deacetylating H4K16 (Cockell, Palladino et al. 1995, Luo, Vega-Palas et al. 2002). This contributes to the "telomere positioning effect" (TPE), referring to the phenomenon that genes artificially placed in the subtelomeric region are transcriptionally repressed (Gottschling, Aparicio et al. 1990). Moreover, Cdc13, Stn1 and Ten1 prevent the binding of RPA to telomeric ssDNA and the subsequent activation of the Mec1-dependent checkpoint cascade and recruitment of DNA repair proteins.

However, telomere protection does not simply depend on the exclusion of proteins pertaining to the DDR. Instead, many of these potentially harmful proteins contribute to proper telomere function:

The MRX complex and Tel1, for example, both contribute to telomere length maintenance (Ritchie and Petes 2000). The Ku70/80 heterodimer, which as described above is recruited early to DSBs due to its affinity for exposed DNA ends, is involved in telomere capping (Fellerhoff, Eckardt-Schupp et al. 2000), while promoting NHEJ at DSBs. At telomeres Ku inhibits nuclease activities and thus helps prevent recombinational processes and checkpoint activation (Maringele and Lydall 2002).

1.6 Telomere attrition causes an irreversible cell cycle arrest called replicative senescence

Apart from the end protection problem, telomeres also face the "end replication problem": Due to the inability of the canonical replication machinery to fully replicate a linear DNA molecule, telomeres shorten with each round of cell division. However, the loss of telomeric sequence is not exclusive to lagging telomere synthesis, which suffers the removal of the outermost RNA primer. The C-rich strand serving as a template for leading strand synthesis can be replicated to its end. The resulting blunt ended telomere needs to be processed to form the G-rich overhang required for proper telomere function (Lingner, Cooper et al. 1995, Soudet, Jolivet et al. 2014).

The mechanistic problem of the end replication of the lagging telomere was first recognized and described by James Watson in 1972 (Watson 1972) and Alexei Olovnikov in 1973 (Olovnikov 1973). Experimental evidence for the relevance of this problem had already unknowingly been established by Leonard Hayflick in 1965 (Hayflick 1965), who found that human diploid fibroblasts can only undergo a finite

number of cell divisions (the "Hayflick limit") when cultured *in vitro*. The irreversible cell cycle arrest triggered by telomere shortening due to cell division is termed replicative senescence. Replicative senescence is thought to be a powerful mechanism for tumour suppression and is likely also involved in aging (Lansdorp 2008).

In most human somatic cells telomeres shorten as cells divide. In human germ cells and, to a lesser extent, in human stem cells telomerase is expressed. Telomerase is a reverse transcriptase able to replenish chromosome ends with telomeric sequences using an associated non-coding RNA as a template (Greider and Blackburn 1985, Greider and Blackburn 1989).

The *S. cerevisiae* telomerase consists of the catalytic subunit Est2, the RNA component encoded by TLC1 and the two regulatory subunits, Est1 and Est3 (Lundblad and Szostak 1989, Lendvay, Morris et al. 1996). The Rap1-Rif1/2 complexes suppress recruitment of telomerase through inhibition of MRX binding. As telomeres shorten, Rap1 binding sites become less abundant, allowing the sequential recruitment of the MRX complex and the Tel1 kinase (Ritchie and Petes 2000, Tsukamoto, Taggart et al. 2001). This leads to extensive resection depending on Sae2, Sgs1, Dna2 and Exo1 (Dionne and Wellinger 1996). The ssDNA is bound predominantly by Cdc13, which in turn recruits Est1 and leads to the assembly of active telomerase, preferentially at short telomeres (Evans and Lundblad 1999, Teixeira, Arneric et al. 2004).

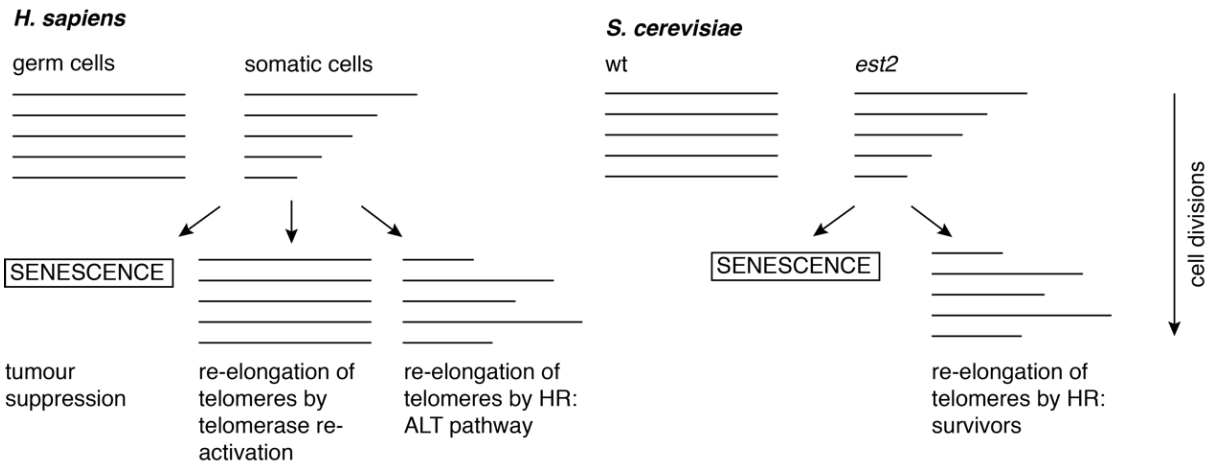

Figure 4 Replicative senescence in *H. sapiens* and *S. cerevisiae*. The lack of telomerase expression in human somatic cells and in *est2* cells in budding yeast causes the loss of telomeric sequence with each cell division, which leads to permanent cell cycle arrest called replicative senescence. A small fraction of cells can overcome this replication barrier. Human tumours re-elongate their telomeres by reactivating telomerase or by homologous recombination (Alternative Lengthening of Telomeres, ALT). In analogy to the human ALT pathway *S. cerevisiae* cells can form survivors. In human germ cells and wt yeast cells telomere length is maintained by telomerase. The situation in human stem cells, which express telomerase to some extent, is not shown.

In telomerase-deficient yeast cells, similar to telomerase-negative mammalian cells, telomeres progressively shorten and cells lose viability over many generations until they stop dividing and arrest at the G2/M border (Figure 4). This state termed "crisis" is characterized by the irreversible activation of DNA damage checkpoints due to eroded telomeres, which are no longer able to fulfil their protective function. Although it has been shown that the G2/M arrest due to telomere attrition depends on Mec1/Ddc2, Rad24, Ddc1/Mec3, Rad9 and Rad53, thus sharing similarities with the response to DNA damage, the signalling of eroded telomeres is not yet fully understood (Enomoto, Glowczewski et al. 2002, Ijpma and Greider 2003, Grandin, Bailly et al. 2005, Deshpande, Ivanova et al. 2011). Nevertheless, mounting evidence suggests that it is the length of the shortest telomere that is of particular importance in determining the onset of replicative senescence (Abdallah, Luciano et al. 2009, Xu 2013). Moreover, telomere processing during replicative senescence also seems to be length dependent (Fallet, Jolivet et al. 2014).

A small fraction of senescent cells is able to regain viability by re-elongating their telomeres based on a homologous recombination-dependent mechanism. These cells are called survivors (Lundblad and Blackburn 1993). They are generally thought to be the yeast equivalent of human ALT (alternative lengthening of telomeres) cancer cells. About 10-15 % of human tumours maintain their telomeres by this

telomerase-independent recombination-mediated mechanism (Cesare and Reddel 2010). A comprehensive review highlighting the significance of budding yeast for the research on replicative senescence is (Teixeira 2013), which served as a basis for this section.

1.7 *RTT101* deletion has pleiotropic effects

Rtt101 is a member of the cullin family of proteins. Cullins are defined by an evolutionarily conserved cullin homology domain and can be found in a wide variety of phylogenetic groups including chordates, nematodes and yeast (Kipreos, Lander et al. 1996, Mathias, Johnson et al. 1996). They act as molecular scaffolds facilitating the assembly of multi-subunit Cullin-RING ubiquitin E3 Ligase complexes (CRL). All cullin proteins possess a conserved C-terminal domain that binds the RING finger protein Hrt1/Roc1, which recruits an E2 ubiquitin-conjugating enzyme. Rtt101 functions with the ubiquitin-conjugating enzyme Cdc34. The N-terminal domain of cullins is more diverse, thus allowing the interaction with a variety of different substrate-specific adaptor proteins (Michel, McCarville et al. 2003, Zaidi, Rabut et al. 2008).

The ubiquitination of a target protein requires the coordinated action of three distinct steps: The ATP-dependent activation of the ubiquitin molecule by an E1 activating enzyme is followed by the transfer of ubiquitin to an E2 ubiquitin-conjugating enzyme in a trans(thio)esterification reaction. An E3 ligase catalyses the formation of an isopeptide bond between the carboxy-terminal glycine residue of ubiquitin and the substrate lysine ε-amino group by bringing substrate and E2 ligase into close proximity. The result of target protein modification by a ubiquitin chain (polyubiquitination) depends on the chain structure. Ubiquitin contains seven lysine residues, which can themselves act as ubiquitin acceptors. Lys48-linked ubiquitin chains generally target substrate proteins for proteasomal degradation while Lys63-linked chains have non-degradative roles and alter protein function (Sarikas, Hartmann et al. 2011).

There are seven cullins in *Homo sapiens* (CUL1 to CUL3, CUL4A, CUL4B, CUL5 and CUL7) and three cullins in *Saccharomyces cerevisiae* (Cdc53, Cul3 and Rtt101). Cdc53 is the only essential budding yeast cullin. It is thought to be the homologue of human CUL1. The Cdc53 assembled complex contains an F-box protein as substrate-specific adaptor, whose interaction with Cdc53 is mediated by Skp1. The

SCF (Skp1, Cullin, F-box) complex promotes the G1-S transition by targeting both G1 cyclins and the Clb-CDK inhibitor, Sic1 for degradation (Willems, Schwab et al. 2004).

Cul3 shares sequence similarities with human CUL3. It forms a complex with Elc1 that polyubiquitinates monoubiquitinated RNA Pol II to trigger its proteasomal destruction after UV irradiation (Ribar, Prakash et al. 2007).

Despite missing sequence similarity Rtt101 has been suggested to be the yeast equivalent of the human CUL4 subfamily since the Rtt101-interacting factor Mms1 was identified as a distant homologue of the CUL4-interacting factor DDB1 (Zaidi, Rabut et al. 2008). Indeed, both Rtt101 and CUL4-assembled complexes have been shown to participate in genome maintenance mechanisms by regulating DNA replication and repair.

Rtt101 (*r*egulator of *T*y1 *t*ransposition 101) was first identified as a suppressor of Ty1 retrotransposon mobility (Scholes, Banerjee et al. 2001). Since then a wide variety of phenotypes have been described for cells lacking Rtt101, only some of which can be discussed here.

rtt101 cells accumulate at the metaphase to anaphase transition (Michel, McCarville et al. 2003). This is likely due to the accumulation of spontaneous DNA damage occurring in S-phase since deletion of the damage checkpoint proteins Mec1 and Rad9 relieves the anaphase delay while deletion of the mitotic checkpoint protein Mad2 does not. The number of repair events as measured by Rad52-GFP and Ddc1-GFP repair foci as well as gross chromosomal rearrangements (GCR), are indeed increased in unchallenged conditions in *rtt101* cells compared to wt. A role for Rtt101 during S-phase is further supported by the observation that replication fork progression through damaged and naturally difficult to replicate regions is impaired in *rtt101* cells (Luke, Versini et al. 2006). The mechanism of how Rtt101 might relieve replisome blockage remains elusive. However, Rtt101 and its putative complex members Mms1 and Mms22 have been suggested to regulate HR-dependent processes in response to replication stress both in fission and budding yeast (Baldwin, Berger et al. 2005, Duro, Vaisica et al. 2008, Dovey, Aslanian et al. 2009, Vaisica, Baryshnikova et al. 2011, Vejrup-Hansen, Mizuno et al. 2011).

Rtt101's role in S-phase is underlined by the fact that *rtt101* cells display a striking hypersensitivity to the genotoxic agents MMS and CPT, which cause DNA damage that is exacerbated in S-phase and leads to replication stress by blocking replication

fork progression (Chang, Bellaoui et al. 2002, Laplaza, Bostick et al. 2004, Parsons, Brost et al. 2004, Luke, Versini et al. 2006). *rtt101* cells are mildly hypersensitive to HU, which causes fork stalling due to nucleotide depletion, and show low sensitivity to ionising radiation and UV treatment (Michel, McCarville et al. 2003, Parsons, Brost et al. 2004, Luke, Versini et al. 2006, Kapitzky, Beltrao et al. 2010). While the checkpoint recovery of *rtt101* cells after MMS treatment is severely delayed, checkpoint deactivation in response to HU occurs with normal kinetics (Luke, Versini et al. 2006).

The sensitivity to MMS and CPT may in part be attributed to Rtt101's role in nucleosome assembly. Rtt101-dependent ubiquitination of H3 upon presentation of the acetylated H3-H4 heterodimer by the histone chaperone Asf1 allows H3-H4 deposition onto newly replicated DNA by reducing its affinity to Asf1. This process is crucial for the establishment of a proper chromatin structure following replication, gene transcription and DNA damage repair. However, the deletion of *RTT101* is additive with ubiquitination-deficient H3 mutants in terms of drug sensitivity (Han, Zhang et al. 2013) indicating that Rtt101-assembled complexes fulfil other functions important for the maintenance of genomic stability in addition to sustaining a proper chromatin structure.

As described in section 1.3 (above) it has been shown that Rtt101 is recruited to chromatin as a consequence of DNA damage induced by MMS and that this recruitment depends on the presence of Rtt107 (Roberts, Zaidi et al. 2008). Moreover, genetic evidence suggests that Rtt107 does not play a role in the nucleosome assembly pathway described above (Pan, Ye et al. 2006, Collins, Miller et al. 2007).

Five different putative substrate specific adaptor proteins have been shown to interact with Rtt101: the DNA repair and replication stress response protein Rtt107, the replication-associated repair protein Esc2, the replisome member Ctf4, the subunit of the origin recognition complex ORC5 and the regulator of RNR gene transcription and DDR protein Crt10. Their interaction with Rtt101 is bridged by the two linker proteins Mms1 and Mms22 (Figure 5A) (Zaidi, Rabut et al. 2008, Mimura, Yamaguchi et al. 2010).

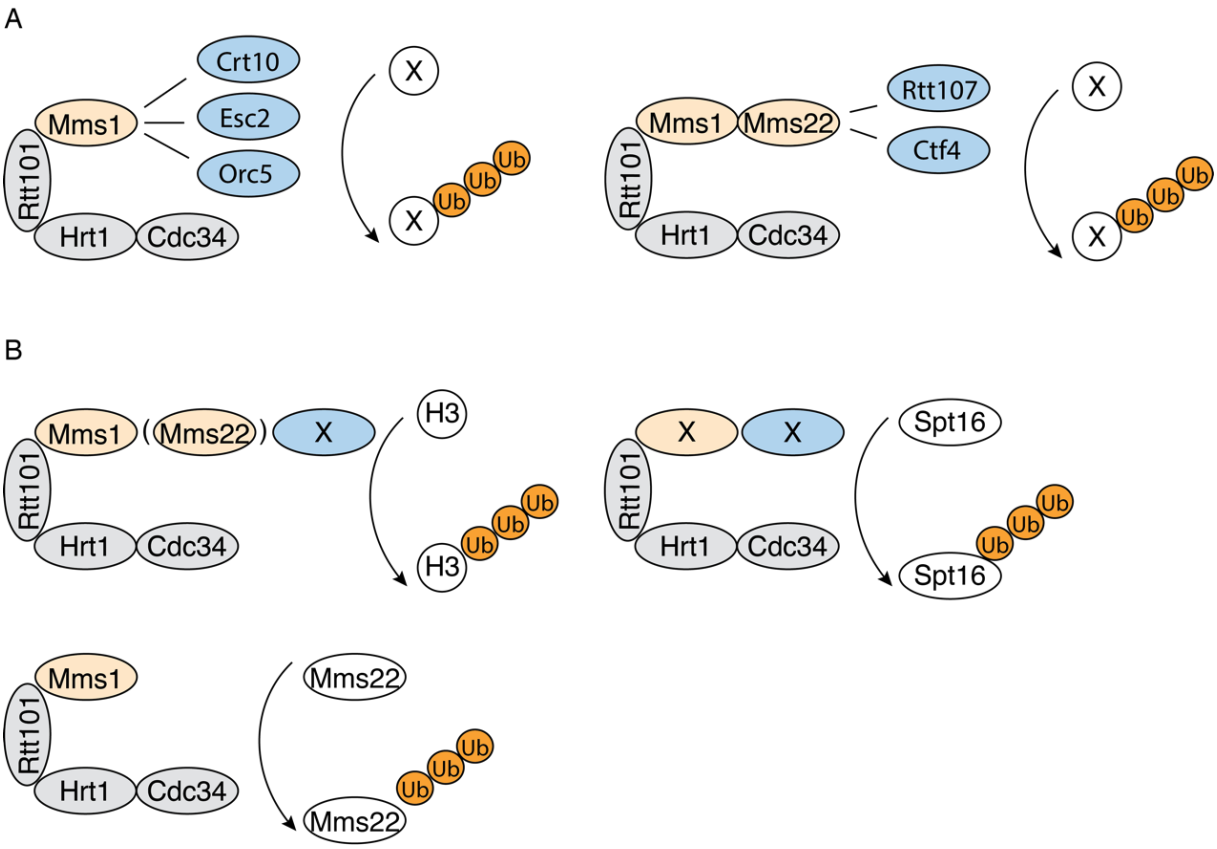

Figure 5 Rtt101 assembles a variety of ubiquitin E3 ligase complexes (A) Rtt101 interacts with its substrate specific adaptor proteins via the linker proteins Mms1 and Mms22. (B) Three target proteins have been identified whose ubiquitination depends on Rtt101. Mms22 seems to be both a linker and a target protein. The exact composition of the ligase complexes ubiquitinating H3 and Spt16 is not known.

Nevertheless, only two *bona fide* targets have so far been identified apart from histone H3. One of them is Spt16, a member of the FACT complex. On the one hand, the FACT complex interacts directly with DNA polymerase α. On the other hand it is part of the replisome progression complex. Deletion of *RTT101* reduces the association of Spt16 and MCM proteins with early replication origins and exacerbates the sensitivity of cells carrying the heat sensitive *spt16-11* allele to replication stress. Han and co-workers conclude that Rtt101-dependent ubiquitination of Spt16 seems to target the FACT complex for replication instead of transcription (Han, Li et al. 2010).

The third confirmed target of Rtt101 is Mms22. Therefore Mms22 is not just a member of the ubiquitin E3 ligase complex $Rtt101^{Mms1Mms22}$. It very likely also becomes its target after having been recruited to sites of DNA damage and having fulfilled its function there. What exactly this function is remains unclear. Nevertheless, the degradation of Mms22 seems to be necessary for yeast cells to re-enter the cell

cycle after G2/M arrest due to MMS-induced DNA damage (Ben-Aroya, Agmon et al. 2010).

The three identified Rtt101 targets indicate that Rtt101 plays a versatile role in replication (Spt16) and replication-associated processes, such as the response to replication-associated DNA damage (Mms22 and Spt16) and replication-coupled (as well as replication-independent) nucleosome assembly (histone H3-H4 heterodimer) in budding yeast.

As mentioned above, $Rtt101^{Mms1}$ has been proposed to be the counterpart of the human $CUL4^{DDB1}$ complex due to the sequence similarity of *MMS1* and *DDB1* (Zaidi, Rabut et al. 2008). *RTT101* shares no significant sequence homology with the two highly similar *CUL4* genes, CUL4A and CUL4B, which seem to be functionally redundant. Just like $Rtt101^{Mms1}$ in *Saccharomyces cerevisiae*, $CUL4^{DDB1}$ promotes both replication-coupled and replication-independent nucleosome assembly by ubiquitinating histones H3.1 and H3.3, which affects their interaction with histone chaperones Asf1a/b, Daxx and HIRA (Han, Zhang et al. 2013). Nakagawa and Xiong could previously show that CUL4 regulates neuronal gene expression by degrading WDR5, a core component of the H3 lysine 4 methyltransferase (Nakagawa and Xiong 2011).

$CUL4^{DDB1}$ also contributes in several ways to the complex balance of factors promoting and suppressing replication in an unperturbed S-phase as well as in the face of DNA damage. In cooperation with PCNA, $CUL4^{DDB1}$ targets CDK inhibitor p21 for degradation after irradiation with low doses of UV (Abbas, Sivaprasad et al. 2008). In a similar mechanism the replication factor Cdt1 is degraded in a $CUL4^{DDB1}$- and PCNA-dependent manner (Higa, Mihaylov et al. 2003, Hu, McCall et al. 2004, Senga, Sivaprasad et al. 2006), a pathway also identified in fission yeast (Ralph, Boye et al. 2006). Thus, human CUL4-based ubiquitin-ligase complexes have been shown to regulate chromatin dynamics and contribute to the maintenance of genome integrity during S-phase. Some of the uncovered pathways seem to be conserved from yeast to human.

In budding yeast, two reports connect Rtt101 to telomere biology. First, *rtt101* cells were shown to be desilenced in the subtelomeric region, suggesting a role for Rtt101 in the maintenance of the telomere position effect (Mimura, Yamaguchi et al. 2010). Whether this is due to the defective chromatin structure of *rtt101* cells has not yet been addressed. Second, a genome-wide screen from the Lydall laboratory identified

RTT101 as one of about 200 genes, many of which implicated in DNA damage repair, whose deletion accelerated entry of telomerase-deficient cells into replicative senescence (Chang, Lawless et al. 2011).

1.8 Aims of this study

The known targets of Rtt101-assembled ubiquitin E3 ligase complexes are not able to explain the phenotypes associated with *RTT101* deletion. Especially, one of the most striking phenotypes of *rtt101* cells, their hypersensitivity to certain genotoxic agents and the role of Rtt101 during S-phase are far from being understood. In this study we aimed to identify potential targets of Rtt101-assembled ubiquitin E3 ligase complexes involved in the cellular response to DNA damage and replication stress.

The second aim of this study was to elucidate Rtt101's role in preventing premature senescence. The biology and maintenance of telomeres is closely connected to the field of DNA damage and repair due to the structural similarity of telomeres with DSBs. Replicative senescence is a natural process that highlights the intimate relation between telomeres and damage as short telomeres provoke a cellular response resembling the DDR. As described, telomeres, in particular short telomeres, are difficult to replicate regions of the genome. This allows the speculation that Rtt101's role during telomere-induced senescence might resemble its role in the response to DNA damage and replication stress.

2 Materials and Methods

2.1 Materials

2.1.1 Yeast strains

The yeast strains used in this study were derived from BY4741 background (*his3-1*, *leu2-0*, *ura3-0*, *met15-0*).

Code	Genotype
YBL7	Wt
YBL1306	*MATα rtt101::NAT*
YBL61	*MATa rtt101::KAN*
YLK297	*MATα rtt101::NAT*
YLK419	*MATα mms1::NAT*
YLK288	*MATa mms22::NAT*
YLK410	*MATα ctf4::NAT*
YMD1500	*MATa esc2::NAT*
YMD1364	*MATa mrc1::KAN*
YMD1348	*MATa pol32::KAN*
YMD1353	*MATa rad27::KAN*
YMD1355	*MATa top1::KAN*
YMD1359	*MATa dpb4::KAN*
YMD1354	*MATa siz2::KAN*
YMD1362	*MATa met7::KAN*
YMD1461	*MATα rtt101::NAT mrc1::KAN*
YMD1388	*MATa rtt101::NAT pol32::KAN*
YMD1400	*MATa rtt101::NAT rad27::KAN*
YMD1412	*MATa rtt101::NAT top1::KAN*
YMD1424	*MATα rtt101::NAT dpb4::KAN*
YMD1368	*MATa rtt101::NAT siz2::KAN*
YMD1445	*MATα rtt101::NAT met7::KAN*
YLK495	*MATa mms1::NAT mrc1::KAN*
YLK432	*MATa mms1::NAT pol32::KAN*

Code	Genotype
YLK434	*MATa mms1::NAT rad27::KAN*
YLK437	*MATa mms1::NAT top1::KAN*
YLK435	*MATa mms1::NAT dpb4::KAN*
YLK430	*MATa mms1::NAT siz2::KAN*
YMD1579	*MATα mms22::NAT mrc1::KAN*
YMD1485	*MATα mms22::NAT pol32::KAN*
YMD1489	*MATa mms22::NAT rad27::KAN*
YMD1497	*MATa mms22::NAT top1::KAN*
YMD1473	*MATa mms22::NAT dpb4::KAN*
YMD1493	*MATα mms22::NAT siz2::KAN*
YMD1477	*MATα mms22::NAT met7::KAN*
YLK422	*MATa ctf4::NAT pol32::KAN*
YLK424	*MATa ctf4::NAT top1::KAN*
YLK426	*MATa ctf4::NAT dpb4::KAN*
YLK420	*MATa ctf4::NAT siz2::KAN*
YMD1522	*MATa esc2::NAT mrc1::KAN*
YMD1506	*MATα esc2::NAT pol32::KAN*
YMD1530	*MATα esc2::NAT rad27::KAN*
YMD1518	*MATa esc2::NAT top1::KAN*
YMD1514	*MATa esc2::NAT dpb4::KAN*
YMD1510	*MATα esc2::NAT siz2::KAN*
YMD1526	*MATa esc2::NAT met7::KAN*
YMD1636	*MATa rad27::KAN*
YMD1637	*MATα rad27::KAN mrc1::NAT*
YMD1600	*MATa ubc13::KAN*
YMD1601	*MATα ubc13::KAN mrc1::NAT*
YMD1624	*MATα csm3::KAN*
YMD1625	*MATa csm3::KAN rtt101::NAT*
YMD1614	*MATa tof1::KAN*
YMD1615	*MATα tof1::KAN rtt101::NAT*
YLK490	*MATa bar1::HIS3*
YLK470	*MATa bar1::HIS3 rtt101::NAT*

Code	Genotype
YLK473	*MATa bar1::HIS3 mrc1::KAN*
YLK478	*MATa bar1::HIS3 rtt101::NAT mrc1::KAN*
YMD1655	*MATa bar1::NAT MRC1-TAP-HIS3*
YMD1657	*MATa bar1::NAT MRC1-TAP-HIS3 rtt101::KAN*
YMD1658	*MATa bar1::NAT MRC1-TAP-HIS3 dia2::HYG*
YLK492	*MATa/MATα RTT101/rtt101::NAT MRC1/mrc1::KAN DIA2/dia2::HYG*
YVK91	*MATa/MATα RTT101/rtt101::HYG MRC1/mrc1::KAN RAD52/rad52::NAT*
YLK268	*MATa/MATα RTT101/rtt101::KAN EST2/est2::HIS3*
YLK379	*MATa/MATα MMS1/mms1::KAN EST2/est2::HIS3*
YLK359	*MATa/MATα MMS22/mms22::KAN EST2/est2::HIS3*
YLK345	*MATa/MATα ESC2/esc2::KAN EST2/est2::HIS3*
YLK347	*MATa/MATα CTF4/ctf4::KAN EST2/ est2::HIS3*
YLK331	*MATa/MATα CRT10/crt10::KAN EST2/est2::HIS3*
YLK362	*MATa/MATα ORC5/orc5-70-KAN EST2/est2::HIS3*
YLK329	*MATa/MATα RTT101/rtt101::KAN RAD52/rad52::NAT EST2/ est2::HIS3*
YLK439	*MATa/MATα RTT101/rtt101::NAT MRC1/mrc1::KAN EST2/ est2::HIS3*

2.1.2 Plasmids

Code	Plasmid
pLK16	*mrc1-aq.kanMX4* in pRS426
pLK18	*mrc1-aq.HIS3* in pRS426
pLK20	pRS415 *LEU2*
pLK23	*MRC1* genomic locus in pRS415
pLK26	$mrc1_{1\text{-}971}$ in pRS415

2.1.3 Oligonucleotides

Code	Name	Sequence (5´-3´)	Exp.
oBL358	1L	GCG GTA CCA GGG TTA GAT TAG GGC TG	telomere PCR
oBL359	oligo-dG	CGG GAT CC$(G)_{18}$	telomere PCR
oBL361	6Y´	TTA GGG CTA TGT AGA AGT GCT G	telomere PCR
oBL207	TERRA	CAC CAC ACC CAC ACA CCA CAC CCA CA	southern blot
oBK295	1L-fwd	CGG TGG GTG AGT GGT AGT AAG TAG A	ChIP
oBL296	1L-rev	ACC CTG TCC CAT TCA ACC ATA C	ChIP
oLK57	15L-fwd	GGG TAA CGA GTG GGG AGG TAA	ChIP
oLK58	15L-rev	CAA CAC TAC CCT AAT CTA ACC CTG T	ChIP
oLK49	6Y´-fwd	GGC TTG GAG GAG ACG TAC ATG	ChIP
oLK50	6Y´-rev	CTC GCT GTC ACT CCT TAC CCG	ChIP
oAM47	rDNA-fwd	TCC AAT TGT TCC TCG TTA AG	ChIP
oAM48	rDNA-rev	ATT CAG GGA GGT AGT GAC AA	ChIP

2.1.4 Antibodies

Antibody	Source
Rad53 EL7.E1	Marco Foiani
Mrc1-TAP	Sigma Aldrich
Pgk1	Life technologies
S9.6 antibody	David Tollervey
Goat Anti-Mouse-HRP Conjugate	BioRad

2.1.5 Liquid media and plates

Plates	YPD
YPD Agar	65 g
ddH_20	1 L
Autoclave	20 min 65 °C

For YPD plates containing antibiotics add:

100 µg/mL for NAT (Nourseothricin or G418), 250 µg/mL for KAN (Kanamycin), and 300 µg/mL for HYG (Hygromycin B)

Plates	SD complete	SD - AA
Yeast synthetic dropout Medium supplement without amino acids	1.92 g	1.92 g
Yeast nitrogen base without amino acids	6.7 g	6.7 g
Agar	24 g	24 g
100 x AA	10 mL	-
dd H_2O	960 mL	960 mL
Autoclave	20 min 65 °C	20 min 65 °C
50 % glucose (final conc. 2 %)	40 mL	40 mL

Plates	Pre-Sporulation Plates
Standard nutrient broth	12 g
Yeast extract	4 g
Agar	8 g
dd H_2O	360 mL
Autoclave	20 min 65 °C
50 % Glucose	40 mL

Liquid medium	**LB**
Yeast extract	5 g
Trypton	10 g
NaCl	10 g
dd H_2O	1 L
Autoclave	20 min 65 °C

For LB medium containing Carbanicillin add 1 mL of Carbanicillin at a concentration of 100 ng/mL.

Plates	**LB**
LB agar	200 g
dd H_2O	5 L
Autocave	20 min 65 °C

For LB plates containing Ampicillin add 100 µg/mL Ampicillin.

Liquid medium	**SOC**
Trypton	20 g
Yeast extract	5 g
NaCl	0.5 g
KCl	0.186 g
Glucose	3.6 g
Adjust pH with 5 M NaOH	about 200 µL
dd H_2O	1 L
Autoclave	20 min 65 °C
Before use add 2 M MgCl2 (prepared of 1 M $MgCl_2$•6 H_2O and 1 M MgSO4•7 H_2O	5 mL

2.1.6 Buffers

10 x TE	
TRIS (1 M, pH 7.5)	400 mL
EDTA (0.5 M)	80 mL
H_2O	3520 mL
Autoclave	20 min 65 °C

10 x TBE	
TRIS	108 g
0.5 M EDTA (set to pH 8 with NaOH)	20 mL
Boric Acid	55 g
dd H_2O	1 L
Autoclave	20 min 110 °C

20 x SSC	
NaCl	175.3 g
Sodium citrate	88.2 g
Adjust to pH 7	HCl
dd H_2O	1 L
Autoclave	20 min 65 °C

10 x PBS	
NaCl	80 g
KCl	2 g
Na_2HPO_4 x 7 H_2O	26.8 g
KH_2PO_4	2.4 g
Adjust to pH 7.4	HCl
dd H_2O	1 L
Autoclave	20 min 65 °C

LiAc Mix	
1 M Lithium Acetate (sterile)	10 mL
10 x TE (sterile)	10 mL
Sterile dd H_2O	80 mL

AE buffer	
Natrium acetate anhydrous	2.05 g
EDTA	1.46 g
Sterile dd H_2O	500 mL
Adjust to pH 5.3	NaOH
Autoclave	20 min 65 °C

SDS	**10 % SDS**	**20 % SDS**
SDS	20 g	40 g
Sterile dd H_2O	200 mL	200 mL
Sterilization	Millipore filter 0.22 µm	Millipore filter 0.22 µm

Hybridization solution	
Formamide	50 mL
20 x SSC	25 mL
50 x Denhardt's solution	10 mL
0.5 M EDTA	1 mL
PIPES 1 M (pH 6.4)	1 mL
Yeast RNA	40 mg in 3 mL H_2O heat to 65 °C and filter sterilize
10 % SDS	10 mL
Sterilize	Heat to 65 °C and use Millipore filter 0.22 µm

PIPES 1M pH 6.4	
PIPES	30.2 g
dd H_2O	100 mL
Adjust to pH 6.4	NaOH
Autoclave	20 min 65 °C

5 x DIG wash buffer	
Maleic acid	58 g
Adjust pH to 7.5	NaOH
NaCl	43.8 g
Tween-20	15 mL
dd H_2O	1 L
Autoclave	20 min 65 °C

Maleic acid buffer	
Maleic acid	11.67 g
Adjust to pH 7.5	NaOH
NaCl	8.76 g
dd H_2O	1 L
Autoclave	20 min 65 °C

DIG detection buffer	
Tris-HCl	15.8 g
NaCl	5.8 g
dd H_2O	1 L
Adjust to pH 9.5	HCl
Autoclave	20 min 65 °C

10 x blocking solution	
Blocking solution powder	10 g
Maleic acid buffer	100 mL
dd H_2O	100 mL

1 x blocking solution	
10 x blocking solution	3 mL
Maleic acid buffer	27 mL

Denaturing solution	
NaOH	16 g
NaCl	35.1 g
dd H_2O	1 L

Neutralizing solution	
NaCl	52.6 g
Trizma -Base	36.3 g
dd H_2O	1 L
Adjust to pH 7.5	

10 x Telomere PCR buffer	
Tris-HCl (pH 8.8)	810 mg
(NH4)2SO4	211 mg
70 % glycerol	7.1 mg
Tween-20 (0.1 %)	10 µL
dd H_2O	10 mL

Elution buffer B	
Tris-HCl pH 7.5	50 mM
SDS	1 %
EDTA pH8.0	10 mM
dd H_2O	250 mL

FA lysis buffer	**-SOD**	**+SOD**
HEPES-KOH pH 7.5	50 mM	50 mM
NaCl	140 mM	140 mM
EDTA pH 8.0	1 mM	1 mM
Triton X-100	1 %	1 %
Sodium deoxycholate	-	0.1 %

FA lysis buffer 500	
HEPES-KOH pH 7.5	50 mM
NaCl	500 mM
EDTA pH 8.0	1 mM
Triton X-100	1 %
Sodium deoxycholate	0.1 %

Buffer III	
Tris-HCl pH 8.0	10 mM
EDTA pH 8.0	1 mM
LiCl	250 mM
NP-40	1 %
Sodium deoxycholate	1 %

Urea loading buffer	
Tris-HCl pH 8.8	1.2 mL (1 M)
5 % glycerol final	714 µL (70 %)
8 M urea final	4.8 g
143 mM β-mercaptoethanol final	100 µL (14.3 M)
8 % SDS final	4 mL (20 %)
dd H_2O	10 mL
Add bromophenol blue to colour the buffer	
Tris-HCl pH 6.8	1.2 mL

Solution 1	
NaOH (10 M)	3.7 mL
dd H_2O	14.78 mL
β-mercaptoethanol	1.52 mL

Solution 2	
TCA 100 %	10 mL
dd H_2O	10 mL

Solution 3	
Acetone	100 %

2.1.7 Other materials

Enzymes	Company
DNase and DNase buffer	New England Biolabs
Phusion Polymerase	New England Biolabs
Proteinase K	Qiagen
RNase A	Applichem
Terminal Transferase	New England Biolabs
Restriction enzymes	New England Biolabs

Ladders	Company
1 kb DNA ladder	New England Biolabs
100 bp DNA ladder	New England Biolabs
DIG-labelled molecular weight marker	Roche

Kits	Company
Puregene Yeast/Bact. Kit B	Qiagen
Qiaquick Gel Extraction Kit	Qiagen
Qiaquick PCR purification Kit	Qiagen
Zero Blunt TOPO PCR cloning Kit for Sequencing	Invitrogen
DirectPrep 96 MiniPrep 3' End labeling Kit 2nd generation	Roche
DyNAmo Flash SYBR Green qPCR Kit	Thermo Scientific

Additional Materials	Company
α-factor	ZymoResearch
Bradford solution	AppliChem
Bromophenol blue indicator	Sigma Aldrich
Camptothecin (CPT)	Sigma Aldrich
CDP-Star	Roche
Denhardt's solution (50x)	AppliChem

Additional Materials	Company
dNTPs	New England Biolabs
Hydroxyurea (HU)	Sigma Aldrich
Lysing Matrix C tubes	MP Biomedicals
Methylmethane sulfonate (MMS)	Sigma Aldrich
Mini Protean TGX Precast Gels	BioRad
Nylon Membrane (positively charged)	GE Healthcare
One Shot DH5α TM-T1 *E. coli*	Invitrogen
Protease inhibitor mix complete Mini tablet EDTA-free	Roche
Protein A Sepharose 4 Fast Flow beads	GE Healthcare
Transblot nitrocellulose membrane	BioRad
Zeocin	Invitrogen

2.1.8 Electronic devices and software

Electronic devices	Company
Bioraptor Twin XD10	Diagenode
Blotting apparatus Trans-Blot Turbo	BioRad
Dissecting Microscope MSM manual	Singer Instruments
Dot blot apparatus	BioRad
Hybridization oven MS incubator	Uniequip GmbH
Incubators MIR154	Sanyo
LAS 4000	FujiFilm
Light Cycler 480	Roche
Microscope with 40 x objective	Optech Technology
Nanodrop 2000C	Thermo Scientific
Photometer Ultraspec 3100pro	Amersham Biosciences
Thermocycler C1000	BioRad
UV Stratalinker 2400	Stratagene

Software	Company
Adobe Illustrator	Adobe
Adobe Photoshop	Adobe

Software	Company
End Note	Thomson Reuters
Excel	Microsoft
FileMaker Pro	FileMaker Inc.
ImageJ	Wayne Rasband (NIH)
MultiGauge	FujiFilm
Prism	Graph Pad
Sequencher	Gene codes Corporation

2.2 Methods

2.2.1 High-throughput screen

A high-throughput screen was carried out as described in (Buser, Kellner et al.): Synthetic Genetic Array (SGA) methodology was used as first reported by Tong and colleagues (Tong, Evangelista et al. 2001). The procedure was modified in the following way: A non-essential heterozygous diploid *S. cerevisiae* knockout collection, kindly provided by M. Knop, was sporulated and crossed to an *rtt101::NAT can1::STE2pr-SpHis5* strain (Y7092, C. Boone). Diploid cells were selected by repinning on YPD plates containing 100 µg/mL nourseothricin and 250 µg/mL of the kanamycin analogue G418. Diploids were then induced to sporulate. Haploid double mutants were selected by repinning on MATa selection plates (SD-his/arg/lys + canavanine + thiolysine) followed by a repinning on MATa selection plates containing 100 µg/mL nourseothricin and 250 µg/mL of the kanamycin analogue G418. Colonies were then repinned onto SD complete, SD + 0.01 % MMS and SD + 5 µM CPT. After 24 h incubation at 30 °C cells were repinned onto the same media, incubated at 30 °C and repinned again after 24 h. Pictures of the last repinning taken after 24 h incubation at 30 °C are shown in Figure 6. Double mutants that showed increased resistance to either MMS or CPT were classified as suppressors. Scoring of the suppressors was done by hand. Validation was carried out by manually crossing and dissecting tetrads from independent starter strains and subsequent duplicate spot assays onto drug containing media.

2.2.2 Transformation of *S. cerevisiae*

25 mL of exponentially growing yeast cells (OD_{600} 0.4 - 0.8) were centrifuged at 3000 rpm for 5 min at RT, washed once in 5 mL LiAc mix and centrifuged again at 3000 rpm. The supernatant was removed and the pellet resuspended in 250 µL LiAc mix. 100 µL of cells were used per transformation and mixed with 500 ng of plasmid DNA, 10 µL of single-stranded carrier DNA (Yeastmaker Carrier DNA, Clontech) and 700 µL of PEG mix and incubated 30 min at RT. Cells were heat shocked for 15 min at 42 °C, pelleted at 3000 rpm and resuspended in 300 µL YPD. Cells were incubated in YPD for 30 min at 30 °C and spread on the appropriate selection plate

with sterile glass beads. The selection plates were incubated for 2-3 days before successfully transformed colonies were picked and restreaked on selective media.

2.2.3 Genomic DNA extraction from *S. cerevisiae*

Genomic DNA was extracted from *S. cerevisiae* using the Puregene Yeast/Bact. Kit B from Qiagen. DNA sample concentrations were measured with the nanodrop ND-1000 Spectrophotometer.

2.2.4 Spotting assay

Yeast cells were incubated overnight at 30 °C in appropriate medium. The cultures were diluted to OD_{600} 0.5 and spotted in ten-fold serial dilutions. 5 µL of each dilution were spotted. The plates were incubated at 30 °C for 3 days and imaged using the LAS4000 (Fujifilm) after 2 and 3 days of incubation.

2.2.5 Yeast protein extraction, SDS-PAGE and western blotting

Appropriate amounts of exponentially growing cells were harvested by centrifugation of culture volumes corresponding to 2 OD_{600} units (13000 rpm for 2 min at RT). Cell pellets were stored at -20 °C if necessary. Cells were resuspended in 150 µL of Solution 1 (0.97 M β-mercaptoethanol, 1.8 M NaOH) and incubated on ice for 10 min before 150 µL of Solution 2 (50 % TCA) were added and cells were again incubated 10 min on ice. Cells were pelleted (13000 rpm for 2 min at 4 °C) and subsequently resuspended in 1 mL acetone. The samples were centrifuged again (13000 rpm for 2 min at 4 °C) and the pellets resuspended in 100 µL urea buffer (120 mM Tris-HCl pH 6.8, 5 % glycerol, 8 M urea, 143 mM 2-mercaptoethanol, 8 % SDS, bromophenol blue indicator). Protein extracts were incubated 5 min at 55 °C and centrifuged (8000 rpm for 30 sec at RT) before they were loaded onto Mini-PROTEAN Precast Gels (BioRad) (7.5 % for detection of Rad53, 4-15 % gradient gels for detection of Mrc1-TAP, Actin and Pgk1). The following antibodies were used: Rad53 (EL7.E1, gift from Marco Foiani) at 1:16, Mrc1-TAP (Sigma Aldrich P1291) at 1:200, Actin (Merck Millipore MAB1501) at 1:1000, Pgk1 (Life technologies, 22C5D8) at 1:25000. Proteins were detected using the Super Signal West Pico Chemiluminescent Substrate (Thermo Scientific) and the LAS4000 (Fujifilm).

2.2.6 Analysis of DNA content by Fluorescence-Activated Cell Sorting (FACS)

In order to collect appropriate amounts of exponentially growing cells, 0.68 OD_{600} units of cell cultures were spun down (3000 rpm for 5 min at RT). Cell pellets were resuspended in 1 mL cold 70 % ethanol and stored at 4 C. Prior to an RNase A treatment (3 h at 37 °C with 10 µL of 10 mg/mL RNase A) cells were washed in 1 mL H_2O (3000 rpm for 5 min at RT) and resuspended in 0.5 mL 50 mM Tris-HCl (pH 8.0). Following the RNase A treatment cells were collected by centrifugation (3000 rpm for 5 min at RT), resuspended in 0.5 mL 50 mM Tris-HCl (pH 7.5) containing 1 mg/mL Proteinase K and incubated for 45 min at 50 °C. After centrifugation (3000 rpm for 5 min at RT) cells were resuspended in 0.5 mL 50 mM Tris-HCl (pH 7.5). 100 µL of cells were used for sonication (five consecutive rounds of sonication, 15 sec each, using the Bioruptor Twin XD10 set to low intensity). 50 µL of cells were mixed with 1 mL of 1 x SYTOX Green (Life Technologies) in 50 mM Tris-HCl (pH 7.5) to stain DNA. Cells were kept dark and the DNA content was analysed immediately using a BD FACSCanto II flow cytometer with the following filters and settings: FSC and SSC were detected with a 488 nm laser with detector settings of 318 V and 360 V, respectively. SYTOX Green was detected with a 502 nm longpass filter and 530/30 nm bandpass filter at 466 V. 20000 events per sample were analysed in each run. BD FACSDiva software was used for data collection and FlowJo v10.0.6 (Miltenyi Biotec) software was used for data analysis.

2.2.7 MMS-induced checkpoint arrest and recovery experiment

20 mL of exponentially growing yeast cells (*bar1* MATa) at OD600 0.6 were arrested in G1 with α-factor (2 µM final concentration) for 2.5 h. To verify efficient arrest shmooing of the cultures was checked using an Optech Technology light microscope. Cells were washed in 40 mL YPD pre-warmed at 30°C (3000 rpm for 2 min at 25 °C). Cells were resuspended in 25 mL of pre-warmed YPD and samples were taken for OD measurement, protein extraction and FACS. Cultures were incubated with MMS (final concentration of 0.01 %) at 30 °C shaking (230 rpm) for 60 min. Cells were collected by centrifugation (3000 rpm for 2 min at 25 °C) and resuspended in 6 mL pre-warmed YPD containing sodium thiosulfate (2.5 % w/v final concentration) to quench MMS. Cells were collected by centrifugation (3000 rpm for 2 min at 25 °C) and resuspended in an appropriate volume of pre-warmed YPD to keep cells in

exponential phase for the following 60 min (OD_{600} ~ 0.8). Samples were taken for OD measurement, protein extraction and FACS.
At four more time points spaced at 60 min intervals samples were taken for OD measurement, protein extraction and FACS during recovery from MMS-induced checkpoint arrest. At each time point the volume of each culture was adjusted with pre-warmed YPD to ensure continued growth in exponential phase.

2.2.8 Protein stability measurement by cyclohexamide chase during recovery from MMS-induced checkpoint arrest

The experiment was performed as described above with the following modifications: After α-factor arrest cells were released into prewarmed YPD containing MMS at a final concentration of 0.03 % and incubated for 45 min. After MMS quenching and wash-out cyclohexamide (CHX) was added to each culture to a final concentration of 200 µg/mL to inhibit protein biosynthesis. After CHX addition samples for protein extraction were taken every 30 min.

2.2.9 Senescence assay

Spore colonies of freshly dissected heterozygous diploids were diluted in 5 mL YPD to a final concentration of OD_{600} 0.01. Cells were incubated for 24 h at 30 °C and the optical density of each culture was measured at 600 nm. Cultures were then re-diluted to OD_{600} 0.01 and incubated for further 24 h at 30 °C. The remaining culture was pelleted and pellets were frozen at -20 °C for further analysis (telomere PCR and Southern blotting). Senescence curves are displayed as the average relative cell density plotted against the average population doublings of all cultures of the same genotype. Population doublings (PD) were calculated as $\log2 (OD_{600}^{24h}/0.01)$. PD values refer to population doublings after the spore had grown on the dissection plate for 2-3 days depending on the growth rate, which corresponds to about 25 population doublings. The relative cell density was calculated by arbitrarily setting the OD_{600} of day 1 to 100 % for each culture. Graphs were made using GraphPad Prism Version 5.0d. Differences in the mean values of relative cell densities of different genotypes were tested for statistical significance using the Mann Whitney test. The test was carried out in GraphPad Prism Version 5.0d. One star indicates a p-value ≤ 0.05, two stars indicate a p-value ≤ 0.01 and three stars indicate a p-value ≤ 0.001.

2.2.10 Telomere length measurement by telomere PCR

Telomere PCR was performed using 100 ng of genomic DNA (Puregene Yeast/Bact. Kit B, Qiagen) in 9 µL 1 x NEB4 buffer. Samples were denatured for 10 min at 96 °C and cooled to 4 °C using the Thermal Cycler (Bio-Rad). For the C-tailing reaction 1 µL of 10 x tailing mix (40 U/µL terminal transferase in 10 x NEB4 buffer and 10 mM dCTPs) was added and samples were incubated for 30 min at 37 °C, 10 min at 65 °C, 5 min at 96 °C before they were cooled to 65 °C. 30 µL of preheated PCR-Mix containing 1 µM oligo dG reverse primer, 1 µM telomere-specific forward primer, 0.267 mM dNTPs, 0.083 U/µL Phusion polymerase (NEB) in PCR buffer (89.11 mM Tris-HCl pH 8.8, 21.28 mM $(NH_4)_2SO_4$, 6.65 % glycerol, 0.0133 % Tween-20) were added and the PCR reaction performed using the following protocol: 3 min at 95 °C, 45 cycles (30 s at 95 °C, 15 s at 63 °C, 20 s at 72 °C), 5 min at 72 °C, hold on 12 °C. Samples were separated on a 1.8 % agarose gel containing 0.005 % RedSafe at 100 V for 25 min. Bands were detected using the LAS4000 (Fujifilm) and telomere length analysed using the Multi Gauge Software (Fujifilm).

2.2.11 Telomere length measurement by Southern blot analysis of terminal restriction fragment lengths

Genomic DNA was extracted from cell pellets (Puregene Yeast/Bact. Kit B, Qiagen), which had been collected during the course of the senescence assay as described above. 20 µg of genomic DNA were digested with 2 µL of XhoI restriction enzyme at 37 °C overnight in a final volume of 50 µL. 2 µL of each digested sample were separated on a 1.2 % agarose gel containing 0.005 % RedSafe at 100 V for 30 min and bands were quantified using ImageJ. 15 µg of digested DNA were loaded onto a 1.2 % agarose gel containing 0.005 % RedSafe and run at 100 V for 15 min and at 25 V overnight. An image of the gel was taken using the LAS4000 (Fujifilm). The DNA was transferred onto a positively charged nylon membrane at 1 Amp for 2 h in 0.5 x TBE at 4 °C. The membrane was rinsed in 2 x SSC before the DNA was crosslinked to the membrane using the UV Stratalinker 2400. The DNA was then denatured by washing the membrane in denaturing solution for 1 h followed by two 10 min washes in neutralizing solution. Following, the membrane was incubated with pre-warmed hybridization solution at 47.5 °C for 1 h. 7.5 µL of DIG labelled probe (oBL207) diluted in 5 mL hybridization solution were denatured at 95 °C for 5 min and

subsequently cooled on ice. For hybridization the membrane was incubated with the denatured, diluted probe at 47.5 °C overnight. Detection was performed as described by the product guidelines of the Roche DIG oligonucleotide 3'-End labelling KIT using the LAS4000 for chemiluminescence detection.

2.2.12 Telomere cloning and sequencing

Telomere cloning and sequencing was carried out as reported in (Chang, Dittmar et al. 2011). QIAquick PCR Purification Kit (Qiagen) was used to purify telomere PCR products. The purified DNA was cloned into a pCR4Blunt-TOPO vector using the Zero Blunt TOPO PCR Cloning Kit for Sequencing, which was used to transform One Shot DH5αTM-T1 E. coli cells. DNA from transformed clones was isolated using the DirectPrep 96 MiniPrep Kit (Qiagen) and analysed with Sequencher software.

2.2.13 Chromatin immunoprecipitation (ChIP)

Crosslinking: Cells were grown to exponential phase at 30 °C in YPD and diluted to OD_{600} 0.74 in 50 mL YPD. Crosslinking was performed by the addition of formaldehyde to a final concentration of 1.2 % for 10 min at RT to the shaking cultures. The crosslinking reaction was quenched by the addition of glycine to a final concentration of 360 mM while cultures were shaking for 5 more minutes at RT. The cells were then put on ice for 5 min, pelleted and washed twice in cold PBS by spinning for 4 min at 3000 rpm at 4 °C. Cell pellets were stored at -80 °C.

Cell lysis: Cells were resuspended in 200 µL cold FA lysis buffer - SOD and lysed at 4 °C in lysing Matrix C tubes using the FastPrep machine at 6.5 M/s for two times 30 sec with 1 min on ice between runs. Cell extracts were recovered by the addition of 800 µL FA Lysis buffer + SOD and pelleted by centrifugation at 13000 rpm for 7 min at 4 °C in fresh Eppendorf tubes. The soluble portion of the lysate was discarded and pellets were resuspended in 1.5 mL FA Lysis buffer + SOD containing 0.26 % SDS and split into three 500 µL for sonication.

Sonication: Chromatin was sheared at 4 °C using the Bioruptor Twin XD10 in 13 cycles with each cycle consisting of 30 sec shearing at high intensity followed by a 30 sec break. Samples were centrifuged for 15 min at 15000 rpm at 4 °C. The supernatant is referred to as the ChIP extract. Protein concentration of the ChIP extract was determined by Bradford assay and the ChIP extract diluted to a protein concentration of 1 mg/mL. To verify the sonication efficiency 100 µL of ChIP extract

were incubated overnight at 65 °C and treated with 7.5 µL of Proteinase K for 2 h at 37 °C. The DNA was purified with QIAquick PCR purification Kit (Qiagen), treated with RNase A solution (Quiagen) for 30 min at 37 °C and analysed by gel electrophoresis on a 1.5 % agarose gel. Efficient sonication results in a bulk fragment size between 100 and 500 bp.

Preclearing and IP: Two times 1 mL of the diluted ChIP extract of each sample was pre-cleared by the addition of 20 µL of protein A sepharose beads for 1 h at 4 °C. The beads had previously been washed with 1 x PBS, incubated with 1 x BSA for 1 h at 4 °C, washed again in 1 x PBS and resuspended in 1 x FA lysis buffer + SOD. After the pre-clearing step RNA-DNA hybrids were precipitated by incubating the samples overnight at 4 °C rotating with 35 µl of 1 x PBS-washed protein A sepharose beads in the presence or absence of a mouse monoclonal S9.6 antibody at a final concentration of 32 µg/mL.

Washes and Elution: The beads were then successively washed in FA lysis buffer + SOD, in FA lysis buffer 500, in 1 x FA buffer III and in 1 x TE (pH 8.0). Each washing step was carried out in 1 mL of liquid at 4 °C rotating for 5 min followed by centrifugation at 3000 rpm for 2 min at 4 °C. The supernatant was removed and the precipitated DNA was eluted from the beads by the addition of 100 µL of Elution buffer B for 8 min at 65 °C. The elution step was repeated with the same volume of elution buffer and the final volume of 200 µL was stored at -80 °C.

Reverse crosslinking and purification: The samples were incubated at 65 °C overnight with 7.5 µL of Proteinase K for protein digestion. The remaining DNA was cleaned with the QIAquick PCR Purification Kit, eluted in 50 µL of water and stored at -20°C.

Quantification by qPCR: Telomeric RNA-DNA hybrid levels were measured by qPCR using the LightCycler480 and the DyNAmo Flash SYBR Green qPCR Kit using the following protocol (10 min at 95 °C for denaturing followed by 40 cycles of 15 sec at 95 °C, 1 min at 60 °C). The final primer concentrations were: 1L (1 µM), 15L (100 nM), Y' (300 nM) and rDNA (500 nM). The input values in percent were calculated as $100*2^{[\text{adjusted input - Ct (IP)}]}$. The adjusted input was calculated as Ct (input) - $\log_2(20)$ to account for the fact that the input fraction is 5 % (dilution factor of 20, which corresponds to $\log_2(20) = 4.322$ cycles).

3 Results

3.1 The ubiquitin E3 ligase Rtt101 affects the replication stress response through Mrc1/Claspin

3.1.1 A genetic screen for mutations suppressing the *rtt101* drug sensitivity reveals potential targets of Rtt101-assembled ubiquitin E3 ligase complexes

In order to identify novel targets of Rtt101, which are ubiquitinated in the response to DNA damage or the ensuing replication stress, we used a genetic approach. We reasoned that in the absence of Rtt101 a variety of its targets would accumulate in their de-ubiquitinated form causing a disturbed or deregulated DNA damage response (DDR) that leads to the striking hypersensitivity of *rtt101* cells to genotoxic agents. Thus, combined deletion of *RTT101* and the gene encoding the potential target protein might relieve the *rtt101* drug sensitivity (Figure 6B). Therefore, we designed a screen, pairwise combining the deletion of *RTT101* with the deletion of about 4800 non-essential genes in *Saccharomyces cerevisiae* and testing the resulting double mutants for growth on MMS and CPT. As described in section 2.2.1 (above), MMS and CPT cause replication stress that ultimately leads to DSBs and other DNA lesions: Synthetic Genetic Array (SGA) methodology was used (Tong, Evangelista et al. 2001) to cross the *rtt101* mutation to a non-essential knockout collection (kindly provided by M. Knop). The resulting haploid double mutants were pinned onto SD plates containing either 0.01 % MMS or 5 µM CPT (Figure 6C and D). The occurrence of suppressors, *i.e.* double mutants that showed increased resistance to either MMS or CPT, was scored manually using pictures of the plates taken after appropriate incubation time. For a more detailed description of the drug sensitivity screen the reader is referred to the "Materials and Methods" section.

Validation by manually crossing and dissecting tetrads from independent starter strains followed by duplicate spot assays onto drug containing media confirmed 16 of 24 candidates yielded by the screen to be true suppressor mutations of *rtt101* drug sensitivity (Figure 6F).

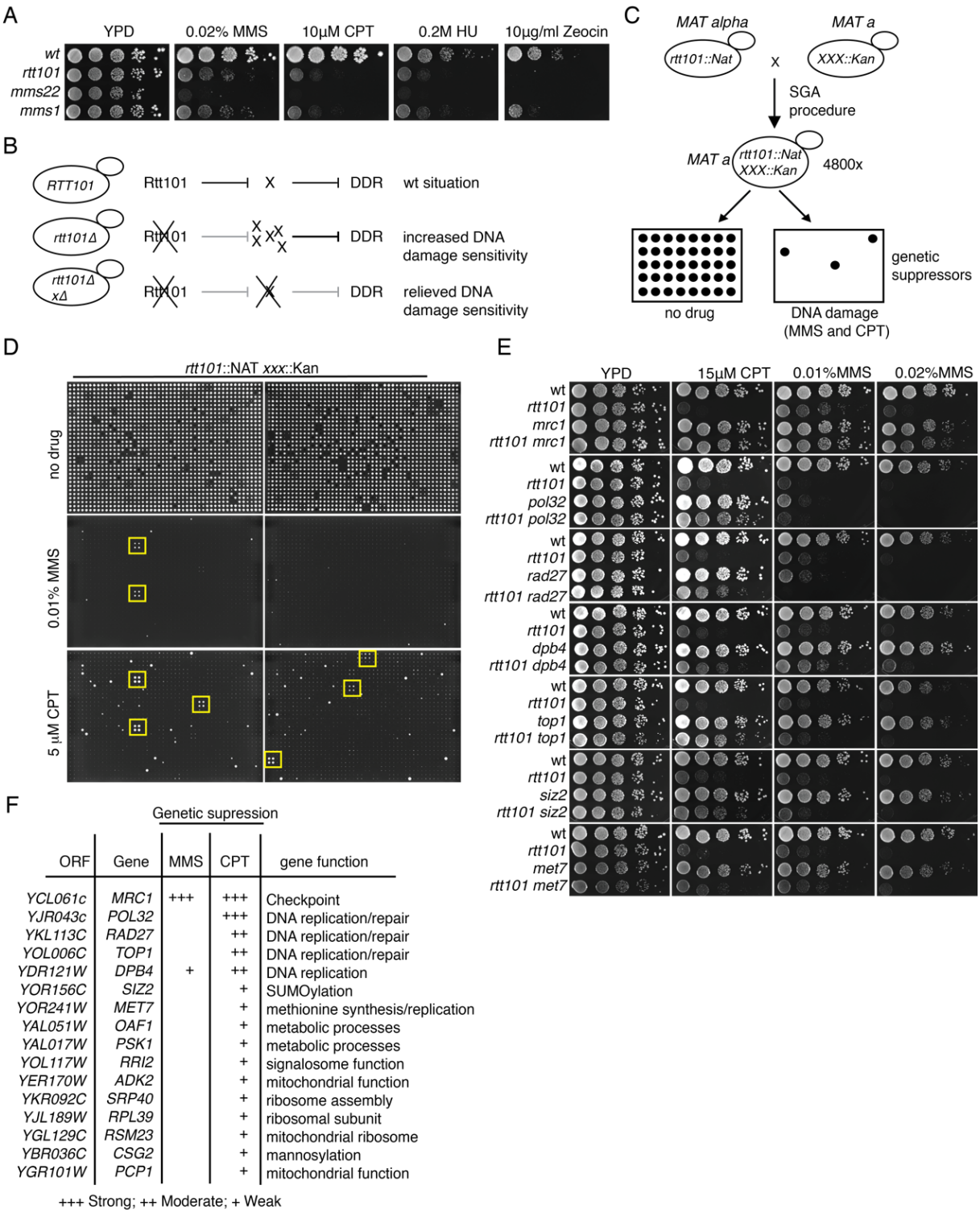

F

Genetic supression

ORF	Gene	MMS	CPT	gene function
YCL061c	MRC1	+++	+++	Checkpoint
YJR043c	POL32		+++	DNA replication/repair
YKL113C	RAD27		++	DNA replication/repair
YOL006C	TOP1		++	DNA replication/repair
YDR121W	DPB4	+	++	DNA replication
YOR156C	SIZ2		+	SUMOylation
YOR241W	MET7		+	methionine synthesis/replication
YAL051W	OAF1		+	metabolic processes
YAL017W	PSK1		+	metabolic processes
YOL117W	RRI2		+	signalosome function
YER170W	ADK2		+	mitochondrial function
YKR092C	SRP40		+	ribosome assembly
YJL189W	RPL39		+	ribosomal subunit
YGL129C	RSM23		+	mitochondrial ribosome
YBR036C	CSG2		+	mannosylation
YGR101W	PCP1		+	mitochondrial function

+++ Strong; ++ Moderate; + Weak

Figure 6 Screen for suppressors of *rtt101* hypersensitivity to MMS and CPT (A) *rtt101*, *mms1* and *mms22* cells are hypersensitive to MMS, CPT, HU and Zeocin (B) Rationale of screen design: combined deletion of *RTT101* and a potential target, whose accumulation inhibits DDR, might relieve *rtt101* drug sensitivity (C) Simplified schematic view of SGA procedure (D) Representative examples of pinning plates (E) Confirmation spottings of seven out of 16 confirmed suppressors (F) List of the 16 confirmed suppressors. Screen and spottings were performed by Martina Dees.

In our further analysis we concentrated on those genes that (i) showed strong or intermediate suppression of *rtt101* drug sensitivity or (ii) had previously been implicated in replication or repair (Figure 6E). These genes encoded the following proteins:

The S-phase checkpoint and replication protein Mrc1, the DNA polymerase δ subunit Pol32, the 5' flap endonuclease Rad27, Topoisomerase I (Top1), the DNA polymerase ε subunit Dpb4, the SUMO E3 ligase Siz2 and the Folylpolyglutamate synthetase Met7.

It is conceivable that the different suppressor proteins affect a number of different pathways required to cope with DNA damage or replicative stress. Nevertheless, it is noteworthy that both Mrc1 and Dpb4 are connected to the leading strand polymerase Pol ε and their deletion was able to relieve the growth defect of *rtt101* cells on both MMS and CPT, with the deletion of *MRC1* resulting in the most striking effect. Deletion of *POL32*, *RAD27* and *TOP1* conferred resistance to CPT only.

The results of the screen suggest that Mrc1, Pol32, Rad27, Top1, Dpb4, Siz2 and Met7 are potential targets of Rtt101-assembled ubiquitin E3 ligase complexes and that their accumulation in the de-ubiquitinated form impairs a proper DDR or replication stress response, either because their destruction by the ubiquitin-proteasome system or alteration of their function by ubiquitination is necessary to allow the appropriate cellular reaction to lesions caused by MMS and CPT.

3.1.2 Rtt101' s function in response to MMS and CPT relies almost fully on Mms1 and Mms22

Rtt101 has been shown to assemble a variety of protein complexes (Collins, Miller et al. 2007, Zaidi, Rabut et al. 2008, Han, Li et al. 2010, Mimura, Yamaguchi et al. 2010, Han, Zhang et al. 2013). The C-terminus of Rtt101 recruits the E2 ubiquitin-conjugating enzyme Cdc34 via the bridging protein Hrt1 (Michel, McCarville et al. 2003). The N-terminus of Rtt101 binds Mms1, which resembles human DDB1 and recruits a number of substrate specific adaptor proteins either directly or via the bridging factor Mms22 (Zaidi, Rabut et al. 2008, Mimura, Yamaguchi et al. 2010). It has, however, also been suggested that Rtt101 can bind at least one of its substrates, Spt16, a member of the FACT complex, in the absence of both Mms1 and Mms22 (Han, Li et al. 2010).

	MMS	CPT	HU	Zeocin
wt	+++	+++	+++	+++
rtt101	+	+	++	++
mrc1	+++	+++	+	++
rtt101 mrc1	+++	+++	+	++
pol32	++	+++	-	++
rtt101 pol32	+	+++	-	++
rad27	+	+++	++	-/+++
rtt101 rad27	-	++	++	++/-
top1	+++	+++	+/++	++
rtt101 top1	++/+	++	++/+	-/++
dpb4	+++	+++	++	++
rtt101 dpb4	++	++	+	++
siz2	+++	+++	+++	+++
rtt101 siz2	+	++	+	++
met7	+++	+++	++/+	-
rtt101 met7	++	++	++/+	-
mms1	+	+	++	++
mrc1	+++	+++	-	++
mms1 mrc1	++	+++	-	++
pol32	++	+++	-	++
mms1 pol32	-	++	-	+/++
rad27	+	+++	+++	-
mms1 rad27	-	++	++	-
top1	+++	+++	+++	+/+++
mms1 top1	++	+++	+++/+	++/-
dpb4	+++	+++	+++	+++
mms1 dpb4	++	++	++	+
siz2	+++	+++	+++	+++
mms1 siz2	+	++	++	++
mms22	+	+	+	+
mrc1	+++	+++	+++	+++
mms22 mrc1	++	++	++	++
pol32	+++	+++	++	+++
mms22 pol32	-	++	-	-
rad27	++	++	++	++
mms22 rad27	-	+	-	-
top1	+++	+++	+++	+++
mms22 top1	+	++	+	+
dpb4	+++	+++	+++	+++
mms22 dpb4	+	++	+	+
siz2	+++	+++	+++	+++
mms22 siz2	+	++	+	+

	MMS	CPT	HU	Zeocin
wt	+++	+++	+++	+++
ctf4	+	+	+	+
mrc1				
ctf4 mrc1				
pol32	++	+++	+	++
ctf4 pol32	-	+	-	-
rad27				
ctf4 rad27				
top1	+++	+++	+++	+++
ctf4 top1	++	+++	+	+
dpb4	+++	+++	+++	+++
ctf4 dpb4	+	++	+	+
siz2	+++	+++	+++	+++
ctf4 siz2	+	++	+	++/+
esc2	++	+++	+++	++
mrc1	+++			++
esc2 mrc1	+++			++
pol32	++			++
esc2 pol32	++			-
rad27	+/-			+/-
esc2 rad27	-/+			+/++
top1	+++			++
esc2 top1	++			++
dpb4	+++			++
esc2 dpb4	++			++
siz2	+++			+++
esc2 siz2	+			++

+++	wt growth
++	sensitive
+	very sensitive
-	dead
	not spotted since double mutant not viable
	not spotted since *esc2* single mutant not sensitive to the drug
	negative synthetic effect: double mutant grows worse than either of the single mutants
	no synthetic effect on drug sensitivity
	positive synthetic effect: double mutant grows better than the more sensitive of single mutants
	inconclusive: either no synthetic effect or negative synthetic effect
	inconclusive: either no synthetic effect or positive synthetic effect
	inconclusive: either positive synthetic effect or negative synthetic effect
	inconclusive for other reasons

Table 1 Overview of the effect of selected suppressor mutations on the sensitivity of *rtt101*, *mms1*, *mms22*, *ctf4* and *esc2* cells to MMS, CPT, HU and Zeocin

Therefore we wanted to explore whether those mutations able to suppress the drug sensitivity of *rtt101* cells were also able to suppress the drug sensitivity of *mms1* and *mms22* cells.

Like *rtt101* cells, both *mms1* and *mms22* are hypersensitive to MMS and CPT (Figure 6A). While the hypersensitivities of *mms1* and *rtt101* to MMS and CPT seems to be identical, *mms22* shows more severe sensitivity to MMS and CPT than *rtt101* (Figure 6A). Hypersensitivity of *mms1* and *mms22* cells to both MMS and CPT are epistatic with that of *rtt101* (Zaidi, Rabut et al. 2008). This suggests that Rtt101's role

in the response to DNA damage is shared by Mms1, and that Mms22's role in the DDR partially overlaps with, but also exceeds that of Rtt101.

The suppressor mutations alleviating *rtt101* drug sensitivity to MMS and CPT also alleviated *mms1* and *mms22* drug sensitivity, with two exceptions: the deletion of *RAD27* did not reduce the hypersensitivity of *mms22* cells to CPT and deletion of *DPB4* only slightly reduced the hypersensitivity of *mms22* cells to MMS. *MET7* was excluded from the analysis because the *met7* strain showed extremely variable growth on YPD. The results of the spotting assays are summarized in Table 1. For the original spotting assays the reader is referred to Supplemental Figure 1 to 5.

The results of these spottings suggest that the functions of Rtt101 in response to lesions induced by MMS and CPT rely fully on the presence of Mms1 and in most instances also on Mms22, while also comprising elements independent of Mms22. In the presence of the genotoxic agents MMS and CPT, Mrc1, Pol32, Rad27, Dpb4 and Siz2 seem to cause toxic intermediates, whose abrogation in the majority of cases requires the concerted action of Rtt101, Mms1 and Mms22.

3.1.3 Mutations alleviating *rtt101* drug sensitivity to MMS and CPT are specific and do not alleviate *rtt101* drug sensitivity to HU or Zeocin

Next, we wanted to determine whether the suppressor mutations identified in our screen also relieved drug sensitivity of *rtt101*, *mms1* and *mms22* cells to HU and Zeocin (Table 1). None of the suppressor mutations was able to increase the resistance of *rtt101, mms1* or *mms22* cells to either HU or Zeocin with the exception of the deletion of *MRC1*, which relieved the hypersensitivity of *mms22* cells to both HU and Zeocin.

Hypersensitivity of *rtt101* and *mms1* cells is particularly severe for lesions induced by MMS and CPT, indicating that Rtt101 and Mms1 contribute substantially to the cellular response to these lesions. By contrast, hypersensitivity of *rtt101* and *mms1* to HU is mild, suggesting that the cellular response to HU relies on mechanisms different from those required in response to MMS and CPT. Thus, it is not surprising that the mutations alleviating *rtt101* and *mms1* drug sensitivity to MMS and CPT are specific and do not alleviate *rtt101* and *mms1* drug sensitivity to HU or Zeocin.

The role of Mms22 in response to DNA damage and replication stress seems to be more general than that of Rtt101 and Mms1 and intimately connected to Mrc1. Hypersensitivity of *mms22* cells to MMS, CPT, HU and Zeocin exceeds that of *rtt101*

and *mms1* cells and is alleviated by *MRC1* deletion for all four drugs. This is in agreement with other studies in yeast and human cells suggesting that Mms22 promotes HR-dependent repair processes independent of Rtt101^{Mms1}, which might contribute to damage repair or fork restart (Baldwin, Berger et al. 2005, Duro, Lundin et al. 2010, O'Donnell, Panier et al. 2010).

Some of our spottings on HU and Zeocin were inconclusive due to varying results or inappropriate drug concentrations. For these cases, it is at this moment not possible to evaluate the effect of the double deletion mutant concludingly.

3.1.4 *ctf4* and *esc2* cells both show major differences and commonalities compared to *rtt101* cells in terms of their drug sensitivity and its suppression

Telomere shortening is a particular type of DNA damage that elicits a response that in many ways resembles that induced by genomic lesions (reviewed in (Dewar and Lydall 2012)). Interestingly, Rtt101 seems to contribute to the maintenance of both shortening telomeres during senescence (Chang, Lawless et al. 2011)(and S. Luke-Glaser personal communication) and telomeric chromatin of wt length telomeres (Mimura, Yamaguchi et al. 2010).

Esc2 is a protein implicated in replication-associated recombination, sister chromatid cohesion and silencing. Ctf4 is part of the replisome and also required for sister chromatid cohesion. Esc2 and Ctf4 have been reported to interact with Rtt101 via Mms1 or via Mms1 and Mms22 respectively (Mimura, Yamaguchi et al. 2010) and share the premature senescence observed in *rtt101* cells (this study, Figure 14). This could indicate that they also share or contribute to Rtt101's role in response to MMS- and CPT-induced lesions. In this case we would expect that the suppressors of *rtt101* drug sensitivity also alleviate drug sensitivity of *esc2* and *ctf4*. The results of our spottings are summarized in Table 1. The original spottings are shown in Supplemental Figure 4 and Supplemental Figure 5.

ctf4 cells show both major differences and commonalities compared to *rtt101* cells in terms of their drug sensitivity and its suppression. *rtt101* cells show severe hypersensitivity to MMS and CPT and mild hypersensitivity to HU and Zeocin. *ctf4* cells are highly sensitive to all four genotoxic agents. Deletion of *TOP1*, *DPB4* and *SIZ2* alleviated the sensitivity of *rtt101* and *ctf4* cells to CPT, indicating that Ctf4 might act in concert with Rtt101, e. g by recruiting the common suppressors for

subsequent ubiquitination. Interestingly, the deletion of *MRC1*, which results in the most striking alleviation of *rtt101* sensitivity to both MMS and CPT, results in synthetic lethality of *ctf4* cells. This result has been published before (Tong, Lesage et al. 2004). The double mutant is inviable due to replication defects that cause permanent checkpoint activation and prevent successful genome duplication (Gambus, van Deursen et al. 2009). A recent study by Luciano and colleagues (Luciano, Dehé et al. 2015) sheds light on the relationship between Ctf4, Mrc1 and an Rtt101-comprising pathway during replicative stress. They show that the deletion of either *CTF4* or *MRC1* is beneficial for CPT-treated *asf1* cells. Since Rtt101 acts downstream of the histone chaperone Asf1 they speculate that Ctf4 and Mrc1 might be targets of Rtt101. This is in agreement with our results and will be discussed in more detail in section 4.2 (Discussion).

esc2 cells are mildly hypersensitive only to MMS and Zeocin. Thus, Esc2 does not seem to be a member of the Rtt101-based complexes assembled in response to CPT and HU. Nevertheless, Esc2 might contribute to the recruitment of Mrc1 and Dpb4 since deletion of these proteins alleviated the hypersensitivity of both *esc2* and *rtt101* cells to MMS (Table 1).

Thus our spottings give clear indications, which of the Rtt101-mediated pathways in response to DNA damage might rely on Ctf4 or Esc2. Further experiments are necessary to test the suggested interactions.

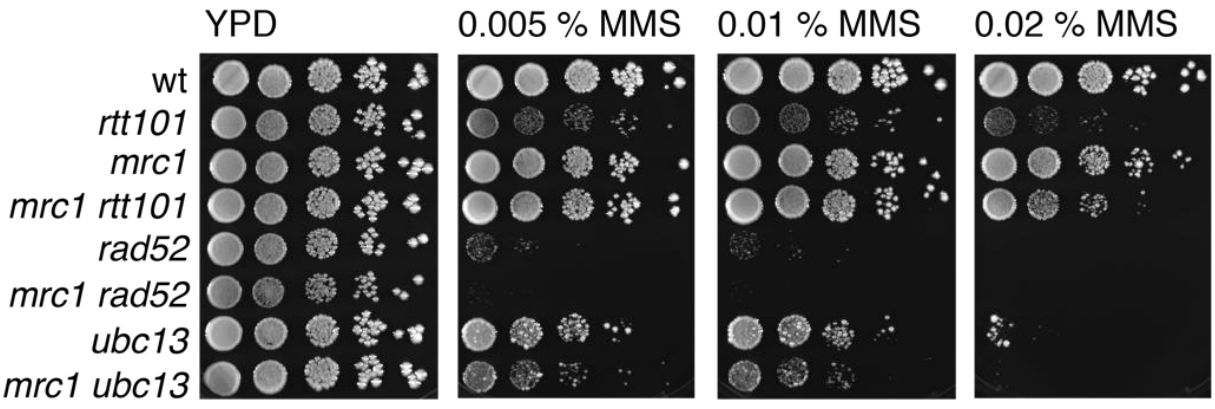

Figure 7 Suppression of drug sensitivity by *MRC1* deletion is specific to the Rtt101-mediated pathway of the DDR: *MRC1* deletion does not rescue the sensitivity of *ubc13* cells to MMS. Spottings were performed by Martina Dees.

3.1.5 The suppression of MMS hypersensitivity by *MRC1* deletion is specific to the Rtt101-mediated pathway of the DDR

Having explored the effects of a selection of suppressors of *rtt101* drug sensitivity on putative Rtt101 complex members, we set out to uncover the mechanistic details of the suppression of *rtt101* drug sensitivity by the deletion of *MRC1* since it conferred the most striking effect on both MMS and CPT.

Mrc1 is a mediator of the replication checkpoint and activates Rad53 in response to replication stress (Alcasabas, Osborn et al. 2001, Tanaka and Russell 2001). It also forms part of the replisome and is required for normal replication progression (Szyjka, Viggiani et al. 2005, Tourriere, Versini et al. 2005, Hodgson, Calzada et al. 2007), in particular due to its role in coupling the CMG helicase to Polε (Lou, Komata et al. 2008, Komata, Bando et al. 2009). Together with Tof1 and Csm3, Mrc1 forms a replication fork pausing complex that stabilizes the replication fork during replication stress (Katou, Kanoh et al. 2003).

The DNA methylating agent MMS and the Topoisomerase I inhibitor CPT create replication obstacles, which cause fork stalling that can lead to the formation of DSBs (Pommier 2006, Wyatt and Pittman 2006) We wondered whether the alleviation of drug sensitivity by the deletion of *MRC1* was indeed specific to cells sensitized to DNA damage by the deletion of *RTT101*, or whether other MMS hypersensitive mutants were also rescued.

Ubc13 is an E2 ubiquitin-conjugating enzyme involved in post-replicative repair (Brusky, Zhu et al. 2000), whose deletion sensitizes cells to MMS. It forms a heteromeric complex with Mms2 and interacts physically with the chromatin-associated RING-finger proteins Rad18 and Rad6. Our spottings in Figure 7 show that MMS sensitivity of *ubc13* cells is not reduced but slightly aggravated by *MRC1* deletion.

Rad52 is the pivotal protein of the *S. cerevisiae* recombination machinery. It promotes the exchange of the abundant ssDNA binding protein RPA for the Rad51 recombinase and catalyses the DNA annealing step in recombination processes (Mortensen, Lisby et al. 2009). Since many repair pathways rely on recombinational processes *rad52* cells are particularly sensitive to a wide range of DNA damaging agents including MMS. MRC1 deletion aggravates the hypersensitivity of *rad52* cells to MMS (Figure 7).

These results indicate that deletion of MRC1 does not generally relieve hypersensitivity to MMS for example by a generally dampened checkpoint response that could allow a variety of DNA repair deficient mutants to continue cell cycle progression despite unrepaired lesions. Instead, the alleviation of hypersensitivity to MMS by *MRC1* deletion seems to be characteristic for those genome maintenance mechanisms that rely on Rtt101.

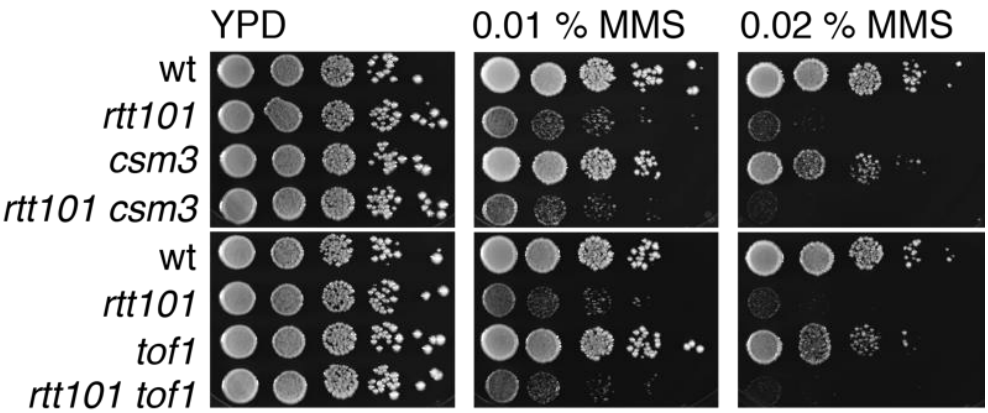

Figure 8 Deletions of CSM3 of TOF1 do not alleviate drug sensitivity of *rtt101* cells. Spottings were performed by Martina Dees.

3.1.6 Deletions of CSM3 or TOF1 do not alleviate drug sensitivity of *rtt101* cells

Mrc1, Csm3 and Tof1 form a heterotrimeric complex that associates with replication forks and is required for normal replication fork progression. It stabilizes stalled forks and promotes sister chromatid cohesion repair after DNA damage (Katou, Kanoh et al. 2003, Bando, Katou et al. 2009). Like Mrc1, Tof1 contributes to Rad53 phosphorylation in response to replication stress, albeit to a lesser extent (Foss 2001). Since Mrc1's functions partially overlap with those of Tof1 and Csm3 we asked whether their deletion might also impact on the drug sensitivity of *rtt101* cells. This is not the case as our spottings in Figure 8 show.

Our results point to a unique function of Mrc1. This could be Mrc1's role in signalling replication stress, its crucial role in replisome stabilization and coupling, the unique combination of these two or a so far uncharacterized function of Mrc1.

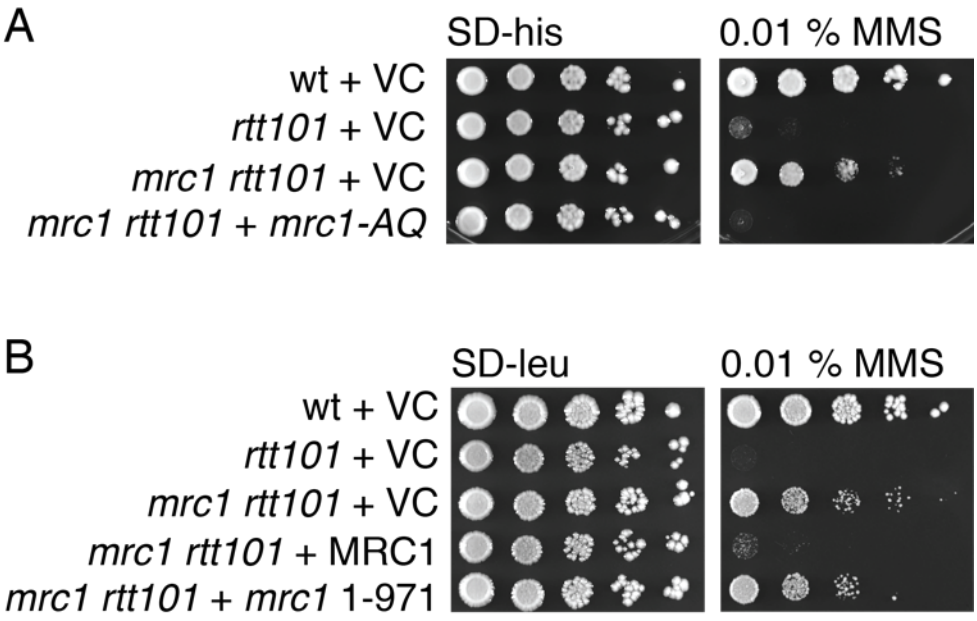

Figure 9 Loss of Mrc1 checkpoint function is not sufficient for the suppression of *rtt101* drug sensitivity (A) The Mrc1-AQ mutant is unable to relieve the hypersensitivity of *rtt101* cells to MMS. (B) The $Mrc1_{1\text{-}971}$ alleviates the hypersensitivity of *rtt101* cells to MMS. Spottings were performed by Martina Dees.

3.1.7 Loss of Mrc1 checkpoint function is not sufficient for the suppression of *rtt101* drug sensitivity

Two separation-of-function alleles of Mrc1 have been described and characterized in detail: the *mrc1-AQ* allele and the $mrc1_{1\text{-}971}$ allele. Both have been described as checkpoint-defective and replication-proficient (Osborn and Elledge 2003, Fong, Arumugam et al. 2013). In order to gain a better understanding of the mechanism underlying the suppression of *rtt101* drug sensitivity by *MRC1* deletion we analysed the effect of both alleles on the MMS sensitivity of *rtt101* cells.

The Mrc1-AQ mutant, in which all Mec1-targeted S/TQ phosphosites are mutated to AQ, was unable to relieve the hypersensitivity of *rtt101* cells to MMS (Figure 9A). Surprisingly, the $Mrc1_{1\text{-}971}$ mutant, which lacks the last 125 amino acids, did indeed phenocopy the alleviation of drug sensitivity, which was seen with the full deletion of Mrc1 (Figure 9B). These results clearly indicate that the loss of Mrc1's checkpoint function is not sufficient to rescue *rtt101* drug sensitivity. Instead, our experiments suggest that Mrc1's C-terminus is toxic for cells under replicative stress lacking Rtt101.

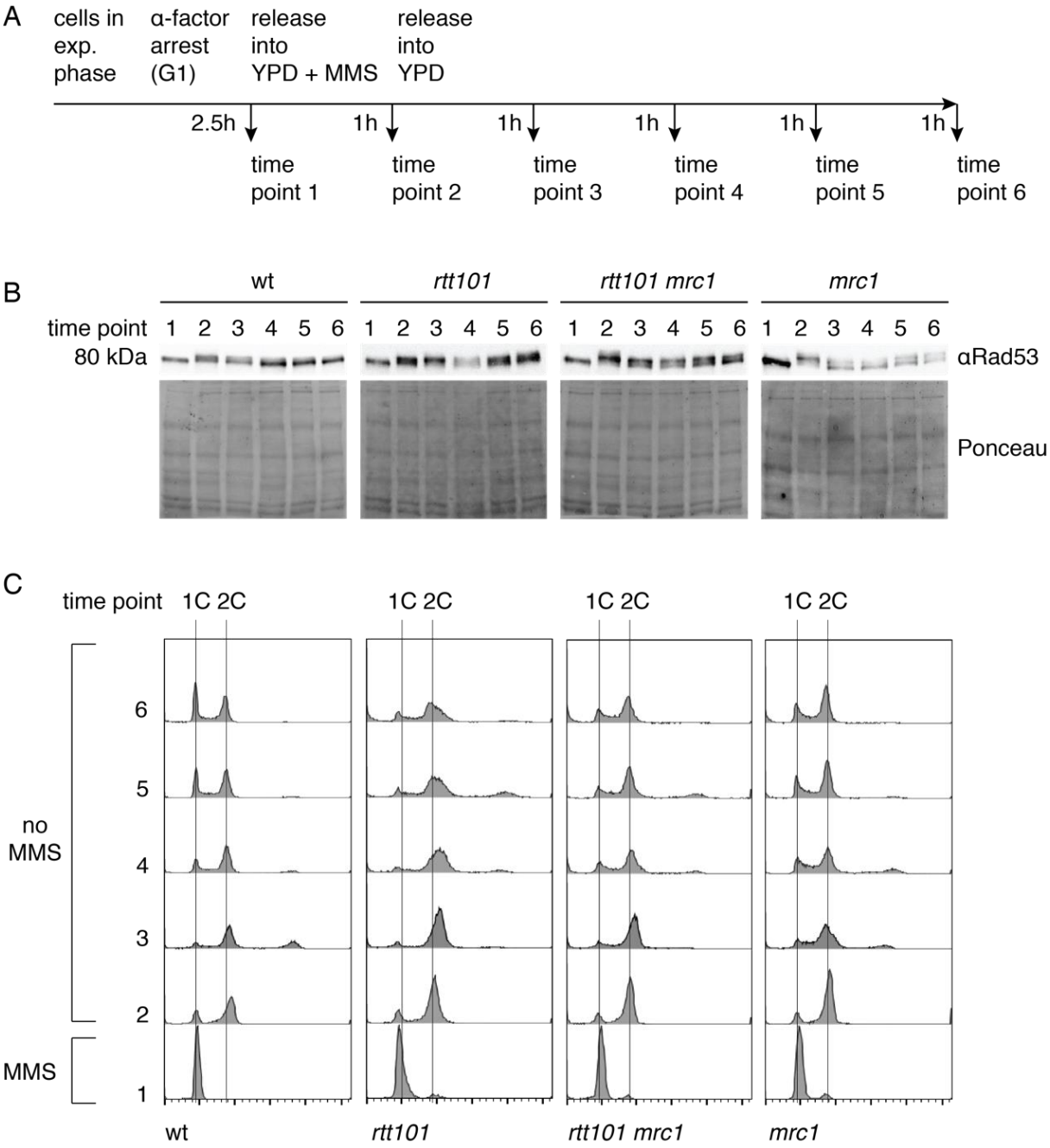

Figure 10 *MRC1* deletion allows timely checkpoint downregulation during recovery from MMS-induced damage. (A) Schematic overview of the experiment: cells in exp. phase were arrested in G1 by the addition of α-factor (2 µM final concentration). Arrested cells were released into YPD containing 0.01 % MMS and released into YPD after 1 h for recovery. At the indicated points in time samples were taken for protein extraction and FACS (B) Western blots with anti Rad53 antibody for the indicated genotypes. In all strains *BAR1* was deleted for efficient α -factor arrest. As reported previously *rtt101* cells show prolonged checkpoint activation as measured by the upshift of the Rad53 band due to Rad53 phosphorylation. *MRC1* deletion allows *rtt101* cells to downregulate their checkpoint during recovery from MMS-induced damage. (C) FACS profiles show that *rtt101 mrc1* cells re-enter the cell cycle in a manner comparable to *mrc1* cells.

Mrc1 interacts directly with Pol2 via two independent binding sites situated in Mrc1's N- and C-terminal domain respectively (Lou, Komata et al. 2008). The *mrc1*$_{1-971}$ mutant strain goes through S-phase normally in unchallenged conditions (Fong, Arumugam et al. 2013). Our results allow the conclusion that Mrc1's C-terminal interaction with Pol2 might be specifically counteracted by Rtt101 in the face of DNA damage-induced replicative stress.

3.1.8 MRC1 deletion allows timely checkpoint downregulation during recovery from MMS-induced damage

One of several phenotypes described for *rtt101* cells is their prolonged checkpoint activation in response to treatment with MMS (Luke, Versini et al. 2006). Prolonged checkpoint activation could be due (i) to a defective checkpoint downregulation after termination of cellular repair activities or (ii) to prolonged persistence of damage due to a defective damage response.

We decided to test the effect of combined deletion of *RTT101* and *MRC1* on the checkpoint activation during recovery from MMS treatment by monitoring the phosphorylation status of Rad53. Therefore, cells were synchronised by the addition of α-factor, released into MMS and allowed to recover from MMS treatment for four hours (Figure 10A).

Deletion of MRC1 did indeed allow *rtt101* cells to dephosphorylate Rad53 in a manner comparable to wt after release from MMS-induced stress (Figure 10B). FACS profiles showed that *rtt101 mrc1* cells were also able to re-enter the cell cycle more efficiently than *rtt101* cells and in a manner comparable to *mrc1* cells, though less efficiently than wt (Figure 10C).

Interestingly, in our experiment *mrc1* cells activated and deactivated the checkpoint with kinetics similar to wt cells. This is in agreement with the fact that the deletion of MRC1 did not alleviate the MMS hypersensitivity of *ubc13* cells, since both results indicate that lack of Mrc1 does not generally hamper the checkpoint activation in response to MMS.

However, our result does not exclude the possibility that checkpoint downregulation following recovery from MMS-induced damage is defective in *rtt101* cells due to the prolonged persistence of Mrc1. Indeed, it has been shown that degradation of Mrc1 is required for checkpoint deactivation during recovery from MMS-induced damage. Mrc1 degradation partially depends on SCF^{Dia2}, a ubiquitin E3 ligase complex

assembled by the cullin Cdc53 (Mimura, Komata et al. 2009, Fong, Arumugam et al. 2013). Therefore, we decided to test if Rtt101 contributes to Mrc1 degradation.

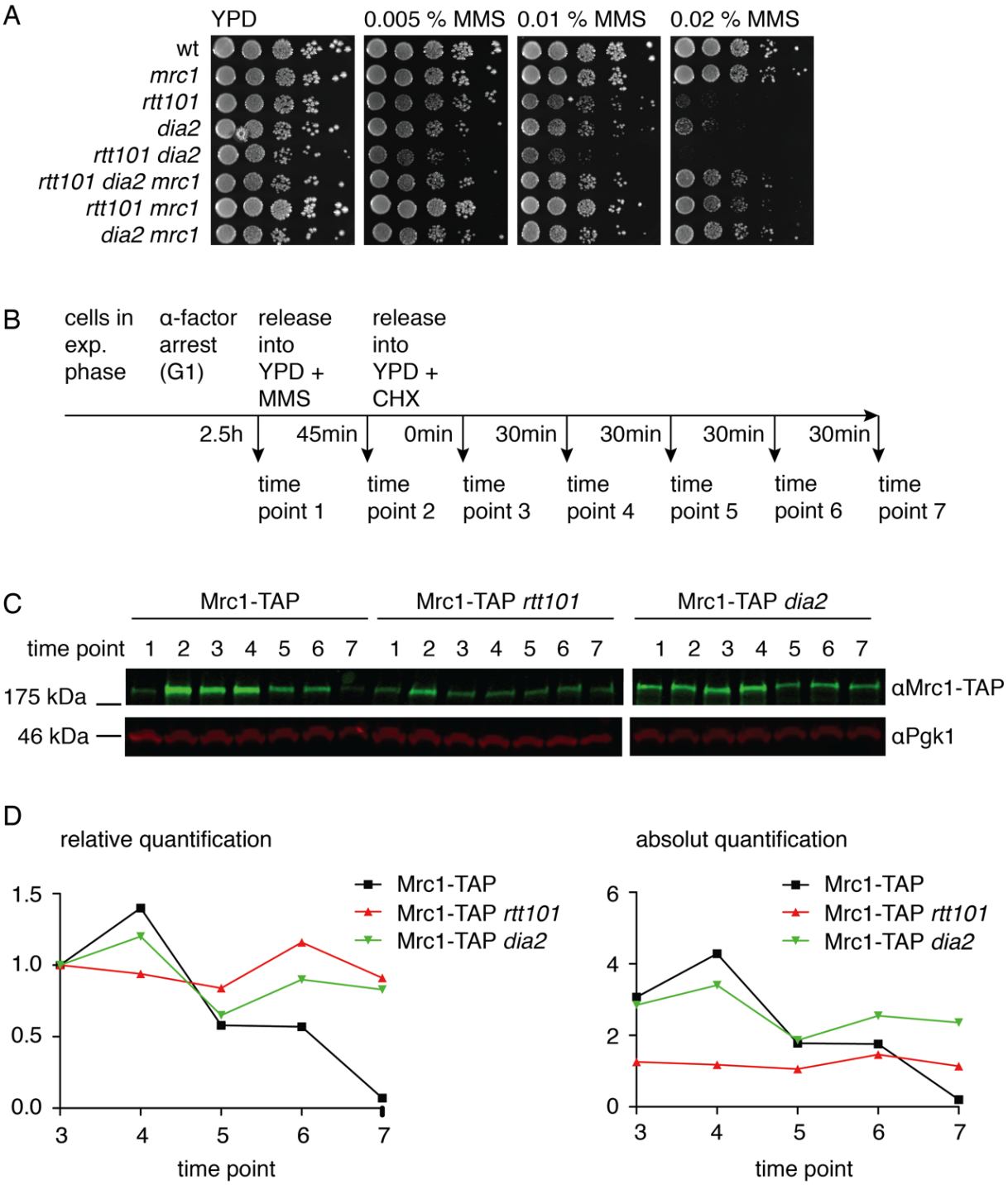

Figure 11 Rtt101 and Dia2 contribute to recovery from MMS-induced damage through Mrc1 by two independent pathways. (A) Combined deletion of *RTT101* and *DIA2* leads to additive sensitivity to MMS. Hypersensitivity of both single mutants and the double mutant can be rescued by the deletion of *MRC1*. Spottings were performed by Vanessa Kellner (B) Schematic overview of the cycloheximide chase experiment to determine the stability of Mrc1 during recovery from MMS-induced DNA damage. Cells in exponential phase were arrested in G1 by the addition of α-factor (2 µM final concentration). Arrested cells were released into

YPD containing 0.03 % MMS. After 45 min cells were released into YPD containing cycloheximide to inhibit protein synthesis during recovery from MMS. Samples for protein extraction were taken at the indicated time points. (C) Western blots with anti-TAP antibody for the indicated genotypes. In all strains *BAR1* was deleted for efficient α-factor arrest. Pgk1 serves as a loading control. (D) Quantification of western blot signals in (C): As reported previously, Mrc1 is degraded in wt cells during recovery from MMS and Mrc1 degradation depends partially on Dia2. Mrc1 is stabilized in *rtt101* cells but absolute Mrc1 levels are lower than in wt. Western blots and their quantification were performed by Martina Dees.

3.1.9 Rtt101 and SCF^{Dia2} contribute to the recovery from MMS-induced damage through Mrc1 by two different pathways

In order to explore whether Rtt101 mediates the degradation of Mrc1 to allow cell cycle resumption after MMS-induced stress in a pathway parallel to SCF^{Dia2} we tested the sensitivity of *rtt101*, *dia2* and *rtt101 dia2* cells to MMS. Combined deletion of *RTT101* and *DIA2* did indeed lead to additive sensitivity to MMS. The hypersensitivity of both single mutants and the double mutant could be rescued by MRC1 deletion (Figure 11A).

To test the effect of *RTT101* deletion on the stability of Mrc1 during recovery from MMS-induced damage cells were synchronised by the addition of α-factor, released into MMS and allowed to recover from MMS treatment in the presence of cyclohexamide for two hours (Figure 11B). As reported by Fong and colleagues, Mrc1 is degraded in wt cells, but stabilized in the absence of Dia2. In *rtt101* cells Mrc1 also seems to be stabilized. However, the absolute quantification of Mrc1 protein levels showed that Mrc1 levels are extremely low in the absence of Rtt101, rendering a role of Rtt101 in Mrc1 degradation unlikely (Figure 11C and D). Since the results of this experiment were variable, *MRC1* was placed under the control of a Gal-inducible promoter. Promoter shut-off experiments carried out by Vanessa Kellner could reproducibly show that Rtt101 does not affect Mrc1 degradation rates (data not shown but published in Buser, Kellner et al. 2016, see appendix 7.2).

The results of the checkpoint recovery experiments described in Figure 10 and Figure 11 indicate that both Rtt101 and Dia2 contribute to the resumption of cell cycle progression after MMS-induced damage through Mrc1. Dia2 contributes to the dephosphorylation of Rad53 by Mrc1 degradation. Accordingly, hypersensitivity of *dia2* cells to MMS is rescued by *MRC1* deletion as well as by both checkpoint defective *mrc1* alleles, *mrc1-AQ* and $mrc1_{1\text{-}971}$ (Fong, Arumugam et al. 2013).

Prolonged checkpoint activation of *rtt101* cells in response to MMS is rescued by MRC1 deletion. Hypersensitivity of *rtt101* cells to MMS is rescued by *MRC1* deletion

and by the *mrc1*$_{1-971}$ allele, but not by the *mrc1-AQ* allele. This indicates that the prolonged Rad53 phosphorylation is due to prolonged persistence of damage rather than to a defective checkpoint downregulation after successful repair.

This is in agreement with the fact that *rtt101* cells show increased levels of Rad52 foci, which likely reflect repair activities (Luke, Versini et al. 2006). *rtt101*, *mms1* and *mms22* cells have also been reported to be deficient in Rad52-dependent repair mechanisms involved in the repair of MMS-induced damage and stalled RFs in both fission and budding yeast (Baldwin, Berger et al. 2005, Duro, Vaisica et al. 2008, Vejrup-Hansen, Mizuno et al. 2011). Therefore we decided to investigate the role of Rad52 for *rtt101* drug sensitivity and its suppression by *MRC1* deletion.

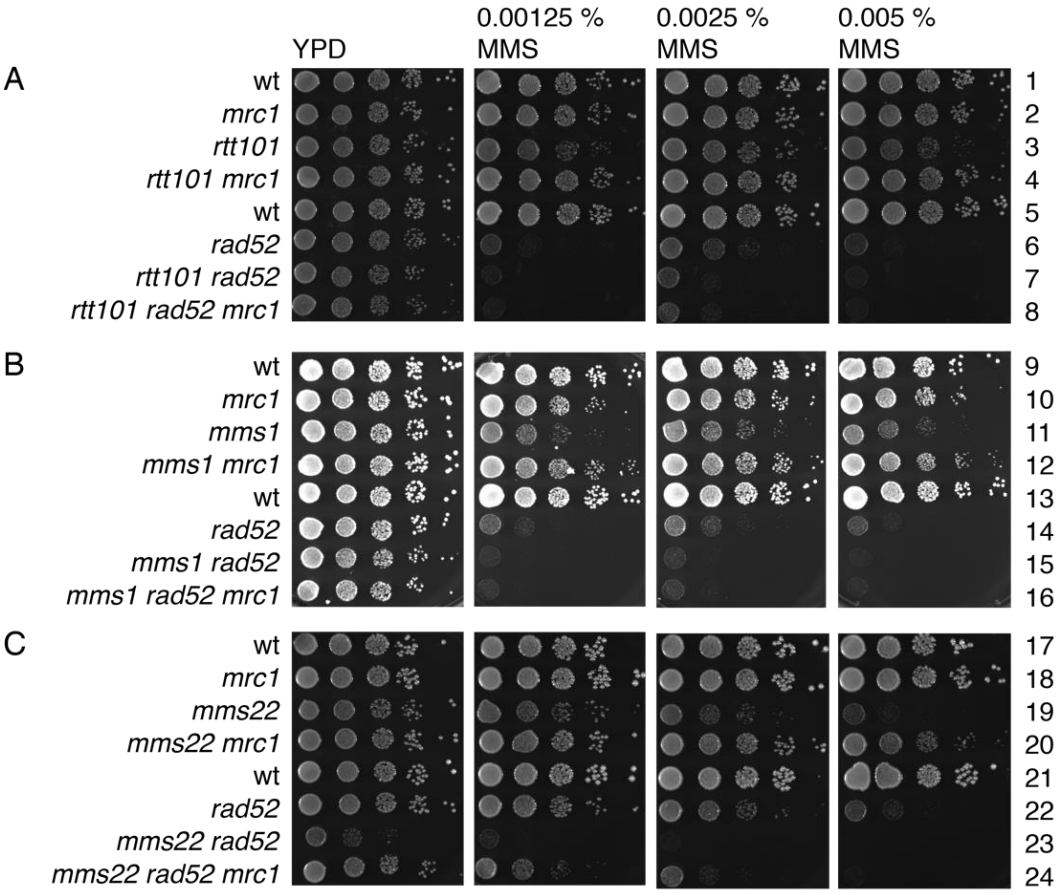

Figure 12 For *rtt101* and *mms1* cells the suppression of hypersensitivity to MMS by *MRC1* deletion depends on the presence of a Rad52. Spottings were performed by Vanessa Kellner.

3.1.10 The suppression of *rtt101* hypersensitivity to MMS by the deletion of *MRC1* depends on a functional recombination machinery

The Rad52 protein is central to virtually all homologous recombination pathways in *S. cerevisiae*. It promotes the exchange of RPA for Rad51 recombinase at ssDNA and catalyses the DNA annealing step in recombination processes (Mortensen, Lisby et al. 2009). Our spottings show that the suppression of *rtt101* MMS hypersensitivity by *MRC1* deletion depends on the presence of *RAD52* (Figure 12A compare lines 6, 7 and 8 of the plate containing 0.0025 % MMS). This is also true for *mms1* cells (Figure 12B compare lines 14, 15 and 16 of the plate containing 0.0025 % MMS). Interestingly, *mms22* cells are still rescued to a certain degree by *MRC1* deletion in the absence of Rad52 (Figure 12C compare lines 22, 23 and 24 of the plate containing 0.00125 % MMS). This means that the rescue of *mms22* cells by *MRC1* deletion is partially independent of HR processes.

We conclude that the $Rtt101^{Mms1Mms22}$ ubiquitin E3 ligase promotes the repair or restart of stalled RFs by a Rad52-dependent mechanism, which probably requires prior ubiquitination of Mrc1 (or an unknown factor regulating Mrc1) by the $Rtt101^{Mms1Mms22}$ complex. Whether Mrc1 is degraded as a result of this process cannot be concluded at the moment. While our results suggest that Mrc1 stability is not affected by Rtt101, proteolysis of Mrc1 might take place at a small subset of stalled replication forks that is not reflected in global Mrc1 levels.

In the absence of Mms22, MRC1 deletion leads to a partial rescue of MMS sensitivity even without a functional HR machinery. This indicates that Mms22 also promotes HR-independent pathways in response to genotoxic stress. This function of Mms22 seems to be independent of Rtt101. Notwithstanding, both the HR-dependent and -independent mechanisms appear to proceed only in the absence of the fork protection protein Mrc1 or require its prior modification.

3.2 The ubiquitin E3 ligase Rtt101 affects replicative senescence through Mrc1/Claspin

3.2.1 Rtt101, Mms1 and Mms22 promote the viability of cells in the presence of short telomeres

The ends of linear chromosomes resemble DSBs and must therefore be protected from the DNA damage response. Telomeres are nucleoprotein structures that protect and maintain chromosome ends. Telomere shortening due to the absence of telomerase leads to a gradual loss of the protective properties of telomeres. Interestingly, Rtt101 is not just required for the proper cellular response to several forms of DNA damage as induced by MMS and CPT, which lead to replication stress. Cells lacking Rtt101 also show accelerated senescence ((Chang, Lawless et al. 2011) and S. Luke-Glaser, personal communication), suggesting that Rtt101 promotes viability of cells in the presence of short telomeres, which represent a DNA damage-like structure. Having explored some aspects of Rtt101's role during replication stress induced by DNA damage, we decided to investigate Rtt101's role in replicative senescence.

Despite the fact that wt yeast cells do not senesce, *S. cerevisiae* has been used for several decades as a valuable model organism to study replicative senescence (reviewed in (Teixeira 2013)). The *EST2* gene encodes the catalytic subunit of the telomerase reverse transcriptase. *TLC1* encodes the telomerase RNA moiety that serves as a template for telomere elongation. Deletion of either of these two genes leads to replicative senescence of budding yeast cells.

As shown in Figure 13, *rtt101 est2* cells senesced faster than *est2* cells. While the viability of *rtt101 est2* cells was identical to the viability of *est2* cells for about 40 population doublings (PDs), *rtt101 est2* cells showed a dramatic loss of viability approximately during population doublings 40 to 70 and a particularly severe crisis (compare the lowest viabilities of *rtt101 est2* and *est2* cells). *rtt101 est2* cells then formed survivors with kinetics and viability similar to *est2* cells.

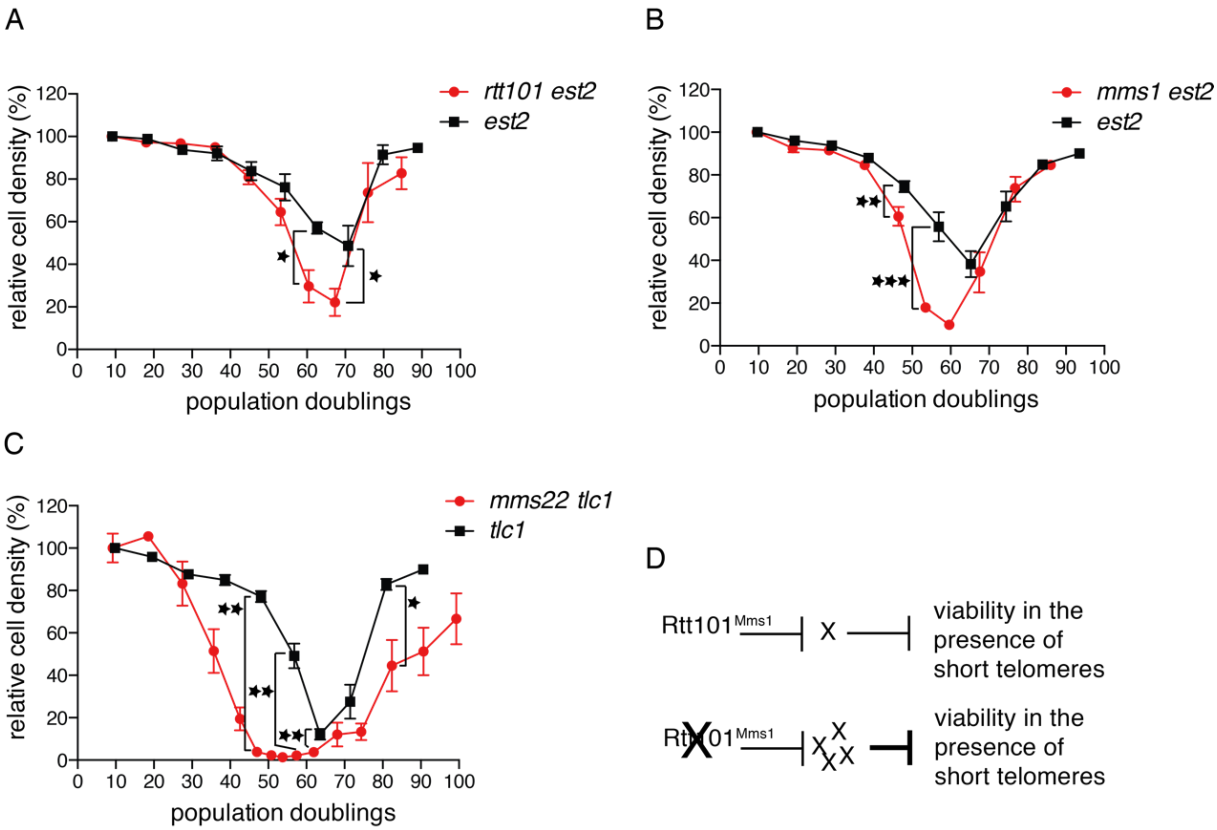

Figure 13 *rtt101 est2*, *mms1 est2* and *mms22 tlc1* cells senesce prematurely. (A-C) Senescence curves showing the accelerated senescence of *rtt101 est2*, *mms1 est2* and *mms22 tlc1* cells compared to *est2* and *tlc1* cells respectively. Each dot represents the mean of n cultures, with n = 6 for *rtt101 est2* and *mms22 tlc1* and n = 10 for *mms1 est2*. Error bars represent s.e.m. Statistical testing was performed using the Mann-Whitney test. p-values of $p \leq 0.05$, $p \leq 0.01$ and $p \leq 0.001$ are represented by one, two and three stars respectively. (D) Simple model of the role of Rtt101 during replicative senescence.

This could indicate that the action of Rtt101 is required particularly when telomeres become critically short and most resemble DNA damage, while Rtt101 seems to be dispensable during early population doublings and for survivor formation.

Rtt101 serves as a platform for the assembly of multi-subunit ubiquitin E3 ligase complexes. The recruitment of target proteins seems to depend on the presence of Mms1 in most cases. Mms1 recruits a variety of substrate specific adaptor proteins either directly of via the bridging factor Mms22 (Collins, Miller et al. 2007, Zaidi, Rabut et al. 2008, Han, Li et al. 2010, Mimura, Yamaguchi et al. 2010, Han, Zhang et al. 2013).

We wandered whether Mms1 and Mms22 shared the premature senescence phenotype just described for *rtt101 est2* cells with the aim of identifying the complex members involved in the Rtt101-dependent pathway required to prevent premature senescence. The senescence curve in Figure 13B shows that the senescence of

mms1 est2 cells resembles that of *rtt101 est2* cells strikingly: *mms1 est2* cells senesced at the same rate as *est2* cells during early population doublings, then underwent a dramatic loss of viability and severe crisis before forming survivors with kinetics and viability similar to *est2* cells.

Since the genomic loci of the *MMS22* and the *EST2* genes are located right next to each other it was not possible to retrieve the *mms22 est2* double mutant by tetrad dissection. Therefore we made use of the *mms22 tlc1* mutant. In comparison to *rtt101 est2*, the premature senescence phenotype of *mms22 tlc1* cells started at earlier population doublings and survivor formation was slower than in *tlc1* control cells (Figure 13C).

We conclude that Mms1 is most likely part of the Rtt101-assembled ubiquitin E3 ligase complex that is active during replicative senescence. Just like in the case of DNA damage sensitivity, the phenotype of *mms22* cells is more severe than that of *rtt101* cells during senescence. Thus Mms22 might well be a member of the Rtt101 complex during senescence, but its functions clearly exceed those of Rtt101. Epistasis analysis by comparing replicative senescence of *rtt101 mms22 tlc1* cells to *rtt101 tlc1* cells and *mms22 tlc1* cells within the same senescence curve was unsuccessful (data not shown).

3.2.2 The two putative substrate-specific adaptors Esc2 and Ctf4 senesce prematurely

The DNA repair and replication stress response protein Rtt107, the replication-associated repair protein Esc2, the replisome member Ctf4, the subunit of the origin recognition complex ORC5 and the regulator of RNR gene transcription and DDR protein Crt10 have been identified as putative members of Rtt101-assembled complexes and could function as substrate specific adaptors recruiting substrates that remain to be determined. Their interaction with Rtt101 depends on the presence of Mms1 and in the case of Rtt107 and Ctf4 also on the presence of Mms22 as linker proteins bridging the interaction to Rtt101 as shown in Figure 5A (Zaidi, Rabut et al. 2008, Mimura, Yamaguchi et al. 2010). We wandered, which of these proteins shared the premature senescence phenotype of *rtt101 est2* cells and performed the corresponding senescence curves.

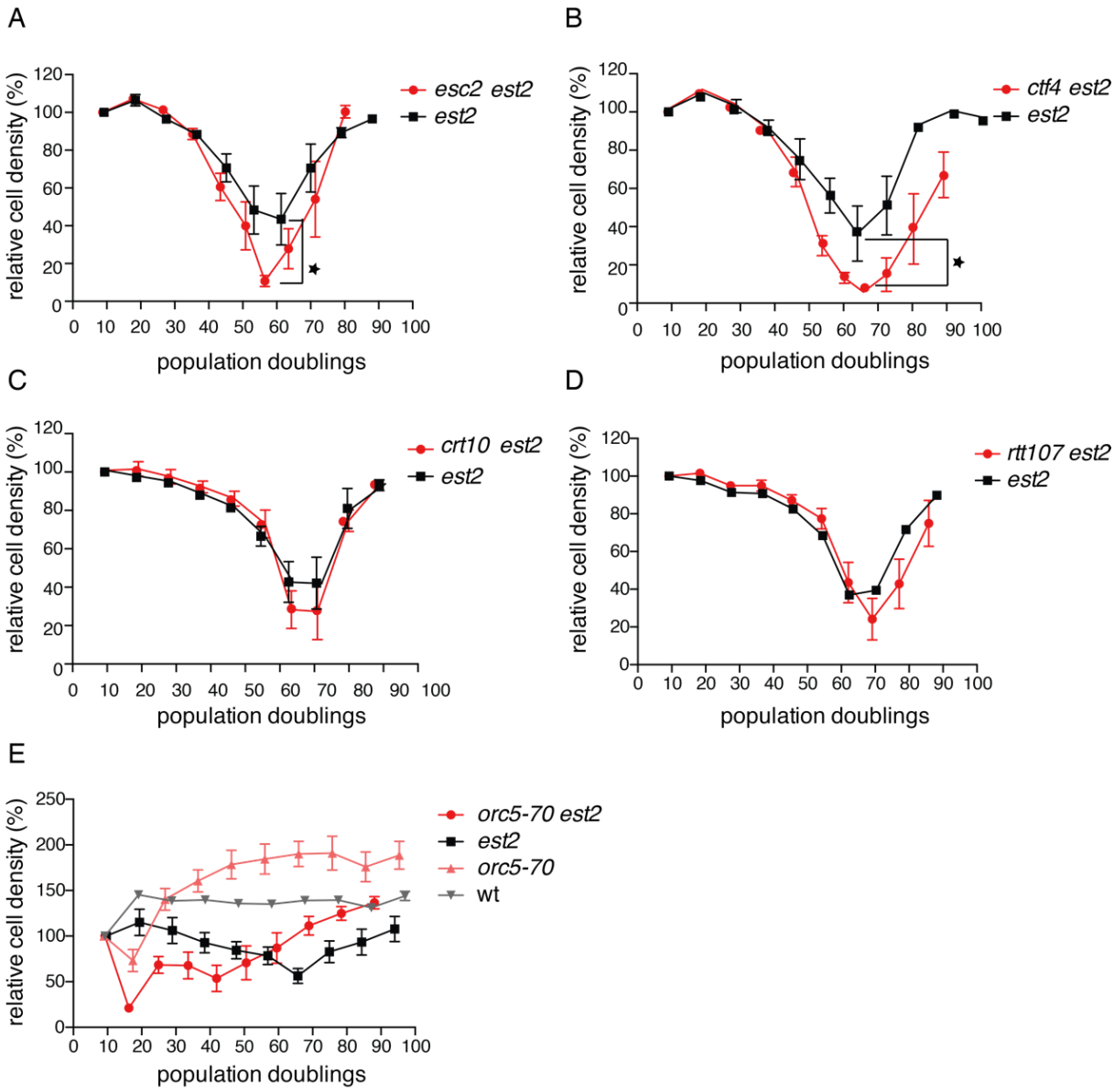

Figure 14 Two out of five putative members of Rtt101-assembled complexes share the premature senescence phenotype of *rtt101* cells. (A-E) Senescence curves for *esc2 est2*, *ctf4 est2*, *crt10 est2, rtt107 est2* and *orc5-70 est2* cells respectively compared to *est2* cells. Each dot represents the mean of n cultures, with n = 5 or n = 4 for all senescence curves displayed in this figure. Error bars represent s.e.m. Statistical testing was performed using the Mann-Whitney test. p-values of $p \leq 0.05$, $p \leq 0.01$ and $p \leq 0.001$ are represented by one, two and three stars respectively.

As the results displayed in Figure 14 show, only *esc2 est2* and *ctf4 est2* cells showed premature or aggravated senescence compared to *est2* cells. Small differences between *crt10 est2* and *rtt107 est2* cells and their respective controls are not significant as assessed by the Mann-Whitney test.

ORC5 is an essential gene. Therefore, the temperature sensitive *orc5-70* allele was used in the senescence curve and *orc5-70* and wt cells from the same dissection were included as controls. The curve was performed at the semipermissive

temperature of 30 °C. The interpretation of the *orc5-70* curve is complicated by the fact that the temperature sensitive strains *orc5-70 est2* and *orc5-70* showed a severe loss of viability at about 15 PDs and subsequently adapted to the semipermissive temperature. Nevertheless, the curve shows that *orc5-70 est2* cells do senesce faster than *est2* cells but the phenotype does not resemble the one shown by *rtt101 est2* cells.

We conclude that Esc2 and Ctf4 are potential members of Rtt101-assembled complexes that might be necessary to promote cell viability in the presence of short telomeres.

3.2.3 Bulk telomere length of *rtt101 est2* cells does not differ from bulk telomere length of *est2* cells during replicative senescence

Replicative senescence as seen in the *est2* or *tlc1* mutants is due to cell cycle arrest caused by shortening telomeres, which elicit the checkpoint response (Ijpma and Greider 2003, Abdallah, Luciano et al. 2009). The premature senescence of *rtt101 est2* cells could be the result of an increased rate of telomere shortening. We therefore analysed telomere length of three different *rtt101 est2* clones and their corresponding *est2* mutants originating from the same tetrad using the genomic DNA of days 1, 3, 5, and 7 of the senescence curve shown in Figure 13A. Telomere length analysis by telomere PCR and by Southern blot of terminal restriction fragments are shown in Figure 15(A-C) and reveal that bulk telomere length of *rtt101 est2* cells did not differ from bulk telomere length of *est2* cells during senescence.

Survivors maintain their telomeres by recombinational processes that lead to very heterogeneous telomere length, which results in a telomeric signal smeared through the whole lane of a Southern blot as seen in Figure 15D. Telomere length analysis of genomic DNA from day 10 (corresponding to 86 PDs approximately) of the senescence curve showed no difference between *rtt101 est2* and *est2* cells.

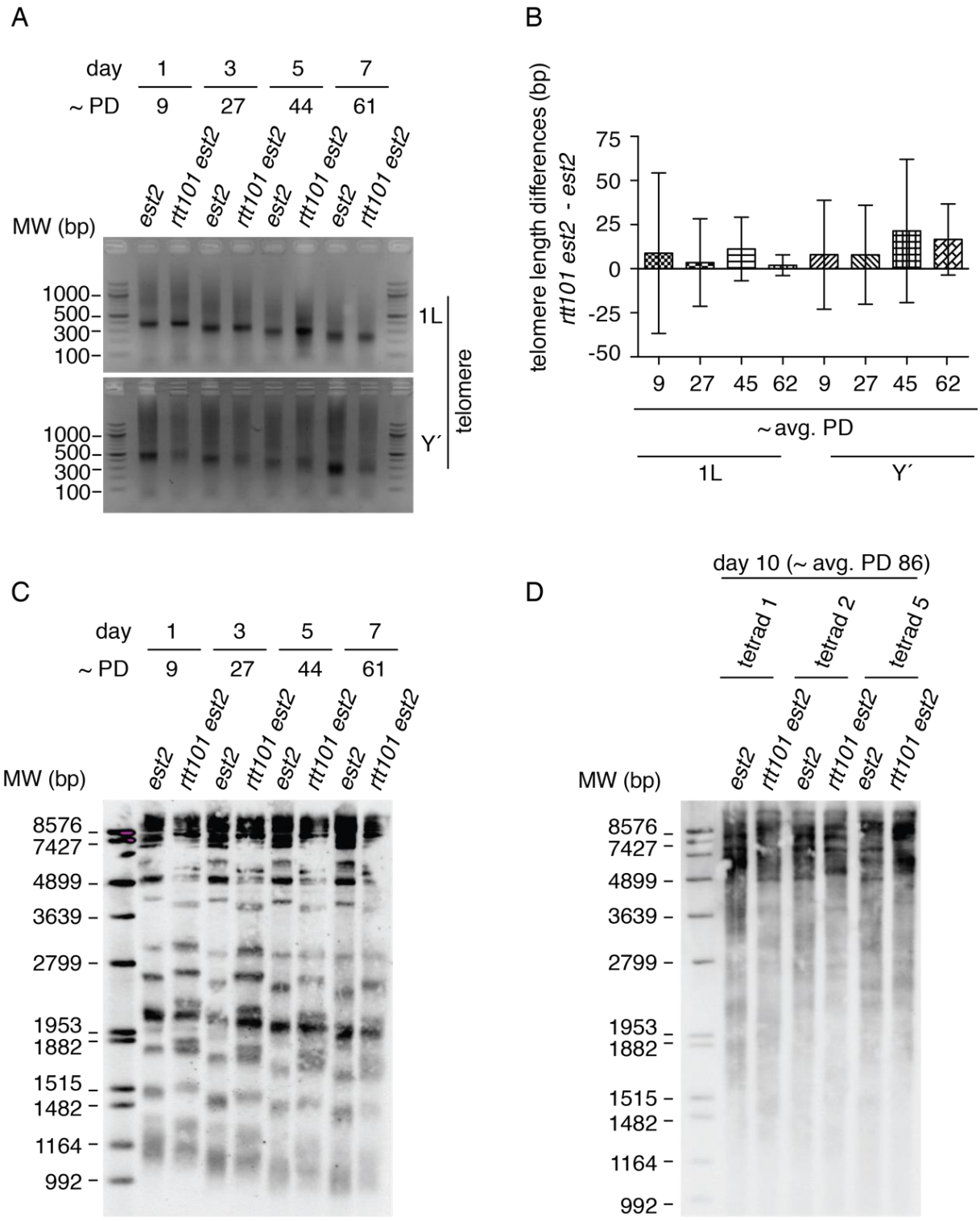

Figure 15 Bulk telomere length of *rtt101 est2* cells does not differ from bulk telomere length of *est2* cells. (A) Representative telomere PCR for telomere 1L and for 6 Y' telomeres. The two mutants originate from the same tetrad. (B) Telomere length differences between *rtt101 est2* and *est2* cells as measured by telomere PCR during senescence are shown. The mean of differences of three pairs of mutants, each pair originating from one tetrad are shown. (C) Telomere length during senescence as measured by Southern blot of terminal restriction fragments: genomic DNA of the two mutants originating from the same tetrad was digested with XhoI, subjected to Southern blotting followed by hybridization with a telomeric probe (D) Southern blot as in (C) for three pairs of mutants after survivor formation.

We also measured the telomere length of cells lacking either of the putative Rtt101-complex members Mms1, Mms22, Esc2, Ctf4, Rtt107 and Crt10 in the presence of telomerase by telomere PCR and Southern blot of terminal restriction fragments. None of the mutants had telomeres shorter than wt (Supplemental Figure 6).

3.2.4 Rtt101 might promote a telomere maintenance mechanism required at critically short telomeres

rtt101 cells have been reported to accumulate spontaneous DNA damage that can be visualized by an increased number of Ddc1-GFP repair foci in unchallenged conditions (Luke, Versini et al. 2006). Like telomere shortening, the accumulation of DNA damage can lead to checkpoint activation and cell cycle arrest. In order to test whether the premature loss of viability observed in the senescence curves of *rtt101 est2*, *mms1 est2*, *mms22 tlc1*, *ctf4 est2* and *esc2 est2* cells was due to a telomere length-independent effect of genomic DNA damage accumulation we propagated the corresponding telomerase proficient strains in unchallenged conditions. As shown in Figure 16A all the tested strains sustained their viability for more than 110 PDs indicating that the premature loss of viability observed in the senescence curves is indeed due to the lack of telomerase and its consequences.

The telomere length distribution in wt budding yeast cells in the presence of telomerase has been described in detail by Xu and co-workers (Xu 2013). The mean telomere length was determined to be 341 ± 41 bp. The mean length of the shortest telomere is about 180 bp. Interestingly, the shortest telomere seems to be separated by a significant gap of approximately 24 nt from the other telomeres. During replicative senescence this gap will most likely be maintained. Indeed, mounting evidence suggests that the length of the shortest telomere, not bulk telomere length is the major determinant of the onset of replicative senescence (Abdallah, Luciano et al. 2009, Khadaroo, Teixeira et al. 2009, Xu 2013). Moreover, it has been proposed that depending on their length telomeres elicit different processing pathways during replicative senescence, with the shortest telomere being subjected to homologous recombination-based (HR) mechanisms that employ the sister chromatid as chromatid as a template (Fallet, Jolivet et al. 2014).

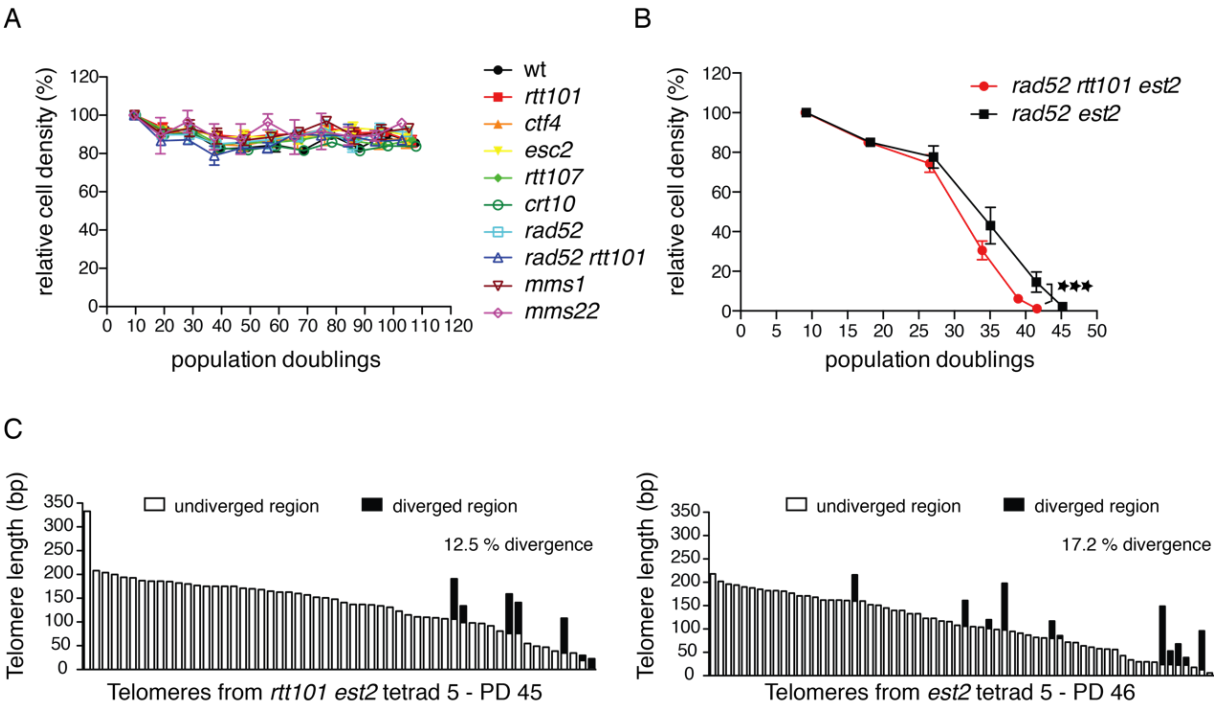

Figure 16 Possible reasons for the premature senescence of *rtt101 est2* cells. (A) In the presence of telomerase cells lacking Rtt101 or any of its putative complex members can be propagated for more than 110 PDs without viability loss. (B) Senescence curve for *rad52 rtt101 est2* cells compared to *rad52 est2* cells. The mean ± s.e.m. of n = 9 cultures per genotype are shown. Statisitical testing was performed using the Mann-Whitney test. Three stars represent a p-value of $p \leq 0.001$. (C) Sequencing of 1L telomere PCR products from tetrad 5, day 5 of the *rtt101 est2* senescence curve shown in Figure 13A. Open bars represent undiverged telomeric sequence, black bars indicate diverged telomeric sequence. For *rtt101 est2* n = 56 telomeres were sequenced, 7 of which showed divergence. For *est2* n = 64 telomeres were sequenced, 11 of which showed divergence.

Strikingly, Rtt101, Mms1, Mms22 have been implicated in sister chromatid exchange and other less well characterized HR pathways (Baldwin, Berger et al. 2005, Duro, Vaisica et al. 2008). Ctf4 is required for sister chromatid cohesion (Hanna, Kroll et al. 2001). Thus, we speculated that Rtt101 could promote an HR-based repair mechanism that might be required specifically at short telomeres to counteract shortening and subsequent checkpoint activation. As already described Rad52 plays a central role in HR pathways in budding yeast. This predicts that the deletion of *RTT101* should be epistatic with the deletion of *RAD52 EST2* in terms of premature senescence.

We performed the senescence curve comparing the *rad52 rtt101 est2* mutant to the *rad52 est2* mutant to test this prediction (Figure 16B). The viabilities of the two mutant strains were almost identical for the greater part of the senescence curve. Towards late population doublings, however, viabilities of *rad52 rtt101 est2* and *rad52 est2* cells differed from each other in a statistically significant manner. This is

in agreement with Rtt101 promoting a Rad52-dependent mechanism during replicative senescence, while also being involved in a Rad52-independent process close to crisis.

Since survivor formation depends on HR-mediated telomere maintenance mechanisms, Rad52-deficient cells are unable to overcome crisis and cell cycle arrest due to telomere shortening is indeed irreversible.

In order to test more directly whether Rtt101 promotes an HR-based pathway at shortening telomeres we cloned and sequenced telomere 1L of *rtt101 est2* and *est2* cells using the genomic DNA extracted from day 5 of the senescence curve shown in Figure 13A. Since budding yeast telomeres are composed of imperfect (TG_{1-3}) repeats the characteristic telomeric sequence of a particular telomere will be maintained in a culture lacking telomerase unless recombination takes place. The sequence of telomeres that have recombined usually differs from bulk telomeric sequence from a point of divergence onward (Teixeira, Arneric et al. 2004, Chang, Dittmar et al. 2011). Our results indicate that telomeric recombination during replicative senescence might be reduced. However, the difference between a recombination rate of 12.5 % in the *rtt101 est2* mutant compared to 17.2 % in the *est2* mutant is not significant according to Fisher's exact test.

To collect further evidence that Rtt101 is required at short telomeres and to be able to sequence a greater number of critically short telomeres we deleted *RTT101* in a strain carrying a construct that allows the Galactose-induced shortening of telomere 7L (Fallet, Jolivet et al. 2014). Unfortunately, the viability of the strain after tetrad dissection was too low both in the presence and absence of *RTT101* to continue experiments (data not shown).

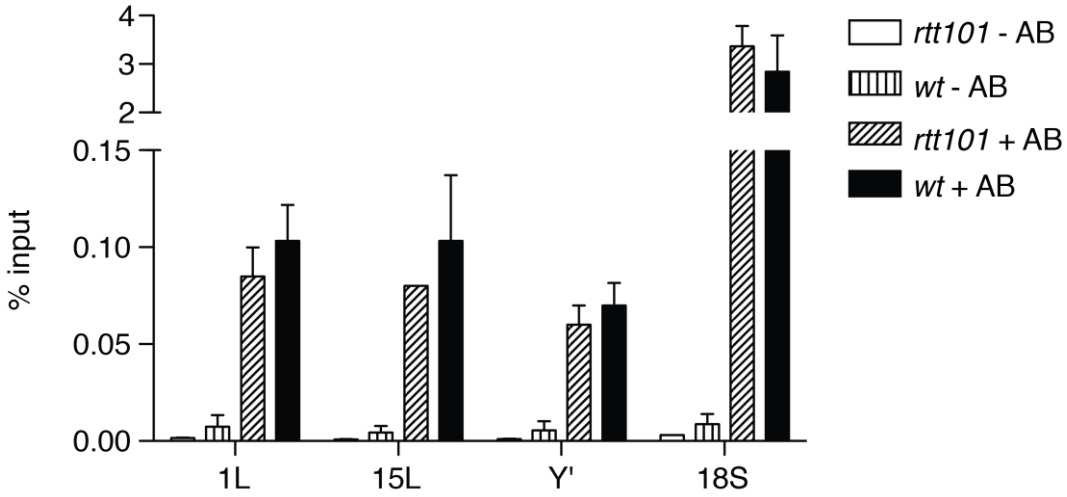

Figure 17 *RTT101* deletion does not influence the levels of RNA-DNA hybrids at telomeres. ChIP with wt and *rtt101* cells using S9.6 antibody, which recognizes RNA-DNA hybrids. Values are shown as percent input. The mean and SD of three independent replicates are shown. The 18S rDNA locus serves as a positive control, since RNA-DNA hybrid levels are known to be increased at this locus.

It has been shown that RNA-DNA hybrids exist at telomeres due to telomeric transcription and that RNA-DNA hybrids promote telomere elongation via homologous recombination thus delaying the onset of cellular senescence (Balk, Maicher et al. 2013). Telomeres start transcribing when they become critically short (Cusanelli, Romero et al. 2013). In order to test whether Rtt101 mediates HR by promoting hybrid formation we determined the level of RNA-DNA hybrids at telomeres in *rtt101* cells by ChIP using the S9.6 antibody, which specifically recognizes the conformation of an RNA-DNA hybrid independent of its sequence (Boguslawski, Smith et al. 1986). No difference in hybrid levels between *rtt101* and wt cells was detected (Figure 17). This, however, does not rule out the possibility that Rtt101 promotes a hybrid-dependent HR pathway, though not by influencing hybrid levels.

3.2.5 Premature senescence of *mrc1 est2* cells is epistatic with premature senescence of *rtt101 est2*

In the first part of this thesis we show that the MMS hypersensitivity of *rtt101* cells is relieved by the deletion of Mrc1 in a Rad52-dependent manner. Based on genetic

evidence we speculated that Rtt101^{Mms1} might promote the restart of RFs that stalled due to MMS-induced lesions.

Evidence from budding yeast, fission yeast and human cells suggests that telomeres are particularly difficult to replicate and replication forks frequently stall in the telomeric and subtelomeric region (Makovets, Herskowitz et al. 2004, Miller, Rog et al. 2006, Verdun and Karlseder 2006). Replication difficulties are exacerbated when telomeres shorten due to the loss of telomeric proteins that facilitate passage of the RF (Miller, Rog et al. 2006). In the absence of appropriate repair mechanisms RF stalling can lead to RF breakdown and the sudden loss of telomeric tracts.

We wandered whether Rtt101^{Mms1} might promote a process at critically short telomeres similar to the one at RFs that stalled due to DNA damage and tested if MRC1 deletion could rescue the premature senescence phenotype of *rtt101 est2* cells.

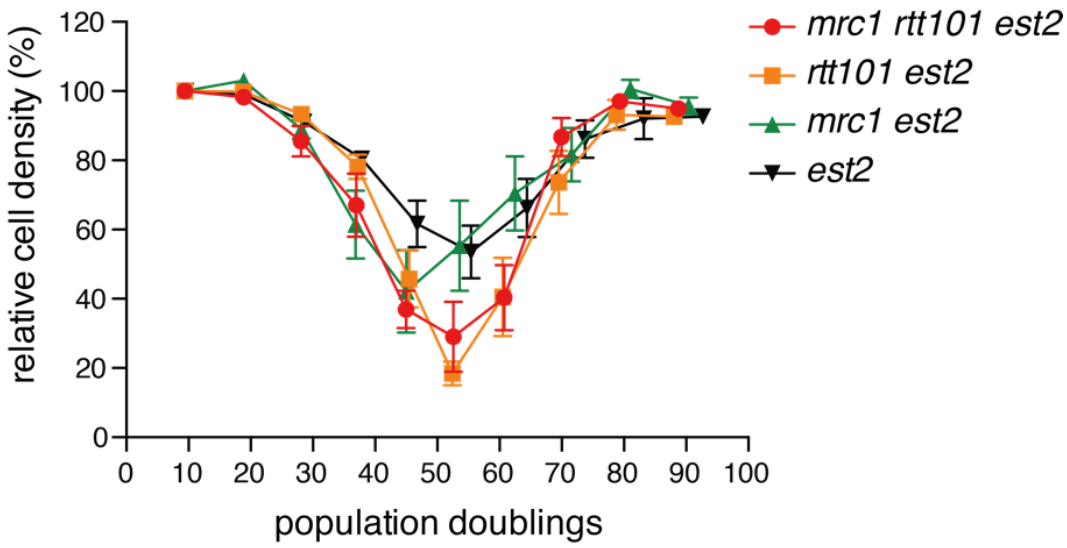

Figure 18 Premature senescence of *mrc1 est2* cells is epistatic with premature senescence of *rtt101 est2* cells. Senescence curves for *est2*, *rtt101 est2*, *mrc1 est2* and *mrc1 rtt101 est2* cells. All genotypes were retrieved from the dissection of the same diploid. The mean and s.e.m of n = 10 cultures are shown.

The senescence curve in Figure 18 shows that this was not the case. Instead *mrc1 est2* cells also senesced fast. As in *rtt101 est2* cells, premature senescence is not due to a global increase in the telomere-shortening rate of telomerase-deficient *mrc1* cells as has been shown by Grandin and colleagues (Grandin and Charbonneau 2007).

Interestingly, *mrc1 est2* cells were epistatic with *rtt101 est2* cells with *rtt101 est2* cells showing a more severe phenotype. This indicates that the early loss of viability or *rtt101 est2* cells undergoing replicative senescence is in part due to the absence of Mrc1. Preliminary experiments suggest that Mrc1 is indeed stabilized during senescence and that Mrc1 stabilization depends on the presence of Rtt101 (data not shown).

This would be in agreement with other studies proposing a protective function of Mrc1 from nucleolytic resection by ExoI at uncapped telomeres (Grandin and Charbonneau 2007, Tsolou and Lydall 2007). Increased exposition of ssDNA during senescence could result in premature checkpoint activation and cell cycle arrest. Further experiments are necessary to confirm these observations and to clarify the role of Rtt101 in this process.

4 Discussion

4.1 Rtt101 affects the replication stress response through Mrc1 but independent of Mrc1's checkpoint function

In order to identify potential targets of Rtt101-assembled ubiquitin E3 ligase complexes we carried out a genetic screen that uncovered 16 suppressor mutations that alleviated the hypersensitivity of *rtt101* cells to either MMS or CPT or to both drugs. We chose to characterize seven of the 16 hits more closely. These hits were chosen either due to their strong suppression phenotype or because they had previously been implicated in DNA replication and repair pathways. They were: the S-phase checkpoint and replication protein Mrc1, the DNA polymerase δ subunit Pol32, the 5' flap endonuclease Rad27, Topoisomerase I (Top1), the DNA polymerase ε subunit Dpb4, the SUMO E3 ligase Siz2 and the Folylpolyglutamate synthetase Met7.

In a first attempt to identify the complexes, which might mediate target ubiquitination, we tested whether the drug sensitivity of the putative Rtt101 complex members Mms1 and Mms22 was also relieved by the deletion of the seven selected screen hits.

The deletions of these genes in *mms1* cells did indeed result in a rescue signature indistinguishable to that of *rtt101* cells. Moreover, *mms1* cells showed a drug sensitivity identical to that of *rtt101* cells. This indicates that Mms1 is likely a constitutive member of Rtt101-assembled complexes in response MMS and CPT. This is in agreement with a wealth of previous studies that could show that the action of Rtt101 depended on the presence of its binding partner Mms1 (Zaidi, Rabut et al. 2008, Ben-Aroya, Agmon et al. 2010, Mimura, Yamaguchi et al. 2010, Han, Zhang et al. 2013). In fact, Spt16 is the only target that has been suggested, so far, to be ubiquitinated by Rtt101 in the absence of Mms1 (Han, Li et al. 2010).

The rescue pattern of *mms22* cells showed some differences compared to *rtt101* cells, in that: deletion of DPB4 only lead to a slight rescue of *mms22* cells on MMS and deletion of RAD27 did not rescue *mms22* cells on CPT. Moreover, hypersensitivity of *mms22* cells to MMS, CPT, HU and Zeocin is more severe than that of *rtt101* and *mms1* cells but could be alleviated in all four cases by *MRC1* deletion. Thus, Mms22 appears to be dispensable for the rescue pathway involving

Rad27 and of minor importance for the Dpb4 pathway. At the same time Mms22 function exceeds that of Rtt101 and Mms1 and fulfils a more general function in response to a broader range of DNA damage that is also intimately connected to the role of Mrc1. This is consistent with the previous suggestions that Mms22 also functions outside of the Rtt101 E3 ligase.

Deletion of MRC1 conferred the most striking rescue of *rtt101* cells and, apart from the DPB4 and MET7 deletions, was the only suppressor that relieved the hypersensitivity of *rtt101* cells to both MMS and CPT. Therefore we were particularly interested in uncovering the mechanistic details of this pathway and chose to characterize it more closely.

How could $Rtt101^{Mms1Mms22}$ act in concert to promote cellular viability via Mrc1 regulation after MMS- and CPT-inflicted DNA damage? Is Mrc1 a direct target of this complex? And why could Mrc1 modification or degradation be beneficial to overcome DNA damage and replication fork stalling?

Mrc1, Tof1 and Csm3 were first suggested to be potential targets of an Rtt101 ubiquitin ligase complex by Collins and co-workers (Collins, Miller et al. 2007) due to positive genetic interactions in an epistatic miniarray profile (E-MAP) exploring different aspects of chromosome biology, including replication and repair, under unchallenged conditions. E-MAPs measure genetic interactions by determining the growth rates of double mutants created by the pairwise combination of gene deletions. The E-MAP comprises a set of selected genes belonging to a specific biological process.

Our screen results are in agreement with this study while underlining the particular and striking positive genetic interaction between *RTT101* and *MRC1* after damage infliction that blocks replication fork progression. Deletion of TOF1 or CSM3 did not however, result in positive genetic interaction with *RTT101* deletion under these conditions (Figure 8).

Mrc1 has been shown to be ubiquitinated and degraded by the proteasome after MMS treatment (Mimura, Komata et al. 2009, Fong, Arumugam et al. 2013). This degradation depends partially but not fully on another ubiquitin E3 ligase complex, the SCF^{Dia2} complex, which is assembled by the cullin Cdc53 (human CUL1). Just like for *rtt101* cells, *MRC1* deletion rescues MMS sensitivity of *dia2* cells and allows timely checkpoint downregulation and cell cycle re-entry. It is tempting to speculate that the $Rtt101^{Mms1Mms22}$ complex might be working in a parallel pathway with

overlapping function and constitute the so far unknown activity that is required for the full reduction of Mrc1 levels during recovery in wt cells.

This possibility is particularly intriguing since CUL4A and CUL1 have been shown to act in concert to ubiquitinate the activated CHK1 protein kinase in human cells (Huh and Piwnica-Worms 2013). Rtt101 is thought to be the equivalent of the human CUL4 subfamiliy of cullin proteins. Furthermore, CHK1 is activated in a Claspin-dependent manner in response to DNA damage and CHK1 degradation is required for efficient cell cycle re-entry after completion of repair activities. Thus CUL4A and CUL1 act together in human cells to promote cell cycle re-entry after MMS-induced damage by degrading the effector kinase while the CUL1 homologue Cdc53 promotes degradation of the mediator molecule Mrc1 together with a so far unknown activity in the equivalent situation in budding yeast.

Two checkpoint defective but replication proficient alleles of Mrc1 have been described. In the *mrc1-AQ* allele all Mec1 target sites are mutated from S/TQ to AQ (Osborn and Elledge 2003). The $mrc1_{1\text{-}971}$ allele encodes a C-terminally truncated version of the protein. Both are able to suppress the MMS sensitivity of *dia2* cells just as well as full *MRC1* deletion. With these results it was concluded that lack of the Mrc1 checkpoint function is sufficient to rescue *dia2* cells (Fong, Arumugam et al. 2013). This indicates that the SCF^{Dia2} complex promotes viability after MMS treatment by disrupting continued checkpoint signalling during the recovery process via destruction of Mrc1.

Our experiments suggest that unlike deletion of *DIA2*, deletion of *RTT101* does not lead to a stabilization of global Mrc1 protein levels during recovery from MMS treatment (Figure 11). These preliminary results were corroborated by experiments by Vanessa Kellner using a Gal-inducible Mrc1 promoter that allowed targeted shut-off of protein production (data not shown, published in Buser, Kellner et al. 2016, see appendix 7.2). We conclude that Rtt101 does not affect the stability of either global or chromatin-associated Mrc1 protein levels (Buser, Kellner et al. 2016).

More importantly however, the *mrc1-AQ* allele did not alleviate the drug sensitivity of *rtt101* cells (Figure 9A). This shows very clearly that unlike for *dia2* cells, the lack of the Mrc1 checkpoint function is not sufficient to rescue *rtt101* cells. Our results do not exclude that Rtt101 targets Mrc1. Indeed, we cannot rule out that Mrc1 might be ubiquitinated locally or transiently at the site of fork stalling, although we were unable to detect such Mrc1 conjugates. However, we exclude that subsequent Mrc1

degradation or alteration of function serves the sole purpose of promoting recovery by dampening checkpoint signalling.

4.2 Rtt101 might mediate selective decoupling at stalled replication forks through Mrc1 to allow repair and replication fork restart

Interestingly, the *mrc1*$_{1\text{-}971}$ allele did indeed alleviate MMS sensitivity of *rtt101* cells almost as well as the full deletion of *MRC1* (Figure 9B). Therefore, loss of the C-terminal Mrc1 function seems to be crucial.

The central portion of Mrc1 (Mrc1$_{312\text{-}655}$) has been shown to interact directly with the C-terminus of Mcm6, which forms part of the replicative helicase. Mrc1 might also interact weakly with Mcm2 and Mcm4 (Komata, Bando et al. 2009). In addition, Mrc1 has been reported to bind Pol2, the catalytic subunit of the leading strand DNA polymerase ε, via two independent interactions. The N-terminus of Mrc1 interacts with the N-terminus of Pol2, while the C-terminus of Mrc1 interacts with the C-terminus of Pol2. The N-terminal interaction has been implicated in the checkpoint response since it is abolished upon phosphorylation of Mrc1, whereas the C-terminal interaction is stable also when Mrc1 is phosphorylated (Lou, Komata et al. 2008).

Coupling of the CMG helicase to the polymerase is crucial for replication of both the leading and the lagging strand in challenged and unchallenged conditions. As described, leading strand coupling is mediated by Mrc1. Lagging strand coupling depends on Ctf4, which trimerizes to bind the CMG helicase subunit Sld5 and polymerase α (Miles and Formosa 1992, Gambus, van Deursen et al. 2009, Simon, Zhou et al. 2014).

In the absence of Mrc1 the rate of replication fork progression is reduced and replication is slower in these cells (Szyjka, Viggiani et al. 2005, Tourriere, Versini et al. 2005, Hodgson, Calzada et al. 2007). After nucleotide depletion due to HU treatment the association of Pol2 with replicating DNA is decreased as shown by chromatin immunoprecipitation in *mrc1* cells (Lou, Komata et al. 2008). The repair or restart of stalled replication forks is thought to be curtailed in these cells due to the inability to stabilize the blocked replisome. (Katou, Kanoh et al. 2003). Cells lacking both Mrc1 and Ctf4 are inviable. Permanent checkpoint activation due to severe replication problems prevents cell cycle completion of these cells (Gambus, van Deursen et al. 2009).

Thus, disruption of the links between the CMG helicase and polymerases ε and α respectively, have been shown to have deleterious effects. However, several lines of evidence indicate that decoupling of the helicase from the polymerase might also be beneficial in some special situations such as replicative stress caused by damage-induced fork stalling. The idea that replisome uncoupling upon blocked RF progression might actually be a natural process and a prerequisite for a number of subsequent repair pathways has been studied in more detail in *E. coli*. Yeeles and colleagues present the current knowledge on this topic in their review (Yeeles, Poli et al. 2013), which served as a basis for the following two paragraphs.

Damage on the lagging strand is generally thought to be a minor problem for replication since repriming of the lagging strand occurs frequently thus allowing reinitiation of replication downstream of the lesion and postreplicative repair of the unreplicated gap. Several studies using site-specific lagging strand damage showed that replication of both the leading and the lagging strand could indeed proceed normally despite lagging strand lesions in bacterial systems (McInerney and O'Donnell 2004, Nelson and Benkovic 2010). However, lesion bypass does not just depend on the ability to reprime. If synthesis continues without removal of the replication block then the replisome must allow dissociation and re-binding of the stalled polymerase. Unlike its eukaryotic equivalent, the prokaryotic replicative helicase travels on the lagging strand template. In this light the results of the above mentioned studies indicate that the bacterial replisome is indeed able to decouple the helicase from the polymerase activity in a controlled manner. Accordingly, single-stranded DNA gaps in the lagging strand have been observed by Higuchi and colleagues (Higuchi, Katayama et al. 2003) following the introduction of a single DNA lesion in an *oriC*-based replication assay *in vitro*.

That repriming of the leading strand is possible in *E. coli* is supported by mounting evidence. Heller and Marians could show that the DnaG primase primed both the leading and the lagging strand outside the origin of replication downstream of an unrepaired leading strand lesion (Heller and Marians 2006). Yeeles and Marians found that introduction of a site specific leading strand damage caused only transient fork stalling followed by repriming that depended on DnaG but not on the canonical replication restart machinery (Yeeles and Marians 2011).

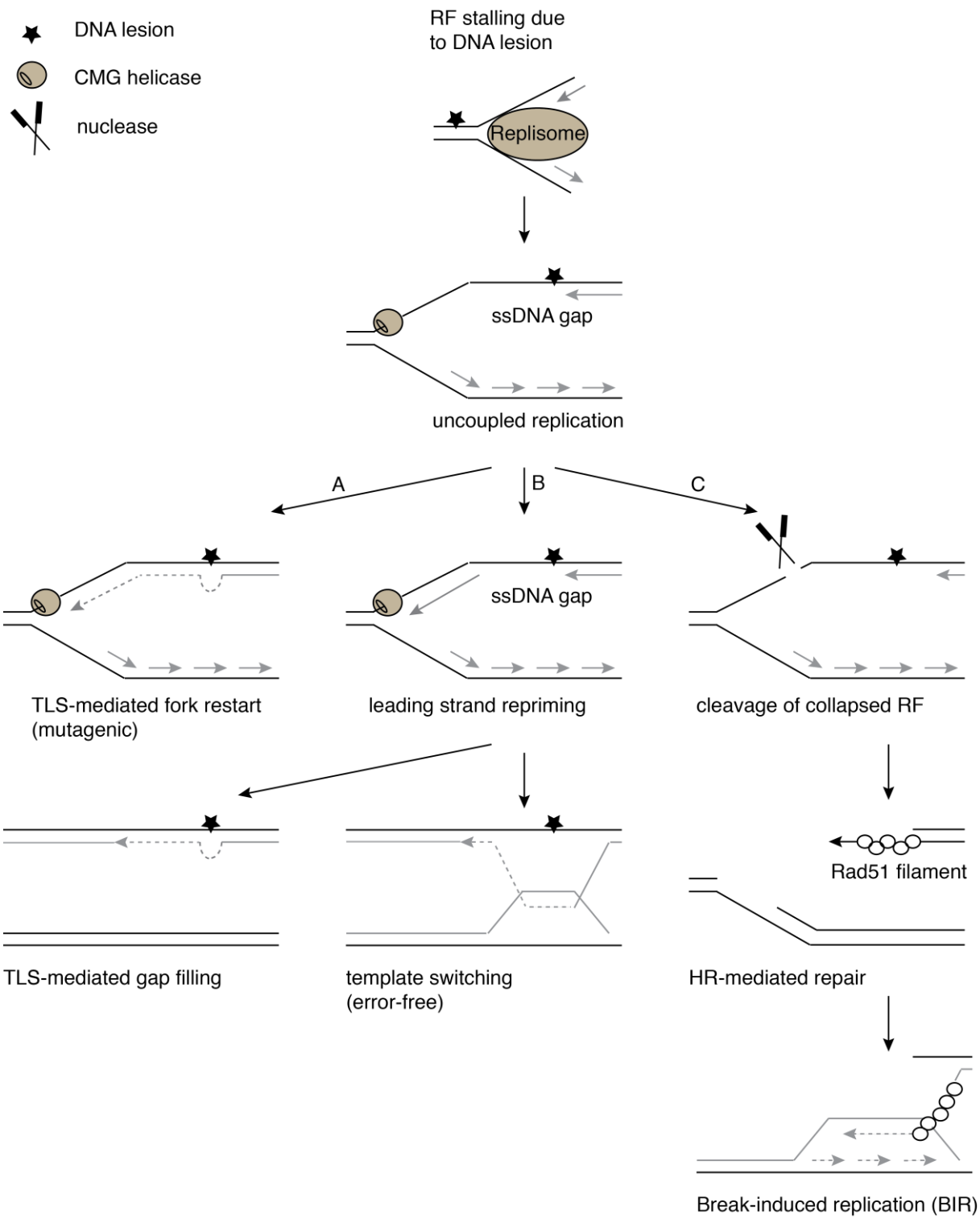

Figure 19 Uncoupling of the CMG helicase from the DNA polymerase ε as a common step preceding different mechanisms that allow the completion of replication despite leading strand damage. Controlled replisome uncoupling has been suggested as a prerequisite for various mechanisms including (A) TLS-mediated fork restart (B) leading strand repriming and (C) cleavage of the collapsed RF. This figure is shown in the introduction of this thesis as Figure 2. It was adapted from (Yeeles, Poli et al. 2013).

In eukaryotic systems both the repriming problem and the decoupling problem coincide on the leading strand. ssDNA gaps in both the leading and the lagging strand and subsequent repair of the gaps has been reported in *S. cerevisiae* after UV irradiation (Lopes, Foiani et al. 2006) and in *Xenopus* egg extracts in response to multiple forms of DNA damage (Byun, Pacek et al. 2005, Van, Yan et al. 2010). However, research has primarily focused on the repair pathways overcoming and filling these gaps postreplicatively rather than on gap creation. Nevertheless replisome uncoupling in order to liberate the CMG helicase from the stalled polymerase has been suggested as a common step preceding TLS, template switching and BIR (see Figure 19 and (Yeeles, Poli et al. 2013)). The uncoupling reaction leads automatically to the production of ssDNA, a potent checkpoint activator, which might well be required upstream of a variety of different repair or restart mechanisms. Thus, the uncoupling reaction might be concomitantly involved in the signalling of a stalled fork (by ssDNA production) and its restart (by gap creation that allows direct repriming or other repair pathways, including those based on HR).

Mrc1 is known to mediate both replisome coupling and stalled fork signalling presenting itself as the perfect leverage to influence both aspects of replication. Our results show that Mrc1 deletion rescues the hypersensitivity of *rtt101*, *mms1* and *mms22* cells to MMS and CPT. This, in theory, would be in agreement with Mrc1 (or an Mrc1 interacting protein) being a target of an Rtt101-assembled E3 ligase complex in response to DNA damage-induced replication fork stalling. We suggest that ubiquitination of Mrc1 (or an Mrc1 interacting protein) by $Rtt101^{Mms1Mms22}$ leads to uncoupling of the CMG helicase from polymerase ε by disrupting the binding of Mrc1 to either Mcm6 or Pol2. It is worth mentioning again that the N-terminal interaction of Mrc1 and Pol2 is abolished upon Mrc1 phosphorylation by Mec1 (Lou, Komata et al. 2008) and recent findings of Uzunova and colleagues suggest that Mrc1 is removed from chromatin after extended exposure to HU (Uzunova, Zarkov et al. 2014), although we were not able to see this upon MMS exposure. Whether Mrc1 ubiquitination leads to its degradation or simply alters its binding behaviour cannot be concluded at the moment and our attempts to detect ubiquitinated Mrc1 conjugates have yielded only negative results. Nevertheless, since the *rtt101* rescue by *MRC1* deletion depends on *RAD52* (Figure 12A), we suggest that modification of Mrc1 by

Rtt101 allows HR-based processes to proceed at the uncoupled fork, which promote replication fork restart or repair.

A similar idea has been brought forward in a recent study by Luciano and colleagues (Luciano, Dehé et al. 2015). They could show that the high sensitivity of *asf1* cells to replication stress induced either by CPT or by the deletion of the DNA helicase Rrm3 is reduced by Ctf4 deletion. Experiments with truncated Ctf4 mutants indicated that it is indeed the uncoupling of the CMG helicase from the polymerase α that confers the rescue. The histone chaperone Asf1 presents the H3-H4 heterodimer to Rtt109 for subsequent acetylation of H3K56. Rtt101, Mms1 and Mms22 have been shown to act downstream of the H3 acetylation event (Tong, Lesage et al. 2004, Pan, Ye et al. 2006, Collins, Miller et al. 2007). While *CTF4* deletion could slightly improve viability of *mms1* and *mms22* cells, it aggravated the growth defect of the *rtt101* mutant caused by MMS treatment. Interestingly, drug sensitivity of *asf1* cells was also relieved by deletion of *MRC1*. Experiments with separation of function mutants revealed that this effect was due to the loss of Mrc1's replicative function and independent of the absence of Mrc1's checkpoint function.

Taken together, the study by Luciano and co-workers indicates that replisome uncoupling might be beneficial for cells lacking a functional H3K56 acetylation pathway when they face replicative stress. This is in agreement with our results. The present thesis complements the understanding of the uncoupling process by focussing on the Mrc1-mediated replisome uncoupling and highlighting the role of Rtt101 in this process. Moreover, it elucidates the relationship between repair/restart mechanisms, which might ensue the uncoupling process, and homologous recombination.

Our results indicate that the rescue of *rtt101* and *mms1* cells by *MRC1* deletion requires Rad52 while *mms22* cells are at least partially rescued by *MRC1* deletion in the absence of Rad52 (Figure 12C). Thus Rtt101 probably assembles different complexes in response to MMS with different functions. As discussed in section 1.7 Mms22 is not just a member of Rtt101-assembled ubiquitin E3 ligase complexes. It is also degraded by the proteasome in an Rtt101-dependent manner after having been recruited to sites of DNA damage and having fulfilled its function there. What exactly this function is remains elusive (Ben-Aroya, Agmon et al. 2010). Mass spectrometry data from Matthias Peter's lab show that Mms22 binds Mrc1 (Buser, Kellner et al. 2016, see appendix 7.2). Therefore, Rtt101 could first assemble an E3 ligase

complex containing both Mms1 and Mms22, which acts upon Mrc1 to promote replisome uncoupling. The Rtt101^{Mms1} complex might then degrade Mms22 and promote recombination at the uncoupled fork by further affecting Mrc1. In this case Rtt101 would be acting both upstream and downstream of the decoupling process. This model is depicted in Figure 20 (Alternative A).

Finally, it is also possible that the decoupling step is mediated by Mms22 independent of Rtt101^{Mms1} (Figure 20, Alternative B). This would be in agreement with Mms22 fulfilling a more general function than Rtt101 and Mms1 in response to DNA damage as indicated by the stronger sensitivity of *mms22* cells to genotoxic agents. Moreover, only *mms22* cells but not *rtt101* and *mms1* cells were rescued on HU and Zeocin by MRC1 deletion (Table 1) and the selective decoupling of stalled forks might well also be necessary in response to these drugs.

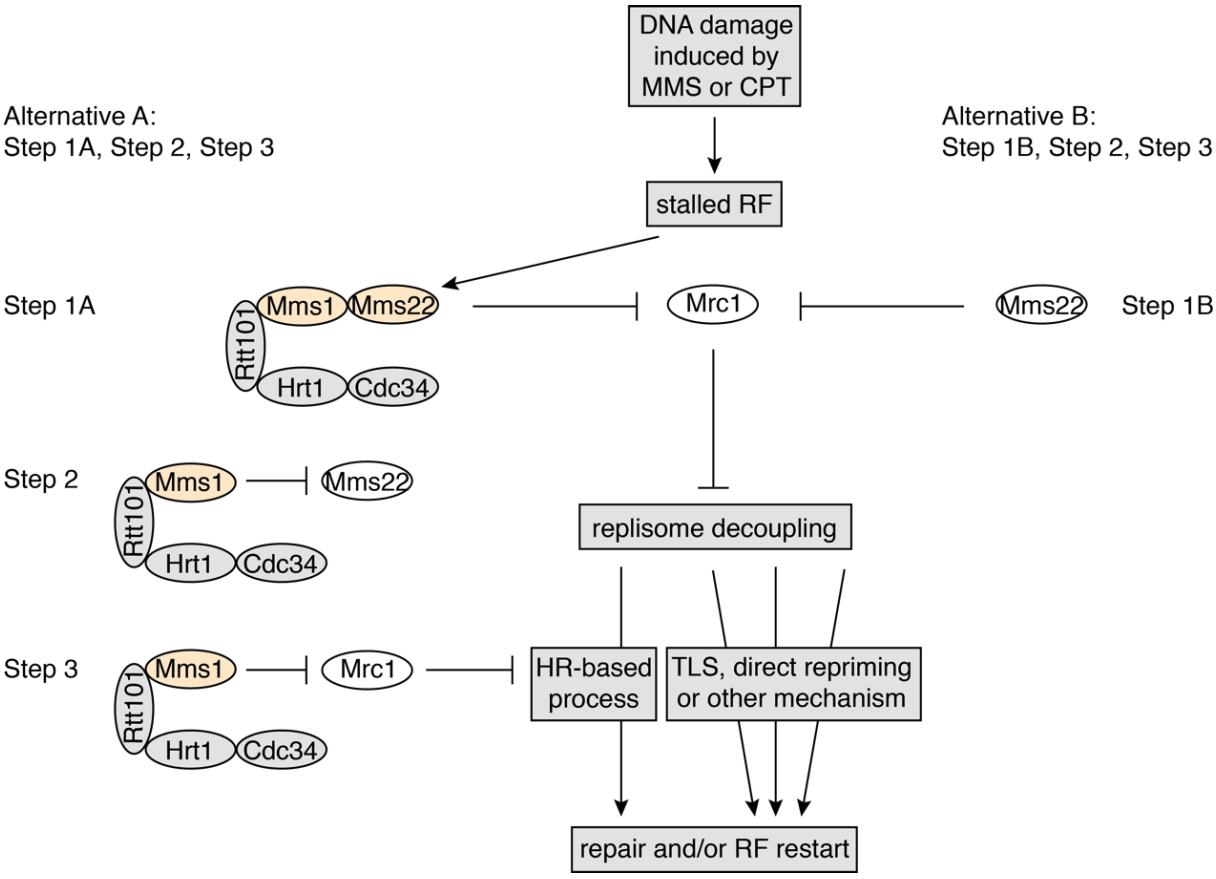

Figure 20 Rtt101 might mediate selective decoupling of the replisome at replication forks that have stalled due to DNA lesions. Rtt101^{Mms1Mms22} could mediate uncoupling of the CMG helicase from Polε through the ubiquitination of Mrc1 (Step 1A). Mms22 might then be degraded by the Rtt101^{Mms1} complex as reported before (Step 2). Rtt101^{Mms1} could then promote recombination at the uncoupled fork by further modifying Mrc1. Other repair or restart mechanisms might still require replisome uncoupling (Step 1) but are independent of further Mrc1 modification and the HR machinery. Alternatively, Step 1 might be mediated by Mms22 independent of Rtt101^{Mms1} (Step 1B).

Our results and their interpretation contradict a hypothesis recently published by Hang and colleagues (Hang, Peng et al. 2015). They showed that loss of Mrc1 increases the survival of *rtt107*, *rtt101*, *mms1 and mms22* cells on MMS containing medium and promotes replication completion of *rtt107* cells under these conditions. They propose that the de-repression of late origins observed in *mrc1* cells is responsible for the rescue. Indeed, the activation of additional origins in *mrc1* cells seemed to be independent of the loss of Mrc1's checkpoint function and could be attributed to the loss of Mrc1's replicative function (Gispan, Carmi et al. 2014). However, our experiments indicate clearly that the rescue of *rtt101* cells depends on a functional HR machinery. Moreover, experiments by Vanessa Kellner using the *sld3-37A dbf4-4A* background suggest that genetic de-repression of late origins is not sufficient to alleviate MMS sensitivity of *rtt101* mutants (data not shown, published in Buser, Kellner et al. 2016, see appendix 7.2), rendering the interpretation of Hang and colleagues unlikely.

Further experiments are certainly necessary to test and develop the ideas suggested here and to pinpoint the pathways, both Rad52-dependent and -independent ones, that seem to proceed more efficiently in the absence of Mrc1 and suppress the hypersensitivity of *rtt101*, *mms1* and *mms22* cells to MMS and CPT.

mms22 cells show reduced HR in response to genotoxic agents while *mrc1* cells are highly recombinogenic (Baldwin, Berger et al. 2005, Duro, Vaisica et al. 2008). Experiments performed in Matthias Peter's lab show that *MRC1* deletion alleviates the low HR frequency of *mms22* cells further indicating that Mrc1 functions downstream of Mms22 to suppress HR (Buser, Kellner et al. 2016, see appendix 7.2). The reduced recombination phenotype observed for *mms22* cells is shared by *rtt101* and *mms1* cells in some experimental settings (Duro, Vaisica et al. 2008).

Co-immunoprecipitation experiments of Mrc1 with Mcm6 (or another component of the MCM complex) and Pol2 respectively could elucidate if Mrc1 does indeed mediate the selective decoupling of stalled forks after MMS treatment. However, since decoupling will only occur at stalled forks it might be difficult to observe changes in the interaction when looking at global Mrc1 levels. Therefore, introduction of a site-specific replication barrier might facilitate insights into whether or not Mrc1's interactions within the replisome change upon fork stalling. Such a system was developed for *S. cerevisiae* in Ian Hickson's lab by introducing the *E. coli* Tus-*Ter* replication fork barrier into budding yeast (Larsen, Sass et al. 2014). This system

would also allow ChIP as an alternative experimental approach to monitor the decoupling reaction. Spatial separation of the signals for the CMG helicase and Pol2 would indicate replisome uncoupling, which might be suppressed in cells lacking Rtt101. If selective decoupling proves to be mediated by the Mrc1/Rtt101 system it will ultimately be interesting to investigate if Claspin/CUL4 system fulfils a similar function in human cells.

As shown in Figure 9 deletion of the Mrc1 C-terminus rescues *rtt101* hypersensitivity almost as well as full deletion of *MRC1*. *MRC1* deletion leads to constitutive decoupling, which despite its deleterious effects during normal replication seems to be beneficial for *rtt101* cells during damage-induced replication stress. We just argued that this could be due to the fact that constitutive decoupling includes the selective decoupling, which might be required for repair or RF restart mechanisms including HR-based ones. The *mrc1*$_{1\text{-}971}$ allele shows no defects during normal replication (Fong, Arumugam et al. 2013). Therefore, it is unlikely that the replisome is constitutively decoupled in *mrc1*$_{1\text{-}971}$ cells. Instead the Mrc1 C-terminus seems to be involved in the selective destabilization of Mrc1 or alteration of its binding behaviour, thus integrating information and remodelling the replisome accordingly. Many Mrc1 binding partners have been found in yeast-two-hybrid assays in budding and fission yeast (Zhao, Tanaka et al. 2003, Tanaka and Russell 2004, Lou, Komata et al. 2008, Mimura, Komata et al. 2009). Identification of binding partners of the Mrc1 C-terminus by yeast-two-hybrid assays using full length Mrc1 and Mrc1$_{1\text{-}971}$ could help to encircle the role of the Mrc1 C-terminus.

4.3 Rtt101 regulates multiple pathways in response to DNA damage and replication stress

As already described, our screen picked up 16 suppressors of *rtt101* drug sensitivity (Figure 6F). We tried to uncover the role of Mrc1 in the Rtt101-mediated pathway activated in response to damage-induced replication stress as discussed in sections 4.1 and 4.2.

However, our screen results show that Rtt101 is certainly required in a variety of pathways in response to DNA damage and replication stress and open up a wealth of possible experiments to test and elucidate the connections between Rtt101 and its drug sensitivity suppressors. Measuring protein levels of the putative targets in the absence and presence of damage-induced replication stress in wt and *rtt101* cells

while inhibiting protein synthesis will give a first indication of whether the suppressor proteins are indeed degraded in an Rtt101-dependent manner. Moreover, the presence of the ubiquitinated form of the suppressors in wt and their absence in *rtt101* cells could be monitored by immunoprecipitation experiments to identify them as true targets of Rtt101-assembled ubiquitin E3 ligase complexes. In default of these data it is nevertheless worthwhile to speculate about possible Rtt101 functions that suggest themselves due to its confirmed drug sensitivity suppressors. In the following paragraphs this is done for the six screen hits whose ability to suppress drug sensitivity of the putative Rtt101 complex members Mms1, Mms22, Esc2 and Ctf4 was tested following the screen. These were the DNA polymerase δ subunit Pol32, the 5' flap endonuclease Rad27, Topoisomerase I (Top1), the DNA polymerase ε subunit Dpb4, the SUMO E3 ligase Siz2 and the Folylpolyglutamate synthetase Met7.

Pol32 is a subunit of DNA polymerase δ, which synthesizes the lagging strand during normal chromosomal DNA replication. Pol32 interacts with Pol31, another Pol δ subunit, with the replication clamp proliferating cell nuclear antigen (PCNA, Pol30) and with Pol1, the large subunit of polymerase α (Johansson, Garg et al. 2004). For translesion synthesis Pol3, the catalytic subunit of Pol δ, is targeted for proteasomal degradation by Def1 (Daraba, Gali et al. 2014). This allows the establishment of a TLS polymerase called Polζ consisting of Pol32, Pol31, Rev3 (catalytic subunit) and Rev7. Interestingly, the assembly of the TLS polymerase is preceded by monoubiquitination of PCNA. Disruption of the Pol32-PCNA binding inhibits PCNA dependent TLS (Makarova, Stodola et al. 2012). Pol32 is also required for BIR, while ubiquitination of PCNA only plays a subordinate role in this process (Lydeard, Lipkin-Moore et al. 2010). Both processes contribute to genome stability in the face of damage-induced replication stress. Our results suggest that ubiquitination by $Rtt101^{Mms1Mms22}$ contributes to the orchestration of one (or both) of these mechanisms. Whether this requirement is rooted in degradation or modification of Pol32 is not obvious at the moment.

Rad27 is a 5' flap endonuclease that is involved in the processing of DNA structural intermediates that arise during the maturation of Okazaki fragments, in base-excision repair and other genome maintenance mechanisms. Interaction of Rad27 with the structure-specific endonuclease Mus81-Mms4 stimulates the cleavage of regressed replication forks (Kang, Lee et al. 2010) and the resolution of toxic intermediates of

HR-based repair (Thu, Nguyen et al. 2015). In the absence of Rad27 stalled RFs accumulate (Guo, Qian et al. 2008). Just like Rad27, its human orthologue FEN1 is involved in Okazaki fragment processing, DNA repair and other genome maintenance pathways. Interestingly, FEN1, has been shown to be degraded at the end of S-phase in a proteasome-dependent manner after a cascade of phosphorylation, sumoylation and ubiquitination (Guo, Kanjanapangka et al. 2012). The action of Rad27 must likely be tightly controlled in yeast, too, in order to prevent aberrant nuclease activity, which might threaten genomic integrity. Whether Rad27 is indeed ubiquitinated and degraded and whether Rtt101 assembles the corresponding ubiquitin E3 ligase complex remains to be determined.

Topoisomerase I (Top1) relaxes supercoiled DNA by cleaving and resealing the phosphodiester backbone. CPT specifically targets Top1 and stabilizes the otherwise transient cleavage complex. Collision of the replisome with enzyme-DNA intermediate lead to the creation DSBs (Pommier 2013). Thus it is not surprising that deletion of the CPT target enzyme Top1 relieves the sensitivity of *rtt101* cells to CPT. It is noteworthy, however, that the putative Rtt101 complex member Mms22 has been shown to be required for the effective cellular response to Etoposide (Baldwin, Berger et al. 2005), which stabilizes Topoisomerase II complexes with DNA. *mms22* cells are hypersensitive to topoisomerase II-mediated DNA breaks and Etoposide-induced homologous recombination is reduced in *mms22* cells. Since *MMS22* is additive with *RAD54*, Mms22 seems to act outside of the single-strand invasion pathway. Baldwin and co-workers also found that *MMS22* is epistatic with *RTT101* in terms of hypersensitivity to Etoposide with *MMS22* conferring the more severe phenotype. These parallels allow the speculation that Mms22 and Rtt101 are required downstream of Etoposide-induced damage and make it interesting to test if *MRC1* deletion can also relieve the sensitivity of *mms22* and *rtt101* cells to the topoisomerase II poison Etoposide. Finally, studies in mammalian cells suggest that Top1 is posttranslationally modified by SUMOylation and ubiquitination and consequently degraded in response to CPT treatment (Desai, Liu et al. 1997, Mao, Sun et al. 2000). Whether this is also true for yeast, and if Rtt101 plays a role in this process remains to be seen.

Dpb4 is a subunit of DNA polymerase ε. It is noteworthy that Dpb4 and Mrc1 are the two suppressors identified in our screen that belong to the part of the replisome responsible for leading strand synthesis while at the same time both suppressors are

able to alleviate drug sensitivity of *rtt101* cells to both MMS and CPT. While the functional details of this observation remain elusive at the moment one might nevertheless speculate that the Dpb4 and the Mrc1 pathways are interconnected. It has indeed been shown that Dpb4 contributes to checkpoint signalling during replication stress (Puddu, Piergiovanni et al. 2011). Moreover, replication is disturbed in *dpb4* cells, probably due to a defective structure of the leading strand polymerase Pol ε (Ohya, Maki et al. 2000) and lack of Dpb4 has been suggested to be the cause of gaps in the leading strand (Aksenova, Volkov et al. 2010). Thus, Dpb4 might contribute to proper Mrc1 function by influencing its interaction with Polε and ultimately contribute to replisome coupling.

The post-translational modifications by ubiquitin and SUMO have been shown to be important and often intertwining regulatory signals of the proteins involved in the DDR in both yeast and mammalian cells (reviewed in (Bologna and Ferrari 2013, Pinder, Attwood et al. 2013)). The SUMOylation of PCNA enhances its subsequent ubiquitination by the SUMO-targeted ubiquitin E3 ligase (STUbL) Rad18, which monoubiquitinates PCNA (Pol30 in yeast) in responses to DNA damage (Parker and Ulrich 2012). This allows the recognition of PCNA by specialised TLS polymerases that replicate across the lesion. On the other hand ubiquitin and SUMO target the same residue within PCNA and can thus become competing or collaborating PTMs, establishing the timing of sequential steps in the progression of replication (Bergink and Jentsch 2009). The fact that deletion of the SUMO E3 ligase *SIZ2* increases the resistance of *rtt101* cells to CPT, albeit moderately, might reflect the competition of SUMOylation and Rtt101-mediated ubiquitination of a common target in response to DNA damage and replication stress.

Finally the Folylpolyglutamate synthetase Met7 was also among the screen hits. We dedicated only limited attention to this suppressor since the *met7* mutant showed extremely variable growth in unchallenged conditions. Suppression of the petite phenotype can be achieved for this mutant by providing exogenous dTMP and deleting TUP7 to allow dTMP uptake as reported by DeSouza and colleagues (DeSouza, Shen et al. 2000). With *MRC1*, *POL32*, *RAD27*, *TOP1* and *DPB4*, five genes identified as suppressor mutations have direct roles in DNA replication and repair. Since the levels of Met7 have also been shown to increase upon replication stress Met7 might also fall into this category (Cherest 2000, Tkach, Yimit et al. 2012).

In summary, our screen results are in agreement with Rtt101 fulfilling a complex and manifold role in genome maintenance. Mrc1, Pol32 and Dpb4 are members of the replisome. By their modification, Rtt101 could contribute directly to reshaping and transforming the replisome in response to replication stress and DNA damage. Immunoprecipitation experiments from Matthias Peter's lab show that Rtt101 interacts with the GINS protein Sld5 during perturbed and unperturbed S-phase (Buser, Kellner et al. 2016, see appendix 7.2). Thus Rtt101 might be a constitutive member of the active replication machinery implementing some of the changes necessary in conditions threatening genomic integrity. On the other hand Rtt101 might also act beyond remodelling of the stalled RF and interfere with repair pathways by targeting members of the DDR such as Rad27 and possibly also Met7 and Top1. The efficiency of one or several of the Rtt101-mediated pathways might also be reduced by SUMOylation in a Siz2-dependent manner. Our screen offers a valuable basis for further experiments and also indicates, which complex members might be required to help Rtt101 fulfil its different functions in response to damage-induced replication stress.

4.4 Rtt101 might suppress precocious senescence signalling by delaying the creation of subtelomeric ssDNA through an Mrc1-dependent mechanism

In the second part of this study we tried to elucidate Rtt101's role in preventing the premature senescence of budding yeast cells, which had been reported previously by the Lydall laboratory (Chang, Lawless et al. 2011). Our data show that bulk telomere length in *rtt101 est2* cells is not shorter than in *est2* cells during senescence (Figure 15). Since the length of the shortest telomere determines the onset of replicative senescence (Abdallah, Luciano et al. 2009, Khadaroo, Teixeira et al. 2009, Fallet, Jolivet et al. 2014) Rtt101 might be involved in a telomere maintenance mechanism required at critically short telomeres. Epistasis analysis revealed that *rtt101 rad52 est2* cells are epistatic with *rad52 est2* cells during early senescence. Towards late population doublings, however, *rtt101 rad52 est2* cells lose viability significantly faster than *rad52 est2* cells indicating that Rtt101 promotes a Rad52-independent process close to crisis (Figure 16B). This is reminiscent of our results for Rtt101's role in response to damage-induced replication stress: on the one hand Rtt101 in conjunction with Mms1 seems to allow a Rad52-dependent process to

proceed at stalled RFs. On the other hand the hypersensitivity of *rtt101* and *rad52* cells is additive suggesting that Rtt101 is also involved in Rad52-independent pathways in response to MMS-inflicted damage (Figure 12A and B).

We also tested putative Rtt101 complex members for their role in senescence and found that Mms1, Mms22, Esc2 and Ctf4 senesce prematurely (Figure 14 and Figure 14). Deletion of *MMS1* conferred a senescence phenotype that was strikingly similar to the deletion of *RTT101*. Deletion of *MMS22* caused a more severe phenotype than deletion of *RTT101*. Both effects are reminiscent of the situation after damage infliction by MMS and CPT. Interestingly, Abdallah and co-workers could show that critically short telomeres are kept in a pre-senescent state, in which senescence signalling through Mec1 is suppressed by a pathway involving Rad52 and Mms1 (Abdallah, Luciano et al. 2009). In the presence of Rad52 and Mms1 cells are able to divide for several cell divisions despite telomere attrition. The absence of Rad52 or Mms1 leads to faster cell cycle arrest but does not affect the size of the critically short telomere, which could be followed specifically in this study by using a strain, where Flp1-dependent excision of telomeric repeats allowed the controlled creation of either a short or a very short 7L telomere. This suggests that the switch from the pre-senescent, non-signalling state to the senescence signalling state does not involve a further reduction in telomere length but could rely on a structural switch, for example the exposure of ssDNA. Since both Rad52 and Mms1 are needed for the repair of stalled RFs by sister chromatid recombination (Tsolou and Lydall 2007, Duro, Vaisica et al. 2008) the authors speculate that short telomeres require Rad52 and Mms1 for their replication. Note that sister chromatid recombination would not lead to a re-elongation of the shortest telomere. Instead, sister chromatid recombination could either maintain the short length or prevent the appearance of ssDNA.

The contribution of Rtt101 to the maintenance of the pre-senescence signalling state was not tested in their study. On the basis of the virtually identical premature senescence phenotypes of *rtt101 est2* and *mms1 est2* cells seen in this study and the fact that Mms1 seems to constitutively function in conjunction with Rtt101 it seems plausible to expand their speculations on Rtt101. Measurement of ssDNA throughout the *rtt101 est2* and *est2* senescence curves could give a first indication if Rtt101 prevents premature senescence by the suppression of Mec1 activation through ssDNA.

The argument brought forward by the Teixeira lab that ssDNA could be the molecular structure causing the switch to the senescence signalling state of the critically short telomere and that HR factors detain its appearance is supported by mounting evidence. RPA has been shown to become enriched at telomeres during replicative senescence (Khadaroo, Teixeira et al. 2009). Moreover, Mec1 was identified in numerous studies to be one of the checkpoint proteins crucial to trigger cell cycle arrest due to telomere attrition (Enomoto, Glowczewski et al. 2002, Ijpma and Greider 2003) and ssDNA is a potent Mec1 activator in the DDR. Finally, Rad52 is recruited to eroding telomeres (Khadaroo, Teixeira et al. 2009) and the accumulation of subtelomeric ssDNA increases specifically at short telomeres of senescing cells in the absence of *RAD52* (Fallet, Jolivet et al. 2014).

Two non-exclusive pathways have been suggested by the Teixeira lab as possible sources of the exposition of ssDNA. One, 5'-3' resection factors could be active at short telomere and two, ssDNA gaps might arise during the replication of short telomeres. Indeed, numerous studies have shown that the MRX complex, Sae2 and Exo1 act on telomeres during replicative senescence (Ballew and Lundblad 2013, Fallet, Jolivet et al. 2014).

Interestingly, Mrc1 has been shown to prevent the accumulation of ssDNA at uncapped telomeres of *cdc13-1* and *yku70* cells, which was at least partially due to Exo1 (Grandin and Charbonneau 2007, Tsolou and Lydall 2007). Since shortening telomeres of senescing cells resemble uncapped telomeres due to the progressive loss of telomeric binding sites it is tempting to speculate that Mrc1 also protects short telomeres from the action of Exo1 and possibly also other nucleases thus preventing the accumulation of ssDNA and subsequent Mec1 activation. This would be in agreement with the premature senescence of *mrc1 est2* cells seen in this study (Figure 18) and reported before (Grandin and Charbonneau 2007).

Our senescence assay showed that the deletions of *RTT101* and *MRC1* are not additive, with *rtt101 est2* cells showing a slightly more severe senescence phenotype. This indicates that the premature senescence of *rtt101 est2* cells is in part attributable to loss of the protective function of Mrc1. These data would be in agreement with a highly speculative model depicted in Figure 21, in which Rtt101 stabilizes Mrc1, possibly by degrading Dia2 or another activity targeting Mrc1 for destruction, thus suppressing the formation of ssDNA and delaying the activation of Mec1 and subsequent cell cycle arrest.

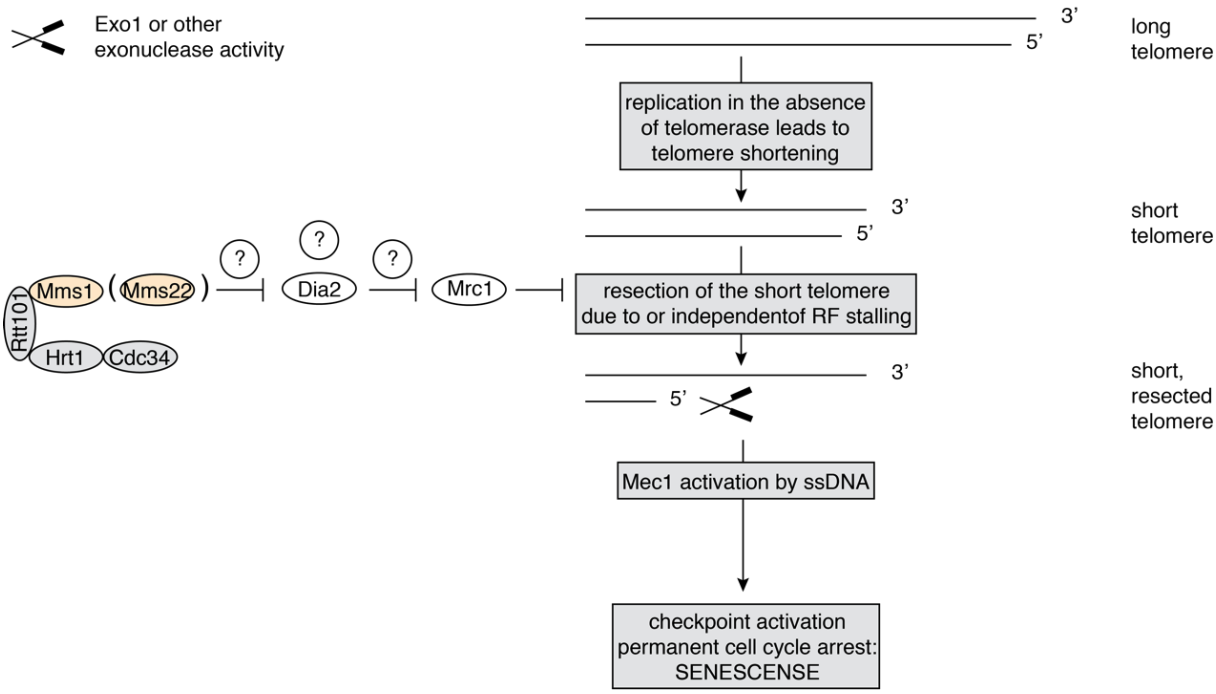

Figure 21 Speculative model on how Rtt101 prevents premature senescence in a pathway depending on Mrc1. In the absence of telomerase telomeres shorten. Short telomeres switch from a pre-senescent, non-signalling state to a senescence-signalling state by resection and exhibition of ssDNA that is partially due to Exo1. Mrc1 prevents ssDNA accumulation. Rtt101 stabilizes Mrc1 thus preventing precocious senescence signalling.

Preliminary data by Martina Dees (Luke lab) support the idea that Mrc1 is indeed stabilized in *est2* cells in an Rtt101-dependent manner.

How Mrc1 protects uncapped telomeres from the action of nucleases remains to be determined. An attractive possibility would be that in the absence of Mrc1 gapped molecules or stalled RFs arise during replication of telomeres allowing nucleolytic attack and excessive production of ssDNA. In this regard it is noteworthy that the 5'-3' exonuclease Exo1 is involved in the resection of both uncapped telomeres (Maringele and Lydall 2002, Zubko, Guillard et al. 2004) and stalled replication forks (Cotta-Ramusino, Fachinetti et al. 2005) highlighting the kinship between these two structures (Tsolou and Lydall 2007). This could allow the ubiquitin E3 ligase Rtt101 to affect both in different ways that are nevertheless connected by their dependence on the replication protein Mrc1: At stalled RFs Rtt101 might mediate selective decoupling thus promoting production of ssDNA and gapped molecules for repair and RF restart. At eroding telomeres Rtt101 might prevent the premature production of ssDNA and precocious cell cycle arrest.

4.5 CUL4A is a promising target for cancer treatment

Complete and faithful chromosome replication is one of the most difficult cellular processes. Replication defects are a major source of genomic instability and a very early feature in the development of cancer (Yeeles, Poli et al. 2013). The *Saccharomyces cerevisiae* ubiquitin E3 ligase protein Rtt101 is required to cope with DNA damage and ensuing replication problems. Rtt101 has also been shown to prevent premature replicative senescence. In this study we tried to shed light on both aspects of Rtt101 function and could identify Mrc1 as a key protein in mediating Rtt101 function.

Rtt101 is thought to be the functional homologue of the human CUL4 subfamily of proteins, which consists of CUL4A and CUL4B. Both CUL4A and CUL4B are overexpressed in various types of cancer including primary breast cancer, squamous cell carcinomas and adrenocortical carcinomas. High expression levels of CUL4A correlate with short patient survival. CUL4A has also been attributed a role in carcinogenesis that is not completely understood, but has been linked to its function in S-phase, the DDR and cell cycle progression. Two drugs expected to interfere with the function of CUL4 and other cullins have been developed as anti-cancer therapeutics. The proteasome inhibitor bortezomib has been approved by the US Food and Drug administration for the treatment of multiple myeloma. The small molecule inhibitor MLN4924, which attenuates cullin activity by preventing cullin neddylation, has entered phase I clinical trials for haematological and solid tumour malignancies. Due to the side effects, which hamper clinical use of bortezomid, the field is currently in search for more selective CUL4A-directed therapeutics. The information used in this paragraph was taken from the following reviews (Lee and Zhou 2010, Sharma and Nag 2014).

Senescence has long been accepted as a powerful tumour suppressor mechanism. The selective induction of senescence as a mechanism of growth suppression has also emerged as a significant strategy in the treatment of cancer, which is exploited in various anticancer agents such as cisplatin. Recent studies suggest that inactivation of cullin ring ligase (CRL) components also triggers senescence in cancer cells. Downregulation of RBX1/ROC1 induces senescence in a variety of cancer cell lines including human colon cancer HCT116 cells, lung cancer H1299

cells, glioma U87 calls and liver cancer cell lines but the exact mechanism remains elusive. The information used in this paragraph was taken from (Pan, Xu et al. 2012). RBX1/ROC1 is a constitutive component of CRL4, which has been shown to target p21 (Abbas, Sivaprasad et al. 2008, Kim, Starostina et al. 2008). Induction of senescence by RBX/ROC1 knockdown depends on p21 in a subset of cell lines. On the basis of our data and in analogy with the function of Rtt101 in *S. cerevisiae* one might speculate that the reported induction of senescence might rely on CRL4 and Claspin.

The accuracy and the significance of this speculation remain to be seen. Irrespective of this it is uncontested that a sound understanding of the cellular processes in response to DNA damage, replication stress and replicative senescence and the crosstalk between them in the model system *Saccharomyces cerevisiae* have the potential to also advance our comprehension of these processes in human cells. In this study we tried to contribute to this goal by elucidating some aspects of Rtt101's role in DNA damage-induced replication stress and replicative senescence.

5 Supplemental Figures

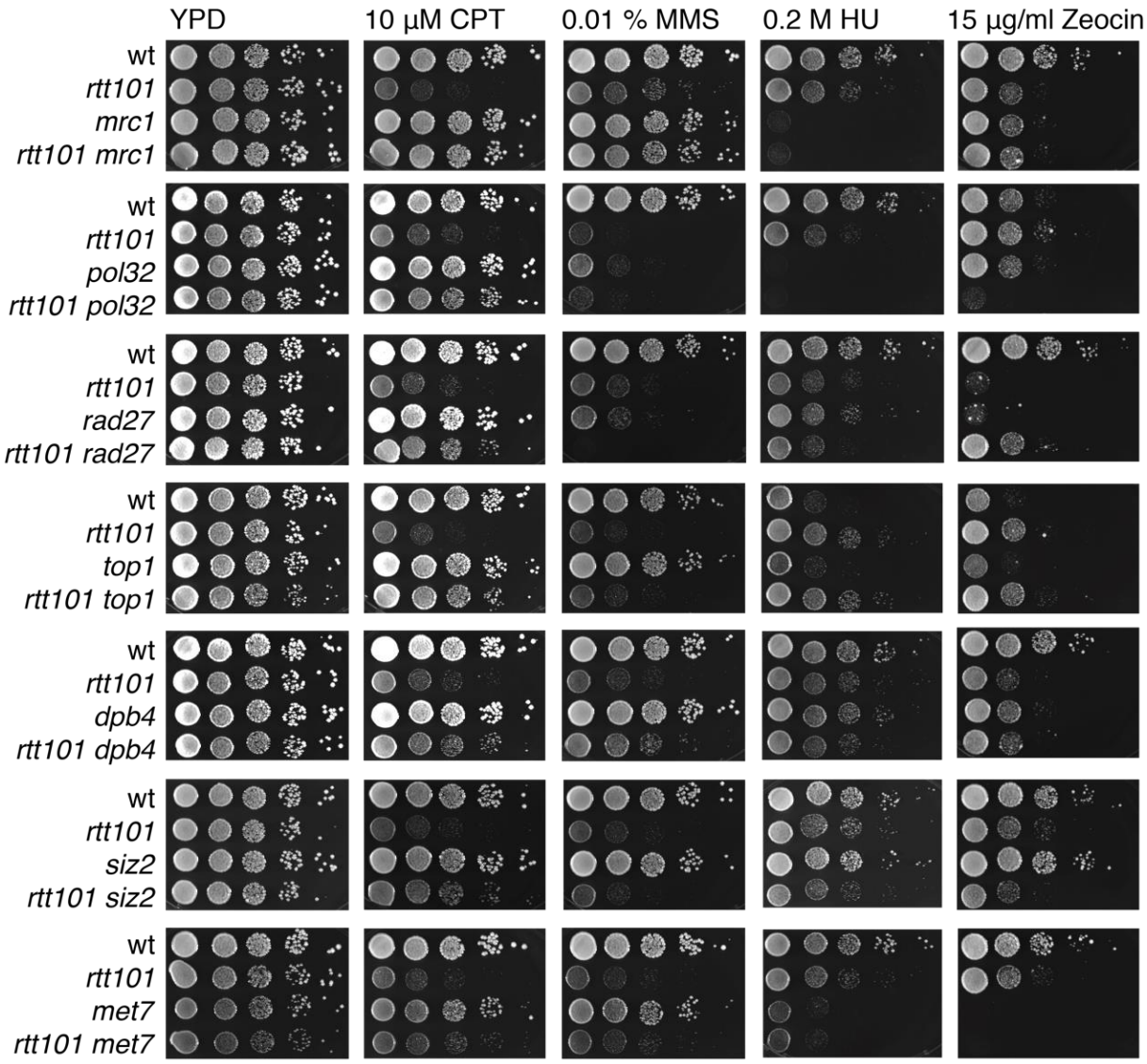

Supplemental Figure 1 Confirmation of screen results: *rtt101* cells were crossed to seven suppressor mutations. Sensitivities of the double and single mutants to CPT and MMS (drugs used in the screen) and to HU and Zeocin were tested. Spottings were performed by Martina Dees.

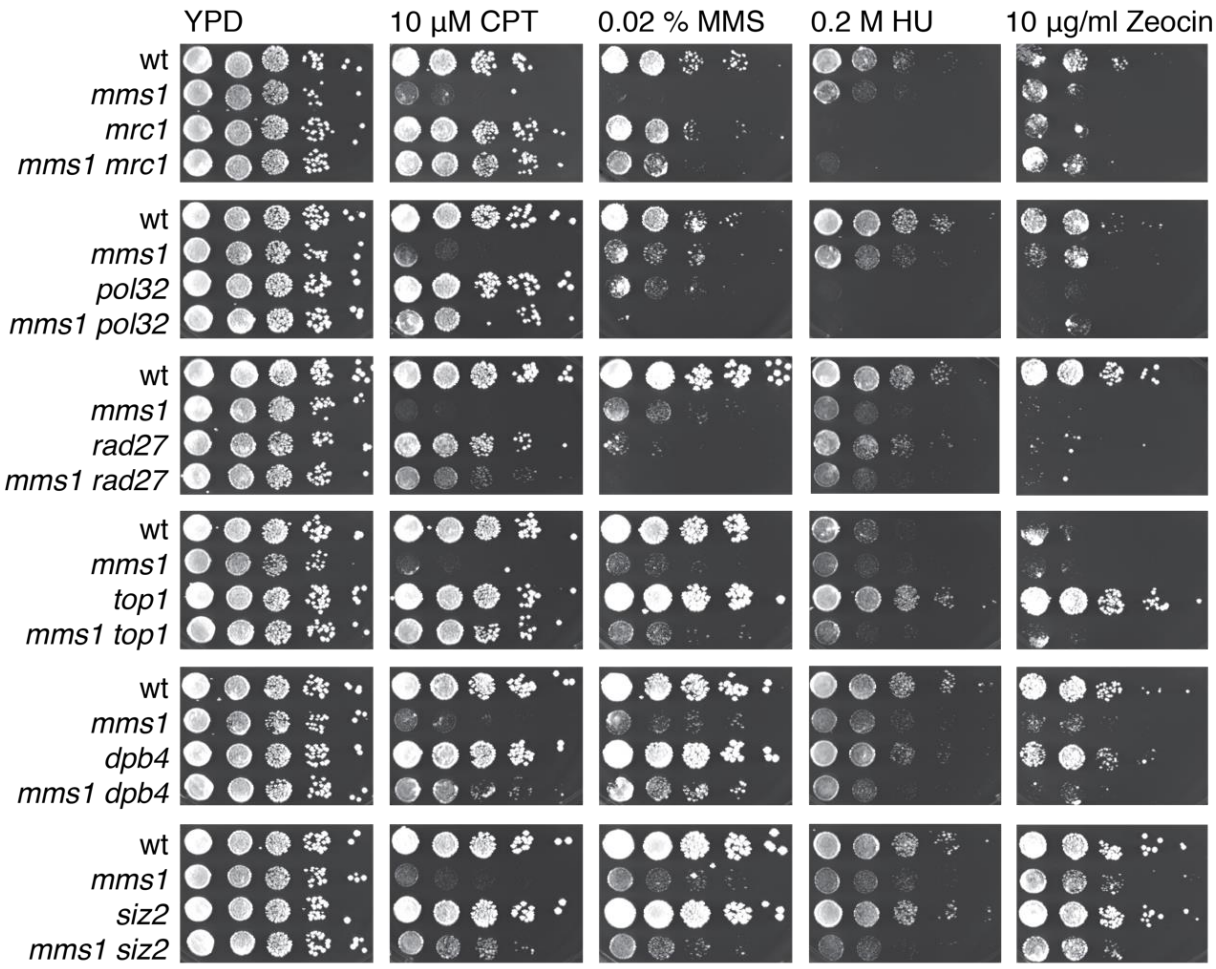

Supplemental Figure 2 The effect of *rtt101* suppressor mutations on the sensitivity of *mms1* cells to CPT, MMS, HU and Zeocin was tested.

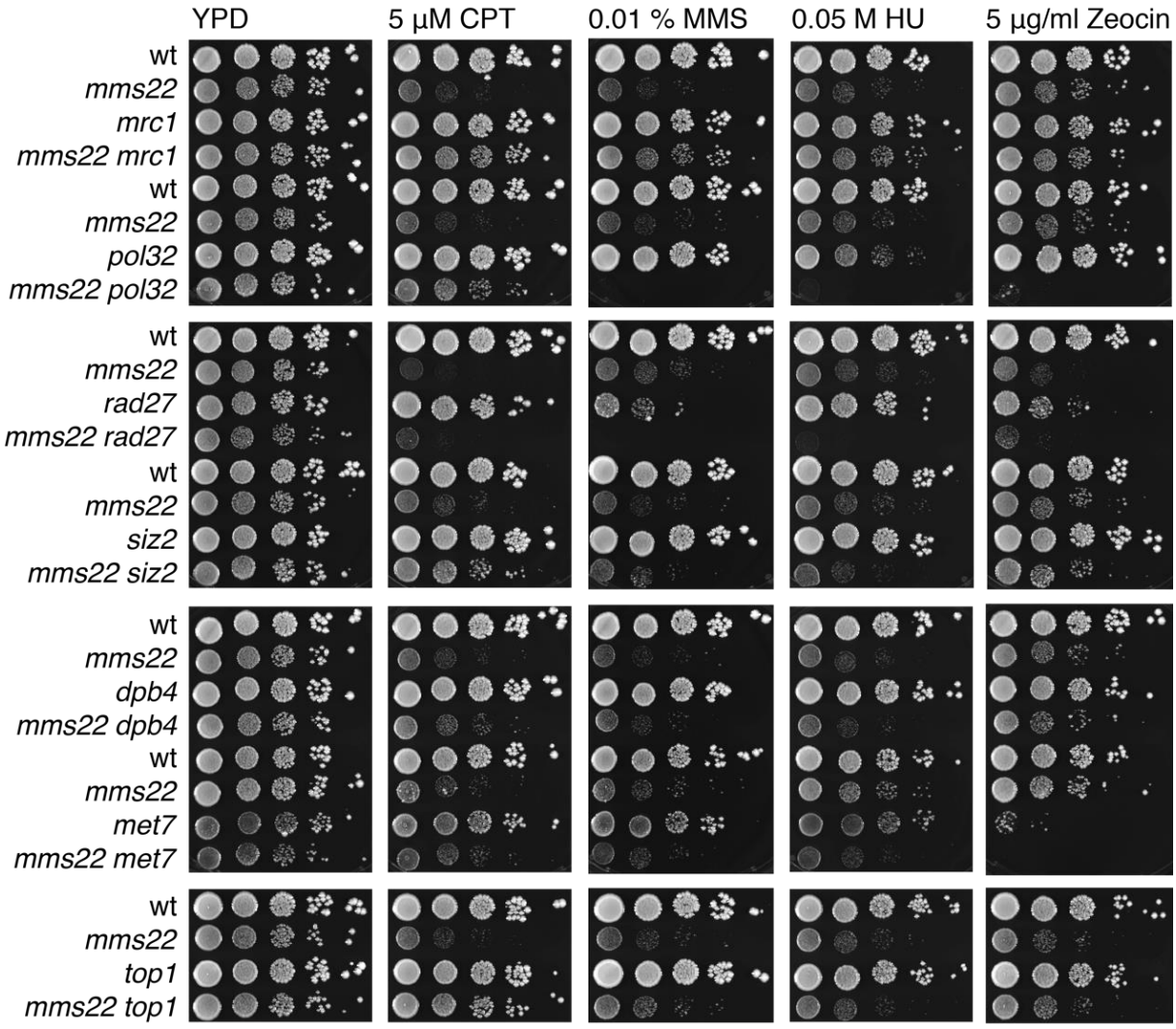

Supplemental Figure 3 The effect of *rtt101* suppressor mutations on the sensitivity of *mms22* cells to CPT, MMS, HU and Zeocin was tested. Spottings were performed by Martina Dees.

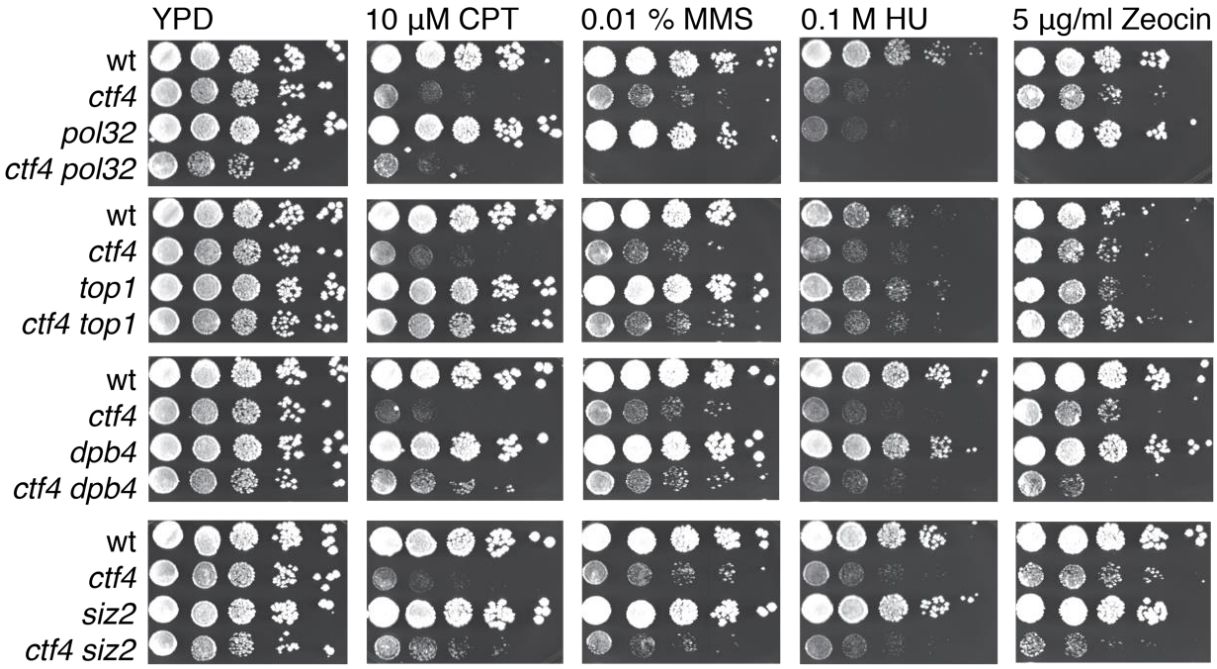

Supplemental Figure 4 The effect of *rtt101* suppressor mutations on the sensitivity of *ctf4* cells to CPT, MMS, HU and Zeocin was tested. The *ctf4 mrc1* and *ctf4 rad27* double mutant were synthetic lethal.

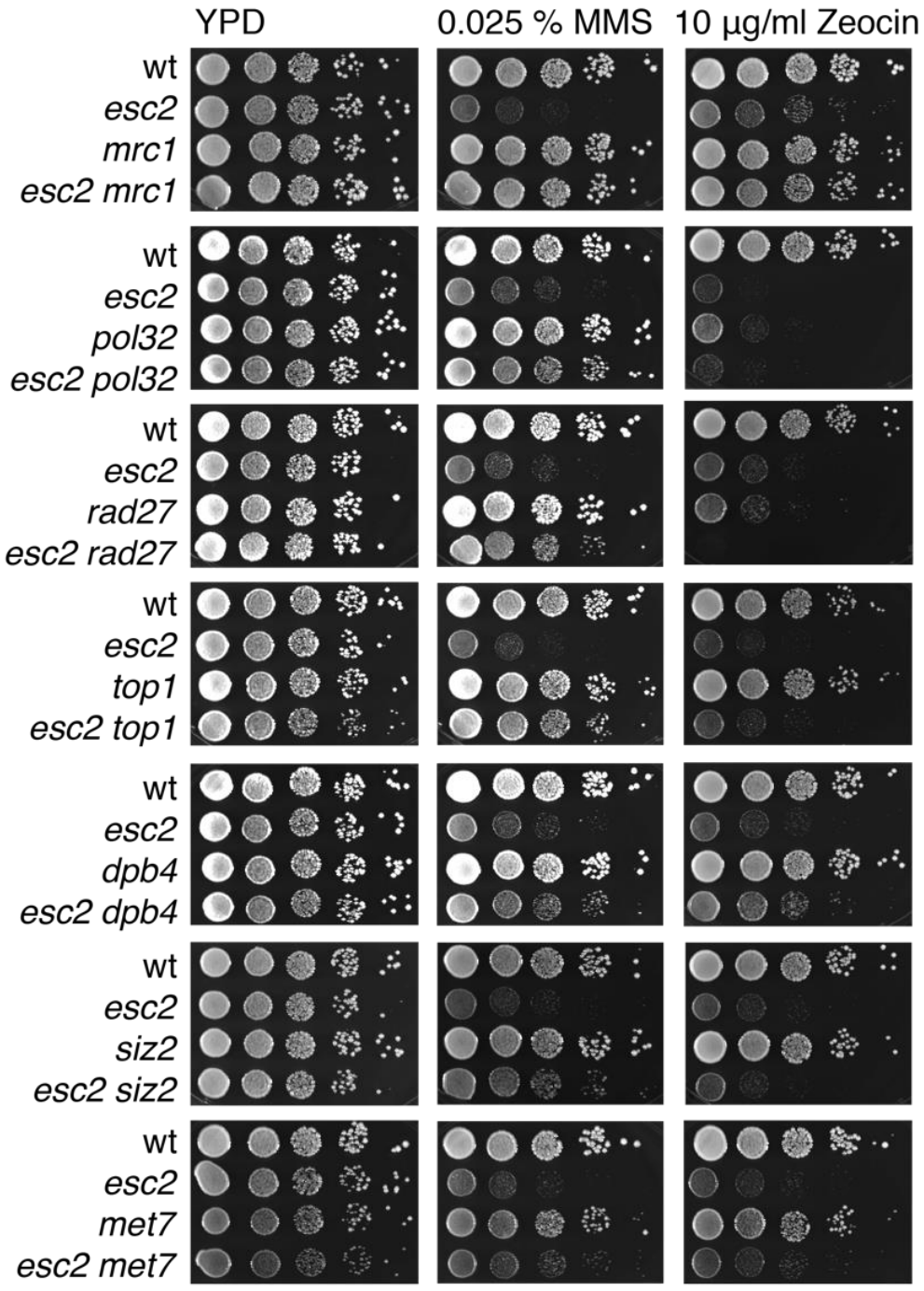

Supplemental Figure 5 The effect of *rtt101* suppressor mutations on the sensitivity of *esc2* cells to MMS and Zeocin was tested. The *esc2* single mutant is not sensitive to CPT and Zeocin. Spottings were performed by Martina Dees.

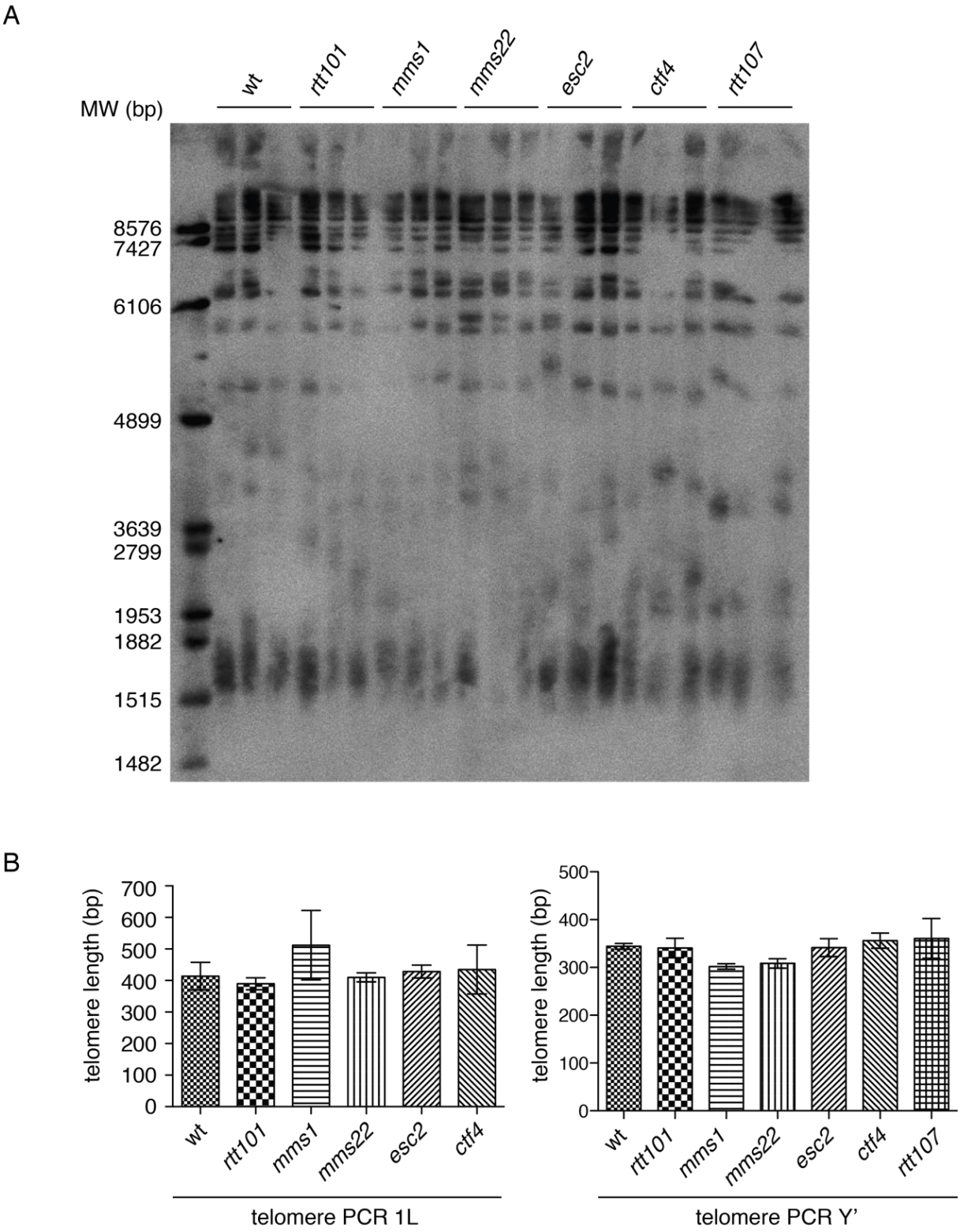

Supplemental Figure 6 Analysis of telomere length in the absence of putative members of Rtt101-assembled complexes. Telomere length measurements in the presence of telomerase were performed after four consecutive streak outs corresponding to approximately 100 PDs. (A) Southern blot of terminal restriction fragments yielded by XhoI digest of genomic DNA. Hybridization was done using a telomeric probe. (B) telomere length as measured by telomere PCR of telomere 1L and 6 Y' telomeres respectively. The mean telomere length and standard deviation of three independent clones are shown.

6 References

Abbas, T., U. Sivaprasad, K. Terai, V. Amador, M. Pagano and A. Dutta (2008). "PCNA-dependent regulation of p21 ubiquitylation and degradation via the CRL4Cdt2 ubiquitin ligase complex." Genes Dev **22**(18): 2496-2506.

Abdallah, P., P. Luciano, K. W. Runge, M. Lisby, V. Geli, E. Gilson and M. T. Teixeira (2009). "A two-step model for senescence triggered by a single critically short telomere." Nat Cell Biol **11**(8): 988-993.

Agarwal, R., Z. Tang, H. Yu and O. Cohen-Fix (2003). "Two distinct pathways for inhibiting pds1 ubiquitination in response to DNA damage." J Biol Chem **278**(45): 45027-45033.

Ahn, J. S., F. Osman and M. C. Whitby (2005). "Replication fork blockage by RTS1 at an ectopic site promotes recombination in fission yeast." EMBO J **24**(11): 2011-2023.

Aksenova, A., K. Volkov, J. Maceluch, Z. F. Pursell, I. B. Rogozin, T. A. Kunkel, Y. I. Pavlov and E. Johansson (2010). "Mismatch repair-independent increase in spontaneous mutagenesis in yeast lacking non-essential subunits of DNA polymerase epsilon." PLoS Genet **6**(11): e1001209.

Alcasabas, A. A., A. J. Osborn, J. Bachant, F. Hu, P. J. Werler, K. Bousset, K. Furuya, J. F. Diffley, A. M. Carr and S. J. Elledge (2001). "Mrc1 transduces signals of DNA replication stress to activate Rad53." Nat Cell Biol **3**(11): 958-965.

Alvino, G. M., D. Collingwood, J. M. Murphy, J. Delrow, B. J. Brewer and M. K. Raghuraman (2007). "Replication in hydroxyurea: it's a matter of time." Mol Cell Biol **27**(18): 6396-6406.

Baldwin, E. L., A. C. Berger, A. H. Corbett and N. Osheroff (2005). "Mms22p protects Saccharomyces cerevisiae from DNA damage induced by topoisomerase II." Nucleic Acids Res **33**(3): 1021-1030.

Balk, B., A. Maicher, M. Dees, J. Klermund, S. Luke-Glaser, K. Bender and B. Luke (2013). "Telomeric RNA-DNA hybrids affect telomere-length dynamics and senescence." Nat Struct Mol Biol **20**(10): 1199-1205.

Ballew, B. J. and V. Lundblad (2013). "Multiple genetic pathways regulate replicative senescence in telomerase-deficient yeast." Aging Cell **12**(4): 719-727.

Bando, M., Y. Katou, M. Komata, H. Tanaka, T. Itoh, T. Sutani and K. Shirahige (2009). "Csm3, Tof1, and Mrc1 form a heterotrimeric mediator complex that associates with DNA replication forks." J Biol Chem **284**(49): 34355-34365.

Ben-Aroya, S., N. Agmon, K. Yuen, T. Kwok, K. McManus, M. Kupiec and P. Hieter (2010). "Proteasome nuclear activity affects chromosome stability by controlling the turnover of Mms22, a protein important for DNA repair." PLoS Genet **6**(2): e1000852.

Bergink, S. and S. Jentsch (2009). "Principles of ubiquitin and SUMO modifications in DNA repair." Nature **458**(7237): 461-467.

Blackburn, E. H., C. W. Greider and J. W. Szostak (2006). "Telomeres and telomerase: the path from maize, Tetrahymena and yeast to human cancer and aging." Nat Med **12**(10): 1133-1138.

Boguslawski, S. J., D. E. Smith, M. A. Michalak, K. E. Mickelson, C. O. Yehle, W. L. Patterson and R. J. Carrico (1986). "Characterization of monoclonal antibody to DNA.RNA and its application to immunodetection of hybrids." J Immunol Methods **89**(1): 123-130.

Bologna, S. and S. Ferrari (2013). "It takes two to tango: Ubiquitin and SUMO in the DNA damage response." Front Genet **4**: 106.

Branzei, D. and M. Foiani (2009). "The checkpoint response to replication stress." DNA Repair (Amst) **8**(9): 1038-1046.

Branzei, D. and M. Foiani (2010). "Maintaining genome stability at the replication fork." Nat Rev Mol Cell Biol **11**(3): 208-219.

Brusky, J., Y. Zhu and W. Xiao (2000). "UBC13, a DNA-damage-inducible gene, is a member of the error-free postreplication repair pathway in Saccharomyces cerevisiae." Curr Genet **37**(3): 168-174.

Burger, R. M. (1998). "Cleavage of Nucleic Acids by Bleomycin." Chemical Reviews **98**(3): 1153-1170.

Buser, R., V. Kellner, A. Melnik, C. Wilson-Zbinden, R. Schellhaas, L. Kastner, W. Piwko, M. Dees, P. Picotti, M. Maric, K. Labib, B. Luke, M. Peter (2016) "The replisome-coupled E3 ubiquitin ligase Rtt101Mms22 counteracts Mrc1 function to tolerate genotoxic stress." PLoS Genet. **12**(2):e1005843

Byun, T. S., M. Pacek, M. C. Yee, J. C. Walter and K. A. Cimprich (2005). "Functional uncoupling of MCM helicase and DNA polymerase activities activates the ATR-dependent checkpoint." Genes Dev **19**(9): 1040-1052.

Cesare, A. J. and R. R. Reddel (2010). "Alternative lengthening of telomeres: models, mechanisms and implications." Nat Rev Genet **11**(5): 319-330.

Chang, H. Y., C. Lawless, S. G. Addinall, S. Oexle, M. Taschuk, A. Wipat, D. J. Wilkinson and D. Lydall (2011). "Genome-wide analysis to identify pathways affecting telomere-initiated senescence in budding yeast." G3 (Bethesda) **1**(3): 197-208.

Chang, M., M. Bellaoui, C. Boone and G. W. Brown (2002). "A genome-wide screen for methyl methanesulfonate-sensitive mutants reveals genes required for S phase progression in the presence of DNA damage." Proc Natl Acad Sci U S A **99**(26): 16934-16939.

Chang, M., J. C. Dittmar and R. Rothstein (2011). "Long telomeres are preferentially extended during recombination-mediated telomere maintenance." Nat Struct Mol Biol **18**(4): 451-456.

Cheng, L., L. Hunke and C. F. Hardy (1998). "Cell cycle regulation of the Saccharomyces cerevisiae polo-like kinase cdc5p." Mol Cell Biol **18**(12): 7360-7370.

Cherest, H. (2000). "Polyglutamylation of Folate Coenzymes Is Necessary for Methionine Biosynthesis and Maintenance of Intact Mitochondrial Genome in Saccharomyces cerevisiae." Journal of Biological Chemistry **275**(19): 14056-14063.

Cockell, M., F. Palladino, T. Laroche, G. Kyrion, C. Liu, A. J. Lustig and S. M. Gasser (1995). "The carboxy termini of Sir4 and Rap1 affect Sir3 localization: evidence for a multicomponent complex required for yeast telomeric silencing." J Cell Biol **129**(4): 909-924.

Collins, S. R., K. M. Miller, N. L. Maas, A. Roguev, J. Fillingham, C. S. Chu, M. Schuldiner, M. Gebbia, J. Recht, M. Shales, H. Ding, H. Xu, J. Han, K. Ingvarsdottir, B. Cheng, B. Andrews, C. Boone, S. L. Berger, P. Hieter, Z. Zhang, G. W. Brown, C. J. Ingles, A. Emili, C. D. Allis, D. P. Toczyski, J. S. Weissman, J. F. Greenblatt and N. J. Krogan (2007). "Functional dissection of protein complexes involved in yeast chromosome biology using a genetic interaction map." Nature **446**(7137): 806-810.

Cortes-Ledesma, F., C. Tous and A. Aguilera (2007). "Different genetic requirements for repair of replication-born double-strand breaks by sister-chromatid recombination and break-induced replication." Nucleic Acids Res **35**(19): 6560-6570.

Cotta-Ramusino, C., D. Fachinetti, C. Lucca, Y. Doksani, M. Lopes, J. Sogo and M. Foiani (2005). "Exo1 processes stalled replication forks and counteracts fork reversal in checkpoint-defective cells." Mol Cell **17**(1): 153-159.

Cusanelli, E., C. A. Romero and P. Chartrand (2013). "Telomeric Noncoding RNA TERRA Is Induced by Telomere Shortening to Nucleate Telomerase Molecules at Short Telomeres." Mol Cell **51**(6): 780-791.

Daraba, A., V. K. Gali, M. Halmai, L. Haracska and I. Unk (2014). "Def1 promotes the degradation of Pol3 for polymerase exchange to occur during DNA-damage--induced mutagenesis in Saccharomyces cerevisiae." PLoS Biol **12**(1): e1001771.

de la Torre-Ruiz, M. A., C. M. Green and N. F. Lowndes (1998). "RAD9 and RAD24 define two additive, interacting branches of the DNA damage checkpoint pathway in budding yeast normally required for Rad53 modification and activation." EMBO J **17**(9): 2687-2698.

de Lange, T. (2005). "Shelterin: the protein complex that shapes and safeguards human telomeres." Genes Dev **19**(18): 2100-2110.

Desai, S. D., L. F. Liu, D. Vazquez-Abad and P. D'Arpa (1997). "Ubiquitin-dependent destruction of topoisomerase I is stimulated by the antitumor drug camptothecin." J Biol Chem **272**(39): 24159-24164.

Deshpande, A. M., I. G. Ivanova, V. Raykov, Y. Xue and L. Maringele (2011). "Polymerase epsilon is required to maintain replicative senescence." Mol Cell Biol **31**(8): 1637-1645.

DeSouza, L., Y. Shen and A. L. Bognar (2000). "Disruption of cytoplasmic and mitochondrial folylpolyglutamate synthetase activity in Saccharomyces cerevisiae." Arch Biochem Biophys **376**(2): 299-312.

Dewar, J. M. and D. Lydall (2012). "Similarities and differences between "uncapped" telomeres and DNA double-strand breaks." Chromosoma **121**(2): 117-130.

Dionne, I. and R. J. Wellinger (1996). "Cell cycle-regulated generation of single-stranded G-rich DNA in the absence of telomerase." Proc Natl Acad Sci U S A **93**(24): 13902-13907.

Dovey, C. L., A. Aslanian, S. Sofueva, J. R. Yates, 3rd and P. Russell (2009). "Mms1-Mms22 complex protects genome integrity in Schizosaccharomyces pombe." DNA Repair (Amst) **8**(12): 1390-1399.

Duro, E., C. Lundin, K. Ask, L. Sanchez-Pulido, T. J. MacArtney, R. Toth, C. P. Ponting, A. Groth, T. Helleday and J. Rouse (2010). "Identification of the MMS22L-TONSL complex that promotes homologous recombination." Mol Cell **40**(4): 632-644.

Duro, E., J. A. Vaisica, G. W. Brown and J. Rouse (2008). "Budding yeast Mms22 and Mms1 regulate homologous recombination induced by replisome blockage." DNA Repair (Amst) **7**(5): 811-818.

Enomoto, S., L. Glowczewski and J. Berman (2002). "MEC3, MEC1, and DDC2 are essential components of a telomere checkpoint pathway required for cell cycle arrest during senescence in Saccharomyces cerevisiae." Mol Biol Cell **13**(8): 2626-2638.

Evans, S. K. and V. Lundblad (1999). "Est1 and Cdc13 as comediators of telomerase access." Science **286**(5437): 117-120.

Fallet, E., P. Jolivet, J. Soudet, M. Lisby, E. Gilson and M. T. Teixeira (2014). "Length-dependent processing of telomeres in the absence of telomerase." Nucleic Acids Res.

Fellerhoff, B., F. Eckardt-Schupp and A. A. Friedl (2000). "Subtelomeric repeat amplification is associated with growth at elevated temperature in yku70 mutants of Saccharomyces cerevisiae." Genetics **154**(3): 1039-1051.

Fong, C. M., A. Arumugam and D. M. Koepp (2013). "The Saccharomyces cerevisiae F-box protein Dia2 is a mediator of S-phase checkpoint recovery from DNA damage." Genetics **193**(2): 483-499.

Foss, E. J. (2001). "Tof1p regulates DNA damage responses during S phase in Saccharomyces cerevisiae." Genetics **157**(2): 567-577.

Gambus, A., F. van Deursen, D. Polychronopoulos, M. Foltman, R. C. Jones, R. D. Edmondson, A. Calzada and K. Labib (2009). "A key role for Ctf4 in coupling the MCM2-7 helicase to DNA polymerase alpha within the eukaryotic replisome." EMBO J **28**(19): 2992-3004.

Gispan A., M. Carmi and N. Barkai (2014). "Checkpoint-independent scaling of the Saccharomyces cerevisiae DNA replication program." BMC Biol 12:79

Gottschling, D. E., O. M. Aparicio, B. L. Billington and V. A. Zakian (1990). "Position effect at S. cerevisiae telomeres: reversible repression of Pol II transcription." Cell **63**(4): 751-762.

Grandin, N., A. Bailly and M. Charbonneau (2005). "Activation of Mrc1, a mediator of the replication checkpoint, by telomere erosion." Biol Cell **97**(10): 799-814.

Grandin, N. and M. Charbonneau (2007). "Mrc1, a non-essential DNA replication protein, is required for telomere end protection following loss of capping by Cdc13, Yku or telomerase." Mol Genet Genomics **277**(6): 685-699.

Greider, C. W. and E. H. Blackburn (1985). "<1-s2.0-0092867485901709-main.pdf>." Cell **43**(2): 405-413.

Greider, C. W. and E. H. Blackburn (1989). "A telomeric sequence in the RNA of Tetrahymena telomerase required for telomere repeat synthesis." Nature **337**(6205): 331-337.

Griffith, J. D., L. Comeau, S. Rosenfield, R. M. Stansel, A. Bianchi, H. Moss and T. de Lange (1999). "Mammalian telomeres end in a large duplex loop." Cell **97**(4): 503-514.

Guo, Z., J. Kanjanapangka, N. Liu, S. Liu, C. Liu, Z. Wu, Y. Wang, T. Loh, C. Kowolik, J. Jamsen, M. Zhou, K. Truong, Y. Chen, L. Zheng and B. Shen (2012). "Sequential posttranslational modifications program FEN1 degradation during cell-cycle progression." Mol Cell **47**(3): 444-456.

Guo, Z., L. Qian, R. Liu, H. Dai, M. Zhou, L. Zheng and B. Shen (2008). "Nucleolar localization and dynamic roles of flap endonuclease 1 in ribosomal DNA replication and damage repair." Mol Cell Biol **28**(13): 4310-4319.

Han, J., Q. Li, L. McCullough, C. Kettelkamp, T. Formosa and Z. Zhang (2010). "Ubiquitylation of FACT by the cullin-E3 ligase Rtt101 connects FACT to DNA replication." Genes Dev **24**(14): 1485-1490.

Han, J., H. Zhang, H. Zhang, Z. Wang, H. Zhou and Z. Zhang (2013). "A Cul4 E3 Ubiquitin Ligase Regulates Histone Hand-Off during Nucleosome Assembly." Cell **155**(4): 817-829.

Hang, L., E., J. Peng, W. Tan, B. Szakal, D. Menolfi, Z. Sheng, K. Lobachev, D. Branzei, W. Feng and X. Zhao (2015). "Rtt107 is a multi-functional scaffold supporting replication progression with partner SUMO and ubiquitin ligases." Mol Cell **60**(2):268-79.

Hanna, J. S., E. S. Kroll, V. Lundblad and F. A. Spencer (2001). "Saccharomyces cerevisiae CTF18 and CTF4 are required for sister chromatid cohesion." Mol Cell Biol **21**(9): 3144-3158.

Harrison, J. C. and J. E. Haber (2006). "Surviving the breakup: the DNA damage checkpoint." Annu Rev Genet **40**: 209-235.

Hartwell, L. H. and T. A. Weinert (1989). "Checkpoints: controls that ensure the order of cell cycle events." Science **246**(4930): 629-634.

Hayflick, L. (1965). "The Limited in Vitro Lifetime of Human Diploid Cell Strains." Exp Cell Res **37**: 614-636.

Heller, R. C. and K. J. Marians (2006). "Replication fork reactivation downstream of a blocked nascent leading strand." Nature **439**(7076): 557-562.

Higa, L. A., I. S. Mihaylov, D. P. Banks, J. Zheng and H. Zhang (2003). "Radiation-mediated proteolysis of CDT1 by CUL4-ROC1 and CSN complexes constitutes a new checkpoint." Nat Cell Biol **5**(11): 1008-15

Higuchi, K., T. Katayama, S. Iwai, M. Hidaka, T. Horiuchi and H. Maki (2003). "Fate of DNA replication fork encountering a single DNA lesion during oriC plasmid DNA replication in vitro." Genes Cells **8**(5): 437-449.

Hirano, Y., K. Fukunaga and K. Sugimoto (2009). "Rif1 and rif2 inhibit localization of tel1 to DNA ends." Mol Cell **33**(3): 312-322.

Hodgson, B., A. Calzada and K. Labib (2007). "Mrc1 and Tof1 regulate DNA replication forks in different ways during normal S phase." Mol Biol Cell **18**(10): 3894-3902.

Hu, J., C. M. McCall, T. Ohta and Y. Xiong (2004) "Targeted ubiquitination of CDT1 by the DDB1-CUL4A-ROC1 ligase in response to DNA damage." Nat Cell Biol **6**(10): 1003-9

Huh, J. and H. Piwnica-Worms (2013). "CRL4(CDT2) targets CHK1 for PCNA-independent destruction." Mol Cell Biol **33**(2): 213-226.

Ijpma A. S. and C. W. Greider (2003). "Short telomeres induce a DNA damage response in Saccharomyces cerevisiae." Mol Biol Cell **14**(3): 987-1001.

Johansson, E., P. Garg and P. M. Burgers (2004). "The Pol32 subunit of DNA polymerase delta contains separable domains for processive replication and proliferating cell nuclear antigen (PCNA) binding." J Biol Chem **279**(3): 1907-1915.

Kang, M. J., C. H. Lee, Y. H. Kang, I. T. Cho, T. A. Nguyen and Y. S. Seo (2010). "Genetic and functional interactions between Mus81-Mms4 and Rad27." Nucleic Acids Res **38**(21): 7611-7625.

Kapitzky, L., P. Beltrao, T. J. Berens, N. Gassner, C. Zhou, A. Wuster, J. Wu, M. M. Babu, S. J. Elledge, D. Toczyski, R. S. Lokey and N. J. Krogan (2010). "Cross-species chemogenomic profiling reveals evolutionarily conserved drug mode of action." Mol Syst Biol **6**: 451.

Katou, Y., Y. Kanoh, M. Bando, H. Noguchi, H. Tanaka, T. Ashikari, K. Sugimoto and K. Shirahige (2003). "S-phase checkpoint proteins Tof1 and Mrc1 form a stable replication-pausing complex." Nature **424**(6952): 1078-1083.

Khadaroo, B., M. T. Teixeira, P. Luciano, N. Eckert-Boulet, S. M. Germann, M. N. Simon, I. Gallina, P. Abdallah, E. Gilson, V. Geli and M. Lisby (2009). "The DNA

damage response at eroded telomeres and tethering to the nuclear pore complex." Nat Cell Biol **11**(8): 980-987.

Kim, Y., N. G. Starostina and E. T. Kipreos (2008). "The CRL4Cdt2 ubiquitin ligase targets the degradation of p21Cip1 to control replication licensing." Genes Dev **22**(18): 2507-2519.

Kipreos, E. T., L. E. Lander, J. P. Wing, W. W. He and E. M. Hedgecock (1996). "cul-1 is required for cell cycle exit in C. elegans and identifies a novel gene family." Cell **85**(6): 829-839.

Komata, M., M. Bando, H. Araki and K. Shirahige (2009). "The direct binding of Mrc1, a checkpoint mediator, to Mcm6, a replication helicase, is essential for the replication checkpoint against methyl methanesulfonate-induced stress." Mol Cell Biol **29**(18): 5008-5019.

Labib, K. (2000). "Uninterrupted MCM2-7 Function Required for DNA Replication Fork Progression." Science **288**(5471): 1643-1647.

Lambert, S., A. Watson, D. M. Sheedy, B. Martin and A. M. Carr (2005). "Gross chromosomal rearrangements and elevated recombination at an inducible site-specific replication fork barrier." Cell **121**(5): 689-702.

Lansdorp, P. M. (2008). "Telomeres, stem cells, and hematology." Blood **111**(4): 1759-1766.

Laplaza, J. M., M. Bostick, D. T. Scholes, M. J. Curcio and J. Callis (2004). "Saccharomyces cerevisiae ubiquitin-like protein Rub1 conjugates to cullin proteins Rtt101 and Cul3 in vivo." Biochem J **377**(Pt 2): 459-467.

Larsen, N. B., E. Sass, C. Suski, H. W. Mankouri and I. D. Hickson (2014). "The Escherichia coli Tus-Ter replication fork barrier causes site-specific DNA replication perturbation in yeast." Nat Commun **5**: 3574.

Lee, J. and P. Zhou (2010). "Cullins and cancer." Genes Cancer **1**(7): 690-699.

Lendvay, T. S., D. K. Morris, J. Sah, B. Balasubramanian and V. Lundblad (1996). "Senescence mutants of Saccharomyces cerevisiae with a defect in telomere replication identify three additional EST genes." Genetics **144**(4): 1399-1412.

Leung G. P., L. Lee, T. I. Schmidt, Shirahige K. and M. S. Kobor (2011) "Rtt107 is required for recruitment of the SMC5/6 complex to DANN double strand breaks." J Biol Chem **286**(29):26250-7.

Lindahl, T. (1993). "Instability and decay of the primary structure of DNA." Nature **362**(6422): 709-715.

Lingner, J., J. P. Cooper and T. R. Cech (1995). "Telomerase and DNA end replication: no longer a lagging strand problem?" Science **269**(5230): 1533-1534.

Lisby, M., J. H. Barlow, R. C. Burgess and R. Rothstein (2004). "Choreography of the DNA damage response: spatiotemporal relationships among checkpoint and repair proteins." Cell **118**(6): 699-713.

Lisby, M. and R. Rothstein (2009). "Choreography of recombination proteins during the DNA damage response." DNA Repair (Amst) **8**(9): 1068-1076.

Lopes, M., M. Foiani and J. M. Sogo (2006). "Multiple mechanisms control chromosome integrity after replication fork uncoupling and restart at irreparable UV lesions." Mol Cell **21**(1): 15-27.

Lou, H., M. Komata, Y. Katou, Z. Guan, C. C. Reis, M. Budd, K. Shirahige and J. L. Campbell (2008). "Mrc1 and DNA polymerase epsilon function together in linking DNA replication and the S phase checkpoint." Mol Cell **32**(1): 106-117.

Luciano, P., P., M., Dehé, S., Audebert, V., Géli, Y., Corda (2015) "Replisome function during replicative stress is modulated by histone h3 lysine 56 acetylation through Ctf4." Genetics **199**(4):1047-63

Luke, B., G. Versini, M. Jaquenoud, I. W. Zaidi, T. Kurz, L. Pintard, P. Pasero and M. Peter (2006). "The cullin Rtt101p promotes replication fork progression through damaged DNA and natural pause sites." Curr Biol **16**(8): 786-792.

Lundblad, V. and E. H. Blackburn (1993). "An alternative pathway for yeast telomere maintenance rescues est1- senescence." Cell **73**(2): 347-360.

Lundblad, V. and J. W. Szostak (1989). "A mutant with a defect in telomere elongation leads to senescence in yeast." Cell **57**(4): 633-643.

Luo, K., M. A. Vega-Palas and M. Grunstein (2002). "Rap1-Sir4 binding independent of other Sir, yKu, or histone interactions initiates the assembly of telomeric heterochromatin in yeast." Genes Dev **16**(12): 1528-1539.

Lydeard, J. R., Z. Lipkin-Moore, Y. J. Sheu, B. Stillman, P. M. Burgers and J. E. Haber (2010). "Break-induced replication requires all essential DNA replication factors except those specific for pre-RC assembly." Genes Dev **24**(11): 1133-1144.

Mailand, N., S. Bekker-Jensen, J. Bartek and J. Lukas (2006). "Destruction of Claspin by SCFbetaTrCP restrains Chk1 activation and facilitates recovery from genotoxic stress." Mol Cell **23**(3): 307-318.

Makarova, A. V., J. L. Stodola and P. M. Burgers (2012). "A four-subunit DNA polymerase zeta complex containing Pol delta accessory subunits is essential for PCNA-mediated mutagenesis." Nucleic Acids Res **40**(22): 11618-11626.

Makovets, S., I. Herskowitz and E. H. Blackburn (2004). "Anatomy and Dynamics of DNA Replication Fork Movement in Yeast Telomeric Regions." Molecular and Cellular Biology **24**(9): 4019-4031.

Mao, Y., M. Sun, S. D. Desai and L. F. Liu (2000). "SUMO-1 conjugation to topoisomerase I: A possible repair response to topoisomerase-mediated DNA damage." Proc Natl Acad Sci U S A **97**(8): 4046-4051.

Maringele, L. and D. Lydall (2002). "EXO1-dependent single-stranded DNA at telomeres activates subsets of DNA damage and spindle checkpoint pathways in budding yeast yku70Delta mutants." Genes Dev **16**(15): 1919-1933.

Martin, S. G., T. Laroche, N. Suka, M. Grunstein and S. M. Gasser (1999). "Relocalization of Telomeric Ku and SIR Proteins in Response to DNA Strand Breaks in Yeast." Cell **97**(5): 621-633.

Mathias, N., S. L. Johnson, M. Winey, A. E. Adams, L. Goetsch, J. R. Pringle, B. Byers and M. G. Goebl (1996). "Cdc53p acts in concert with Cdc4p and Cdc34p to control the G1-to-S-phase transition and identifies a conserved family of proteins." Mol Cell Biol **16**(12): 6634-6643.

McInerney, P. and M. O'Donnell (2004). "Functional uncoupling of twin polymerases: mechanism of polymerase dissociation from a lagging-strand block." J Biol Chem **279**(20): 21543-21551.

Michel, J. J., J. F. McCarville and Y. Xiong (2003). "A role for Saccharomyces cerevisiae Cul8 ubiquitin ligase in proper anaphase progression." J Biol Chem **278**(25): 22828-22837.

Miles, J. and T. Formosa (1992). "Protein affinity chromatography with purified yeast DNA polymerase alpha detects proteins that bind to DNA polymerase." Proc Natl Acad Sci U S A **89**(4): 1276-1280.

Miller, K. M., O. Rog and J. P. Cooper (2006). "Semi-conservative DNA replication through telomeres requires Taz1." Nature **440**(7085): 824-828.

Mimura, S., M. Komata, T. Kishi, K. Shirahige and T. Kamura (2009). "SCF(Dia2) regulates DNA replication forks during S-phase in budding yeast." EMBO J **28**(23): 3693-3705.

Mimura, S., T. Yamaguchi, S. Ishii, E. Noro, T. Katsura, C. Obuse and T. Kamura (2010). "Cul8/Rtt101 forms a variety of protein complexes that regulate DNA damage response and transcriptional silencing." J Biol Chem **285**(13): 9858-9867.

Moldovan, G. L., B. Pfander and S. Jentsch (2007). "PCNA, the maestro of the replication fork." Cell **129**(4): 665-679.

Mortensen, U. H., M. Lisby and R. Rothstein (2009). "Rad52." Curr Biol **19**(16): R676-677.

Nakagawa T. and Y. Xiong (2011). "X-linked mental retardation gene CUL4B targets ubiquitylation of H3K4 methyltransferase component WDR5 and regulates neuronal gene expression." Mol Cell **43**(3):381-91.

Nelson, S. W. and S. J. Benkovic (2010). "Response of the bacteriophage T4 replisome to noncoding lesions and regression of a stalled replication fork." J Mol Biol **401**(5): 743-756.

O'Donnell, L., S. Panier, J. Wildenhain, J. M. Tkach, A. Al-Hakim, M. C. Landry, C. Escribano-Diaz, R. K. Szilard, J. T. Young, M. Munro, M. D. Canny, N. K. Kolas, W. Zhang, S. M. Harding, J. Ylanko, M. Mendez, M. Mullin, T. Sun, B. Habermann, A. Datti, R. G. Bristow, A. C. Gingras, M. D. Tyers, G. W. Brown and D. Durocher (2010). "The MMS22L-TONSL complex mediates recovery from replication stress and homologous recombination." Mol Cell **40**(4): 619-631.

O'Neill, B. M., S. J. Szyjka, E. T. Lis, A. O. Bailey, J. R. Yates, 3rd, O. M. Aparicio and F. E. Romesberg (2007). "Pph3-Psy2 is a phosphatase complex required for Rad53 dephosphorylation and replication fork restart during recovery from DNA damage." Proc Natl Acad Sci U S A **104**(22): 9290-9295.

Ohya, T., S. Maki, Y. Kawasaki and A. Sugino (2000). "Structure and function of the fourth subunit (Dpb4p) of DNA polymerase epsilon in Saccharomyces cerevisiae." Nucleic Acids Res **28**(20): 3846-3852.

Ohouo, P. Y., F. M. Bastos de Oliveira, B. S. Almeida and M. B. Smolka (2010). "DNA damage signaling recruits the Rtt107-Slx4 scaffold via Dpb11 to mediate replication stress response." Mol Cell **39**(2):300-6.

Olovnikov, A. M. (1973). "A theory of marginotomy. The incomplete copying of template margin in enzymic synthesis of polynucleotides and biological significance of the phenomenon." J Theor Biol **41**(1): 181-190.

Osborn, A. J. and S. J. Elledge (2003). "Mrc1 is a replication fork component whose phosphorylation in response to DNA replication stress activates Rad53." Genes Dev **17**(14): 1755-1767.

Pan, X., P. Ye, D. S. Yuan, X. Wang, J. S. Bader and J. D. Boeke (2006). "A DNA integrity network in the yeast Saccharomyces cerevisiae." Cell **124**(5): 1069-1081.

Pan, Y., H. Xu, R. Liu and L. Jia (2012). "Induction of cell senescence by targeting to Cullin-RING Ligases (CRLs) for effective cancer therapy." Int J Biochem Mol Biol **3**(3): 273-281.

Pardo, B. and S. Marcand (2005). "Rap1 prevents telomere fusions by nonhomologous end joining." EMBO J **24**(17): 3117-3127.

Parker, J. L. and H. D. Ulrich (2012). "A SUMO-interacting motif activates budding yeast ubiquitin ligase Rad18 towards SUMO-modified PCNA." Nucleic Acids Res **40**(22): 11380-11388.

Parsons, A. B., R. L. Brost, H. Ding, Z. Li, C. Zhang, B. Sheikh, G. W. Brown, P. M. Kane, T. R. Hughes and C. Boone (2004). "Integration of chemical-genetic and genetic interaction data links bioactive compounds to cellular target pathways." Nat Biotechnol **22**(1): 62-69.

Peschiaroli, A., N. V. Dorrello, D. Guardavaccaro, M. Venere, T. Halazonetis, N. E. Sherman and M. Pagano (2006). "SCFbetaTrCP-mediated degradation of Claspin regulates recovery from the DNA replication checkpoint response." Mol Cell **23**(3): 319-329.

Pinder, J. B., K. M. Attwood and G. Dellaire (2013). "Reading, writing, and repair: the role of ubiquitin and the ubiquitin-like proteins in DNA damage signaling and repair." Front Genet **4**: 45.

Pommier, Y. (2006). "Topoisomerase I inhibitors: camptothecins and beyond." Nat Rev Cancer **6**(10): 789-802.

Pommier, Y. (2013). "Drugging topoisomerases: lessons and challenges." ACS Chem Biol **8**(1): 82-95.

Poschke, H., M. Dees, M. Chang, S. Amberkar, L. Kaderali, R. Rothstein and B. Luke (2012). "Rif2 promotes a telomere fold-back structure through Rpd3L recruitment in budding yeast." PLoS Genet **8**(9): e1002960.

Povirk, L. F. (1996). "DNA damage and mutagenesis by radiomimetic DNA-cleaving agents: bleomycin, neocarzinostatin and other enediynes." Mutat Res **355**(1-2): 71-89.

Puddu, F., G. Piergiovanni, P. Plevani and M. Muzi-Falconi (2011). "Sensing of replication stress and Mec1 activation act through two independent pathways involving the 9-1-1 complex and DNA polymerase epsilon." PLoS Genet **7**(3): e1002022.

Ralph E., E. Boye and S. E. Kearsey (2006). "DNA damage induces Cdt1 proteolysis in fission yeast through a pathway dependent on Cdt2 and Ddb1." EMBO Rep **7**(11): 1134-9.

Redon, C., D. R. Pilch, E. P. Rogakou, A. H. Orr, N. F. Lowndes and W. M. Bonner (2003). "Yeast histone 2A serine 129 is essential for the efficient repair of checkpoint-blind DNA damage." EMBO Rep **4**(7): 678-684.

Ribar, B., L. Prakash and S. Prakash (2007). "ELA1 and CUL3 are required along with ELC1 for RNA polymerase II polyubiquitylation and degradation in DNA-damaged yeast cells." Mol Cell Biol **27**(8): 3211-3216.

Ritchie, K. B. and T. D. Petes (2000). "The Mre11p/Rad50p/Xrs2p complex and the Tel1p function in a single pathway for telomere maintenance in yeast." Genetics **155**(1): 475-479.

Roberts, T. M., I. W. Zaidi, J. A. Vaisica, M. Peter and G. W. Brown (2008). "Regulation of rtt107 recruitment to stalled DNA replication forks by the cullin rtt101 and the rtt109 acetyltransferase." Mol Biol Cell **19**(1): 171-180.

Rogakou, E. P., D. R. Pilch, A. H. Orr, V. S. Ivanova and W. M. Bonner (1998). "DNA Double-stranded Breaks Induce Histone H2AX Phosphorylation on Serine 139." Journal of Biological Chemistry **273**(10): 5858-5868.

Rouse, J. and S. P. Jackson (2002). "Interfaces between the detection, signaling, and repair of DNA damage." Science **297**(5581): 547-551.

Rouse, J. and S. P. Jackson (2002). "Lcd1p recruits Mec1p to DNA lesions in vitro and in vivo." Mol Cell **9**(4): 857-869.

Sanchez, Y. (1999). "Control of the DNA Damage Checkpoint by Chk1 and Rad53 Protein Kinases Through Distinct Mechanisms." Science **286**(5442): 1166-1171.

Sarikas, A., T. Hartmann and Z. Q. Pan (2011). "The cullin protein family." Genome Biol **12**(4): 220.

Scholes D. T., M. Banerjee, B. Bowen and M. J. Curcio (2001). "Multiple regulators of Ty1 transposition in Saccharomyces cerevisiae have conserved roles in genome maintenance." Genetics **159**(4):1449-65.

Senga T., U. Sivaprasad, W. Zhu, J. H. Park, E. E. Arias, J. C. Walter and A. Dutta (2006) "PCNA is a cofactor for Cdt1 degradation by CUL4/DDB1-mediated N-terminal ubiquitination." J Biol Chem **281**(10): 6246-52.

Sharma, P. and A. Nag (2014). "CUL4A ubiquitin ligase: a promising drug target for cancer and other human diseases." Open Biol **4**: 130217.

Simon, A. C., J. C. Zhou, R. L. Perera, F. van Deursen, C. Evrin, M. E. Ivanova, M. L. Kilkenny, L. Renault, S. Kjaer, D. Matak-Vinkovic, K. Labib, A. Costa and L. Pellegrini (2014). "A Ctf4 trimer couples the CMG helicase to DNA polymerase alpha in the eukaryotic replisome." Nature **510**(7504): 293-297.

Soudet, J., P. Jolivet and M. T. Teixeira (2014). "Elucidation of the DNA end-replication problem in Saccharomyces cerevisiae." Mol Cell **53**(6): 954-964.

Szyjka, S. J., C. J. Viggiani and O. M. Aparicio (2005). "Mrc1 is required for normal progression of replication forks throughout chromatin in S. cerevisiae." Mol Cell **19**(5): 691-697.

Takeuchi, Y., T. Horiuchi and T. Kobayashi (2003). "Transcription-dependent recombination and the role of fork collision in yeast rDNA." Genes Dev **17**(12): 1497-1506.

Tanaka, H., Y. Katou, M. Yagura, K. Saitoh, T. Itoh, H. Araki, M. Bando and K. Shirahige (2009). "Ctf4 coordinates the progression of helicase and DNA polymerase alpha." Genes Cells **14**(7): 807-820.

Tanaka, K. and P. Russell (2001). "Mrc1 channels the DNA replication arrest signal to checkpoint kinase Cds1." Nat Cell Biol **3**(11): 966-972.

Tanaka, K. and P. Russell (2004). "Cds1 phosphorylation by Rad3-Rad26 kinase is mediated by forkhead-associated domain interaction with Mrc1." J Biol Chem **279**(31): 32079-32086.

Teixeira, M. T. (2013). "Saccharomyces cerevisiae as a Model to Study Replicative Senescence Triggered by Telomere Shortening." Front Oncol **3**: 101.

Teixeira, M. T., M. Arneric, P. Sperisen and J. Lingner (2004). "Telomere length homeostasis is achieved via a switch between telomerase- extendible and -nonextendible states." Cell **117**(3): 323-335.

Thu, H. P., T. A. Nguyen, P. R. Munashingha, B. Kwon, Q. Dao Van and Y. S. Seo (2015). "A physiological significance of the functional interaction between Mus81 and Rad27 in homologous recombination repair." Nucleic Acids Res **43**(3): 1684-1699.

Tkach, J. M., A. Yimit, A. Y. Lee, M. Riffle, M. Costanzo, D. Jaschob, J. A. Hendry, J. Ou, J. Moffat, C. Boone, T. N. Davis, C. Nislow and G. W. Brown (2012). "Dissecting

DNA damage response pathways by analysing protein localization and abundance changes during DNA replication stress." Nat Cell Biol **14**(9): 966-976.

Toh, G. W., A. M. O'Shaughnessy, S. Jimeno, I. M. Dobbie, M. Grenon, S. Maffini, A. O'Rorke and N. F. Lowndes (2006). "Histone H2A phosphorylation and H3 methylation are required for a novel Rad9 DSB repair function following checkpoint activation." DNA Repair (Amst) **5**(6): 693-703.

Tong, A., H., G. Lesage, G. D. Bader, H. Ding, H, Xu, X. Xin, J. Young, G. F. Berriz, R. L. Brost, M. Chang, Y. Chen, X. Cheng, G. Chua, H. Friesen, D. S. Goldberg, J. Haynes, C. Humphries, G. He, S. Hussein, L. Ke, N. Krogan, Z. Li, J. N. Levinson, H. Lu, P. Ménard, C. Munyana, A. B. Parsons, O. Ryan, R. Tonikian, T. Roberts, A. M. Sdicu, J. Shapiro, B. Sheikh, B. Suter, S. L. Wong, L. V. Zhang, H. Zhu, C. G. Burd, S. Munro, C. Sander, J. Rine, J. Greenblatt, M. Peter, A. Bretscher, G. Bell, F. P. Roth, G. W. Brown, B. Andrews, H. Bussey and C. Boone (2004). "Global mapping of the yeast genetic interaction network." Science **303**(5659): 808-13.

Tong, A. H., M. Evangelista, A. B. Parsons, H. Xu, G. D. Bader, N. Page, M. Robinson, S. Raghibizadeh, C. W. Hogue, H. Bussey, B. Andrews, M. Tyers and C. Boone (2001). "Systematic genetic analysis with ordered arrays of yeast deletion mutants." Science **294**(5550): 2364-2368.

Tourriere, H., G. Versini, V. Cordon-Preciado, C. Alabert and P. Pasero (2005). "Mrc1 and Tof1 promote replication fork progression and recovery independently of Rad53." Mol Cell **19**(5): 699-706.

Tsolou, A. and D. Lydall (2007). "Mrc1 protects uncapped budding yeast telomeres from exonuclease EXO1." DNA Repair (Amst) **6**(11): 1607-1617.

Tsukamoto, Y., A. K. Taggart and V. A. Zakian (2001). "The role of the Mre11-Rad50-Xrs2 complex in telomerase- mediated lengthening of Saccharomyces cerevisiae telomeres." Curr Biol **11**(17): 1328-1335.

Uzunova, S. D., A. S. Zarkov, A. M. Ivanova, S. S. Stoynov and M. N. Nedelcheva-Veleva (2014). "The subunits of the S-phase checkpoint complex Mrc1/Tof1/Csm3: dynamics and interdependence." Cell Div **9**: 4.

Vaisica, J. A., A. Baryshnikova, M. Costanzo, C. Boone and G. W. Brown (2011). "Mms1 and Mms22 stabilize the replisome during replication stress." Mol Biol Cell **22**(13): 2396-2408.

Van, C., S. Yan, W. M. Michael, S. Waga and K. A. Cimprich (2010). "Continued primer synthesis at stalled replication forks contributes to checkpoint activation." J Cell Biol **189**(2): 233-246.

Vejrup-Hansen, R., K. Mizuno, I. Miyabe, O. Fleck, C. Holmberg, J. M. Murray, A. M. Carr and O. Nielsen (2011). "Schizosaccharomyces pombe Mms1 channels repair of perturbed replication into Rhp51 independent homologous recombination." DNA Repair (Amst) **10**(3): 283-295.

Verdun, R. E. and J. Karlseder (2006). "The DNA damage machinery and homologous recombination pathway act consecutively to protect human telomeres." Cell **127**(4): 709-720.

Walmsley, R. W., C. S. Chan, B. K. Tye and T. D. Petes (1984). "Unusual DNA sequences associated with the ends of yeast chromosomes." Nature **310**(5973): 157-160.

Waris, G. and H. Ahsan (2006). "Reactive oxygen species: role in the development of cancer and various chronic conditions." J Carcinog **5**: 14.

Watson, J. D. (1972). "Origin of concatemeric T7 DNA." Nat New Biol **239**(94): 197-201.

Wellinger, R. J., A. J. Wolf and V. A. Zakian (1993). "Saccharomyces telomeres acquire single-strand TG1-3 tails late in S phase." Cell **72**(1): 51-60.

Willems, A. R., M. Schwab and M. Tyers (2004). "A hitchhiker's guide to the cullin ubiquitin ligases: SCF and its kin." Biochim Biophys Acta **1695**(1-3): 133-170.

Wu, D., L. M. Topper and T. E. Wilson (2008). "Recruitment and dissociation of nonhomologous end joining proteins at a DNA double-strand break in Saccharomyces cerevisiae." Genetics **178**(3): 1237-1249.

Wyatt, M. D. and D. L. Pittman (2006). "Methylating agents and DNA repair responses: Methylated bases and sources of strand breaks." Chem Res Toxicol **19**(12): 1580-1594.

Xu, Z., Duc, K. H., Holcman, D., Teixeira, M. T. (2013). "The Length on the Shortest Telomere as the Major Determinant of the Onset of Replicative Senescence." Genetics.

Yeeles, J. T. and K. J. Marians (2011). "The Escherichia coli replisome is inherently DNA damage tolerant." Science **334**(6053): 235-238.

Yeeles, J. T., J. Poli, K. J. Marians and P. Pasero (2013). "Rescuing stalled or damaged replication forks." Cold Spring Harb Perspect Biol **5**(5): a012815.

Zaidi, I. W., G. Rabut, A. Poveda, H. Scheel, J. Malmstrom, H. Ulrich, K. Hofmann, P. Pasero, M. Peter and B. Luke (2008). "Rtt101 and Mms1 in budding yeast form a CUL4(DDB1)-like ubiquitin ligase that promotes replication through damaged DNA." EMBO Rep **9**(10): 1034-1040.

Zhao, H., K. Tanaka, E. Nogochi, C. Nogochi and P. Russell (2003). "Replication checkpoint protein Mrc1 is regulated by Rad3 and Tel1 in fission yeast." Mol Cell Biol **23**(22): 8395-8403.

Zhao, X., A. Chabes, V. Domkin, L. Thelander and R. Rothstein (2001). "The ribonucleotide reductase inhibitor Sml1 is a new target of the Mec1/Rad53 kinase cascade during growth and in response to DNA damage." EMBO J **20**(13): 3544-3553.

Zhao, X. and R. Rothstein (2002). "The Dun1 checkpoint kinase phosphorylates and regulates the ribonucleotide reductase inhibitor Sml1." Proc Natl Acad Sci U S A **99**(6): 3746-3751.

Zhou, Z. and S. J. Elledge (1993). "DUN1 encodes a protein kinase that controls the DNA damage response in yeast." Cell **75**(6): 1119-1127.

Zubko, M. K., S. Guillard and D. Lydall (2004). "Exo1 and Rad24 differentially regulate generation of ssDNA at telomeres of Saccharomyces cerevisiae cdc13-1 mutants." Genetics **168**(1): 103-115.

7 Appendix

7.1 Abbreviations

A	alanine
AA	amino acid
Ab	antibody
ALT	alternative lengthening of telomeres
APC	anaphase promoting complex
Arg	arginine
ATP	adenosine triphosphate
BER	base excision repair
BIR	break-induced replication
bp	base pairs
CDK	cyclin-dependent kinase
ChIP	chromatin immunoprecipitation
CMG	Cdc45-MCM-GINS
CPT	camptothecin
CRL	cullin-RING ubiquitin E3 ligase
CST	Cdc13-Stn1-Ten1
dCTP	deoxycytidine triphosphate
dd	double-distilled
DDR	DNA damage response
DMSO	dimethyl sulfoxide
DNA	deoxyribonucleic acid
dNTP	deoxyribonucleotide
ds	double-stranded
DSB	double-strand break
dTMP	deoxythymidine monophosphate
E-MAP	epistatic miniarray profile
EtOH	ethanol
ExoI	exonuclease I
FACS	fluorescence-activated cell sorting

g	gram
Gal	galactose
GCR	gross chromosomal rearrangements
GFP	green fluorescent protein
h	hour
HDR	homology-directed repair
His	histidine
HR	homologous recombination
H. sapiens	*Homo sapiens*
HU	hydroxyurea
Hyg	hygromycin B
K	lysine
Kan	kanamycin
kb	kilobases
L	litre
Leu	leucine
Lys	lysine
LiAc	lithium acetate
M	molar
mg	milligram
µg	microgram
MCM	minichromosome maintenance
mM	millimolar
MMS	methylmethane sulfonate
min	minute
mL	millilitre
µL	microlitre
µM	micromolar
µm	micrometre
Nat	nourseothricin
NER	nucleotide excision repair
ng	nanogram
NHEJ	non-homologous end joining
nM	nanomolar

nm	nanometre
nt	nucleotide
OD	optical density
PCR	polymerase chain reaction
PCNA	proliferating cell nuclear antigen
PD	population doubling
Pol	polymerase
PTM	post-translational modification
Q	glutamine
RF	replication fork
RC	replicative complex
RFC	replication factor C
rDNA	ribosomal DNA
RNA	ribonucleic acid
RNR	ribonucleotide reductase
RPA	replication protein A
rpm	rounds per minute
RT	room temperature
S	serine
S. cerevisiae	*Saccharomyces cerevisiae*
SCF	Skp1 Cullin F-box
SD	synthetic dropout
SDS	sodium dodecyl sulphate
sec	second
s.e.m.	standard error of the mean
SGA	synthetic genetic array
ss	single-stranded
S-phase	synthesis phase
T	threonine
TLS	translesion synthesis
TMM	telomere maintenance mechanism
Top1	topoisomerase I
TRF	terminal restriction fragment
Ura	uracil

UV	ultra violet
V	Volt
wt	wild type
YPD	yeast extract peptone dextrose

7.2 This thesis contributed to the following publication

PLOS | GENETICS

RESEARCH ARTICLE

The Replisome-Coupled E3 Ubiquitin Ligase Rtt101^{Mms22} Counteracts Mrc1 Function to Tolerate Genotoxic Stress

Raymond Buser[1☯], Vanessa Kellner[2☯¤], Andre Melnik[1], Caroline Wilson-Zbinden[1], René Schellhaas[2¤], Lisa Kastner[2], Wojciech Piwko[1], Martina Dees[2], Paola Picotti[1], Marija Maric[3], Karim Labib[3], Brian Luke[2¤*], Matthias Peter[1*]

1 Institute of Biochemistry, Department of Biology, ETH Zurich, Zürich, Switzerland, **2** Zentrum für Molekulare Biologie der Universität Heidelberg (ZMBH), Heidelberg, Germany, **3** MRC Protein Phosphorylation and Ubiquitylation Unit, College of Life Sciences, University of Dundee, Dundee, Scotland, United Kingdom

☯ These authors contributed equally to this work.
¤ Current address: Institute of Molecular Biology (IMB), Mainz, Germany
* b.luke@imb-mainz.de (BL); matthias.peter@bc.biol.ethz.ch (MP)

OPEN ACCESS

Citation: Buser R, Kellner V, Melnik A, Wilson-Zbinden C, Schellhaas R, Kastner L, et al. (2016) The Replisome-Coupled E3 Ubiquitin Ligase Rtt101^{Mms22} Counteracts Mrc1 Function to Tolerate Genotoxic Stress. PLoS Genet 12(2): e1005843. doi:10.1371/journal.pgen.1005843

Editor: Judith L. Campbell, California Institute of Technology, UNITED STATES

Received: May 21, 2015

Accepted: January 12, 2016

Published: February 5, 2016

Data Availability Statement: All relevant data are within the paper and its Supporting Information files.

Funding: RB was funded by an EMBO short-term fellowship (ASTF 162-2012; http://www.embo.org/funding-awards/fellowships/short-term-fellowships) and VK by the International PhD Program (IPP). Work in the Luke laboratory is supported by the IMB and the Peter laboratory by the Swiss National Science Foundation, an ERC senior award and ETHZ. Work in Karim Labib's group is funded by the Medical Research Council and the Wellcome Trust (reference 102943/Z/13/Z for a senior investigator

Abstract

Faithful DNA replication and repair requires the activity of cullin 4-based E3 ubiquitin ligases (CRL4), but the underlying mechanisms remain poorly understood. The budding yeast Cul4 homologue, Rtt101, in complex with the linker Mms1 and the putative substrate adaptor Mms22 promotes progression of replication forks through damaged DNA. Here we characterized the interactome of Mms22 and found that the Rtt101^{Mms22} ligase associates with the replisome progression complex during S-phase via the amino-terminal WD40 domain of Ctf4. Moreover, genetic screening for suppressors of the genotoxic sensitivity of *rtt101Δ* cells identified a cluster of replication proteins, among them a component of the fork protection complex, Mrc1. In contrast to *rtt101Δ* and *mms22Δ* cells, *mrc1Δ rtt101Δ* and *mrc1Δ mms22Δ* double mutants complete DNA replication upon replication stress by facilitating the repair/restart of stalled replication forks using a Rad52-dependent mechanism. Our results suggest that the Rtt101^{Mms22} E3 ligase does not induce Mrc1 degradation, but specifically counteracts Mrc1's replicative function, possibly by modulating its interaction with the CMG (Cdc45-MCM-GINS) complex at stalled forks.

Author Summary

Post-translational protein modifications, such as ubiquitylation, are essential for cells to respond to environmental cues. In order to understand how eukaryotes cope with DNA damage, we have investigated a conserved E3 ubiquitin ligase complex required for the resistance to carcinogenic chemicals. This complex, composed of Rtt101, Mms1 and Mms22 in budding yeast, plays a critical role in regulating the fate of stalled DNA replication. Here, we found that the Rtt101^{Mms22} E3 ubiquitin ligase complex interacts with the replisome during S-phase, and orchestrates the repair/restart of DNA synthesis after

award to KL). The funders had no role in study design, data collection and analysis, decision to publish, or preparation of the manuscript.

Competing Interests: The authors have declared that no competing interests exist.

stalling by activating a Rad52-dependent homologous recombination pathway. Our findings indicate that Rtt101^{Mms22} specifically counteracts the replicative activity of Mrc1, a subunit of the fork protection complex, possibly by modulating its interaction with the CMG (Cdc45-MCM-GINS) helicase complex upon fork stalling. Altogether, our study unravels a functional protein cluster that is essential to understand how eukaryotic cells cope with DNA damage during replication and, thus deepens our knowledge of the biology that underlies carcinogenesis.

Introduction

DNA replication is a process through which cells duplicate their entire genome prior to cell division. To achieve accurate replication, eukaryotes have evolved intricate surveillance systems that allow fine-tuning of the replication machinery. In order to continually provide the replicative polymerase with a single stranded DNA template, replisomes must adapt to chromatin heterogeneities such as aberrant DNA structures, condensed chromatids, transcriptional obstacles and DNA-protein barriers [1]. In *Saccharomyces cerevisiae*, this adaptation is regulated by proteins such as Mrc1, Tof1, Csm3 and Ctf4, which assemble around the CMG (Cdc45-MCM-GINS) DNA helicase at replication forks. These components form the 'Replisome Progression Complex' (RPC), a replisome sub-assembly that exists exclusively at replication forks [2]. The RPC functions in coupling DNA polymerases to the CMG helicase [3,4], and in regulating fork progression [5–9]. Moreover, these replisome components also limit mutagenic frequency and prevent unscheduled homologous recombination (HR) events at stalled forks [10–12]. Mrc1 possesses two polymerase epsilon (Pol ε) binding sites [13] as well as an Mcm6 interaction motif [14], and is required for checkpoint activation in response to replication stress [15]. Tof1 and Csm3 help to link Mrc1 to fork components [16,17] but also have distinct functions not shared with Mrc1 [9]. Conversely, the replication fork progression defect is enhanced in *mrc1Δ* compared to *tof1Δ* and *csm3Δ* mutants [1], implying that Mrc1 also promotes replication functions independent of Tof1 and Csm3. Ctf4, the yeast homologue of human AND1, bridges the interaction of the primase, DNA polymerase-α, to the CMG helicase [3,5,18]. Although the coupling of the CMG to leading and lagging strand DNA polymerases preserves genome integrity during unperturbed DNA replication, this mechanism is partially disrupted when forks encounter replication stress. Indeed, significant stretches of ssDNA generated by uncoupling can promote HR-mediated replication re-start via either a template switch or break-induced replication (BIR) [19].

Growing evidence implicates Cullin-RING containing E3 ligases (CRL's) in regulating DNA replication and repair [20]. For example, Cdc53/Cul1 in a complex with the F-box adaptor protein Dia2 (SCF^{Dia2}) promotes the ubiquitylation of the Mcm7 subunit of the CMG helicase, which triggers Cdc48/p97-dependent disassembly of CMG at the end of DNA replication [21]. In addition, SCF^{Dia2} has been reported to antagonize Mrc1 upon replication stress, possibly by inducing degradation of phosphorylated Mrc1 to recover from checkpoint arrest following repair [22–24]. Cullin4 (CRL4)-based E3 ubiquitin ligases regulate DNA replication and repair both in yeast and mammalian cells, in part by controlling histone dynamics at active replication forks [25]. Rtt101, the budding yeast analogue of human Cul4 [26], has been reported to target Spt16, a subunit of the FACT complex that reorganizes nucleosomes during DNA replication [27]. Moreover, Rtt101 promotes replication fork progression through DNA lesions and natural pause sites [28]. This function is dependent on *MMS1* and *MMS22*, which encode a DDB1-like linker protein and a putative substrate specific adaptor,

respectively [26]. However, the underlying mechanisms and function of the Rtt101-Mms1-Mms22 complex (termed Rtt101^{Mms22}) remain largely elusive. Recent results suggest that the sensitivity of *mms1Δ*, *mms22Δ* and *rtt101Δ* cells to the DNA-damaging drugs CPT and MMS could be rescued by further deleting *MRC1* [18,29], possibly by de-regulating late firing origins [29].

Here we show that the Rtt101^{Mms22} E3 ubiquitin ligase genetically and biochemically interacts with components of the replication fork. We found that the WD40 domain of Ctf4, a protein required for coupling the CMG complex to the replicative polymerases, recruits Mms22 to active forks during S-phase. Moreover, Mms22 physically associates with Mrc1 and deletion of the *MRC1* gene suppresses the defects of *rtt101Δ*, *mms1Δ* and *mms22Δ* cells, including genotoxic sensitivity, prolonged checkpoint activation and reduced HR rates. Importantly, our results suggest that de-repression of late replication origins is not sufficient to bypass the need of Rtt101^{Mms22} E3-ligase activity. Instead, *MRC1* deletion promotes HR-mediated repair of replication forks that have paused in response to replication stress. Based on genetic and biochemical data we propose that the Rtt101^{Mms22} complex specifically counteracts the replicative, and not the checkpoint, function of Mrc1, possibly by modulating its interaction with the CMG helicase complex upon fork stalling.

Results

RTT101, *MMS1* and *MMS22* interact genetically with proteins involved in replication

To elucidate the role of the Rtt101^{Mms22} E3 ubiquitin ligase in DNA replication, we employed an automated SGA approach [30] to screen for genes that, when deleted, would suppress the growth defects of *rtt101Δ* cells exposed to either the alkylating agent methyl methanesulfonate (MMS) or the topoisomerase 1 (Top1) poison camptothecin (CPT) [31] (Figs 1A and S1). The SGA screen was performed in duplicate and only suppressors that appeared in both screens were considered for further analysis. The combined results for MMS and CPT conditions initially identified 63 suppressor genes that were scored by visual inspection as either strong, medium or weak (S1 Table). Only the strong and medium hits were validated by crossing the single deletion mutants to an independent *rtt101Δ* strain, in which double mutants were derived by manual tetrad dissection. Cells were then spotted in biological duplicate on MMS and CPT containing media as depicted in Fig 1C–1E. Using this workflow, we confirmed a list of 16 genes that when deleted improved the growth of *rtt101Δ* cells (Fig 1B). Among the most potent suppressors are genes directly involved in DNA replication, including *MRC1*, *POL32*, *RAD27*, *TOP1*, *SIZ2* and *DPB4*. Additional suppressor mutations implicated in other biological processes were also confirmed (Fig 1B), but were not further characterized in this study. Some suppressors such as the lagging strand polymerase subunit Pol32 only restored growth on CPT containing media (Fig 1B–1D), indicating that the screening approach could isolate functional protein sub-clusters. The slow growth phenotype of other Rtt101-based E3 ubiquitin ligase component mutants, including those lacking the linker protein Mms1 (Fig 1D) as well as mutants deleted for the putative substrate specific adaptor Mms22 (Fig 1E), were rescued by deleting the identical replication gene cluster that suppressed the *rtt101Δ* cell phenotype. These data indicate that Rtt101 likely acts as a fully assembled E3 ubiquitin ligase in a process associated with replication stress. Indeed, deletion of *MRC1* suppressed the growth defects of cells expressing the neddylation-deficient Rtt101-K791R mutant [32], implying that loss of *MRC1* suppresses the phenotypes correlated with inactivation of Rtt101^{Mms22} E3 ligase activity (S2 Fig). In contrast, deletion of *MRC1* did not rescue the MMS sensitivity of *ubc13Δ* cells defective for PCNA polyubiquitylation (S3 Fig), indicating that the genetic suppression is specific to the

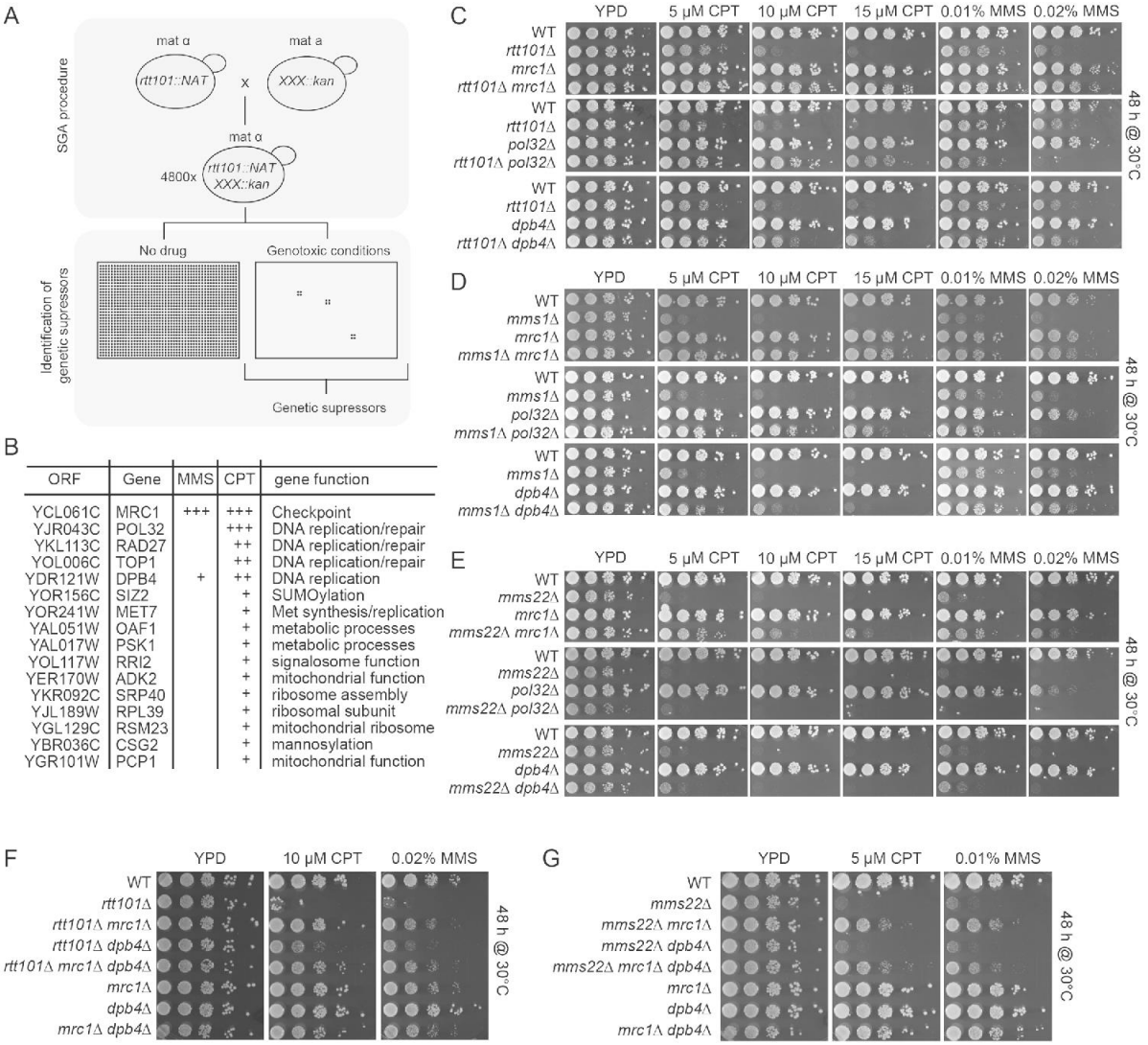

ORF	Gene	MMS	CPT	gene function
YCL061C	MRC1	+++	+++	Checkpoint
YJR043C	POL32		+++	DNA replication/repair
YKL113C	RAD27		++	DNA replication/repair
YOL006C	TOP1		++	DNA replication/repair
YDR121W	DPB4	+	++	DNA replication
YOR156C	SIZ2		+	SUMOylation
YOR241W	MET7		+	Met synthesis/replication
YAL051W	OAF1		+	metabolic processes
YAL017W	PSK1		+	metabolic processes
YOL117W	RRI2		+	signalosome function
YER170W	ADK2		+	mitochondrial function
YKR092C	SRP40		+	ribosome assembly
YJL189W	RPL39		+	ribosomal subunit
YGL129C	RSM23		+	mitochondrial ribosome
YBR036C	CSG2		+	mannosylation
YGR101W	PCP1		+	mitochondrial function

Fig 1. The Rtt101-Mms1-Mms22 E3 ubiquitin ligase genetically interacts with genes involved in DNA replication. (A) and (B) Schematic representation of the synthetic genetic array (SGA) screening procedure (A), and table summarizing cellular functions of the main hits (B). Genotoxic conditions included MMS (0.01%) and CPT (5 μM) and colony size was qualitatively scored after 72 hours at 30°C. (+) weak suppression, (++) medium suppression, (+++) strong suppression. See Materials and Methods for a detailed description of the screening procedure and S1 Fig for an example of the raw data. (C) *RTT101* genetically interacts with the replication genes *MRC1*, *POL32* and *DPB4*. Serial dilution of wild-type (WT) or *rtt101Δ*, *mrc1Δ*, *rtt101Δ mrc1Δ*, *pol32Δ*, *rtt101Δ pol32Δ*, *dpb4Δ* and *rtt101Δ dpb4Δ* mutants were assayed on normal growth media (YPD), and media containing 5 μM, 10 μM and 15 μM CPT or 0.01% and 0.02% MMS. Cells were imaged after 48 hours of incubation at 30°C.(D) *MMS1* phenocopies the genetic interactions of *RTT101* with *MRC1*, *POL32* and *DPB4*. Serial dilution of wild-type (WT) or *mms1Δ*, *mrc1Δ*, *mms1Δ mrc1Δ*, *pol32Δ*, *mms1Δ pol32Δ*, *dpb4Δ* and *mms1Δ dpb4Δ* mutants were assayed on normal growth media (YPD), and media containing 5 μM, 10 μM and 15 μM CPT or 0.01% and 0.02% MMS. Cells were imaged after 48 hours of incubation at 30°C. (E) *MMS22* phenocopies the genetic interactions of *RTT101* and *MMS1* with *MRC1* and *DPB4*, but not *POL32*. Serial dilution of wild-type (WT) or *mms22Δ*, *mrc1Δ*, *mms22Δ mrc1Δ*, *pol32Δ*, *mms22Δ pol32Δ*, *dpb4Δ* and *mms22Δ dpb4Δ* mutants were assayed on normal growth media (YPD), and media containing 5 μM, 10 μM and 15 μM CPT or 0.01% and 0.02% MMS. Cells were imaged after 48 hours of incubation at 30°C. (F) and (G). *mrc1Δ* and *dpb4Δ* rescue *rtt101Δ* and *mms22Δ* in an epistatic manner. Cells were spotted on the indicated media and imaged as described above in (C, D and E).

doi:10.1371/journal.pgen.1005843.g001

loss of Rtt101^{Mms22} function and not other ubiquitylation-defective mutants involved in lesion bypass repair [33].

MRC1 and *DPB4* are both linked to the putative leading strand polymerase, Pol ε, and deletion of these genes showed suppression on both MMS and CPT containing media, albeit to varying extents. Furthermore, when the deletions of *DPB4* and *MRC1* were combined in the absence of either *RTT101* or *MMS22*, we observed that the genetic rescue was not additive (Fig 1F and 1G). Unlike in *rtt101Δ* or *mms1Δ* cells, the deletion of *POL32* did not rescue the CPT sensitivity of *mms22Δ* cells (Fig 1E), supporting the notion that Mms22 has additional functions independent of the E3 ligase complex [34]. Taken together, these data demonstrate that deletion of replication genes such as *MRC1* and *DPB4* can alleviate the growth defects associated with impaired Rtt101^{Mms22} E3 ubiquitin ligase activity in response to multiple genotoxic agents.

The Rtt101^{Mms22} complex associates with replisomes during S-phase

The above genetic data suggests that the Rtt101^{Mms22} complex may directly interact with the replisome. Since specificity of a CRL complex is mainly conferred by the substrate adaptor [35], we immunoprecipitated Mms22 from S-phase synchronized cells and identified associated proteins by an unbiased mass-spectrometry method referred to as shotgun LC-MS/MS (Fig 2A). As expected, Mms22 co-purified with the E3 ligase subunits Rtt101, Mms1 and Hrt1, with the core histones Htb2, Hhf1, Hta1, and Hht1, as well as with the FACT complex (Spt16, Pob3), a nucleosome re-organizer that likely facilitates the interactions between DNA replication and transcription. These findings are consistent with previously published data showing that Rtt101-Mms1 associates with histone H3 [25] and ubiquitylates the Spt16 subunit of FACT [27]. We also detected a cluster of replication factors, including components of the GINS- (go-ichi-ni-san), the fork protection- and the MCM helicase complexes (Fig 2A, see also S2 Table for a complete list of Mms22-interacting proteins). These results strengthen the genetic interaction clusters that were found to suppress the growth defects of *rtt101Δ* cells, and strongly suggest a function of Rtt101^{Mms22} at replisomes during S-phase.

To better characterize the interaction of Mms22 with replisome components, we immunoprecipitated functional epitope-tagged versions of Mms22 (PA-Mms22) (Fig 2C) and the GINS complex (TAP-Sld5) (Fig 2D) from cells synchronized in G1 and S-phase with normal or genotoxic stress (0.03% MMS) growth conditions (Fig 2B). We observed that Mms22 and Rtt101 interact with all tested components of the replisome progression complex during S-phase (Fig 2C and 2D). Remarkably, Ctf4 and the FACT complex showed affinity for Mms22 in both G1 and S-phase, although both interactions were more prominent during S-phase. The induction of DNA damage through MMS treatment did not alter the observed interactions, suggesting that the Rtt101^{Mms22} E3 ligase is not specifically recruited to replisomes upon genotoxic insult, but rather constitutively associates with the active replication machinery.

Ctf4 tethers the Rtt101^{Mms22} E3 ubiquitin ligase to active replisomes

We next examined how the Rtt101^{Mms22} E3 ligase is recruited to active replisomes. Ctf4 was an intriguing candidate as it was previously found to interact with Mms22 [3,18,36]. Indeed, genetic analysis revealed that the growth defect of *ctf4Δ* cells on genotoxic drugs was epistatic with *RTT101* and even slightly suppressed the sensitivity of *mms22Δ* cells (Fig 3A), consistent with previous findings [36]. To test whether Ctf4 tethers Mms22 to the replisome, we compared the presence of replisome components in Mms22 purifications prepared from wild-type and *ctf4Δ* cells (Fig 3B). Notably, Mms22 failed to interact with the replication factors

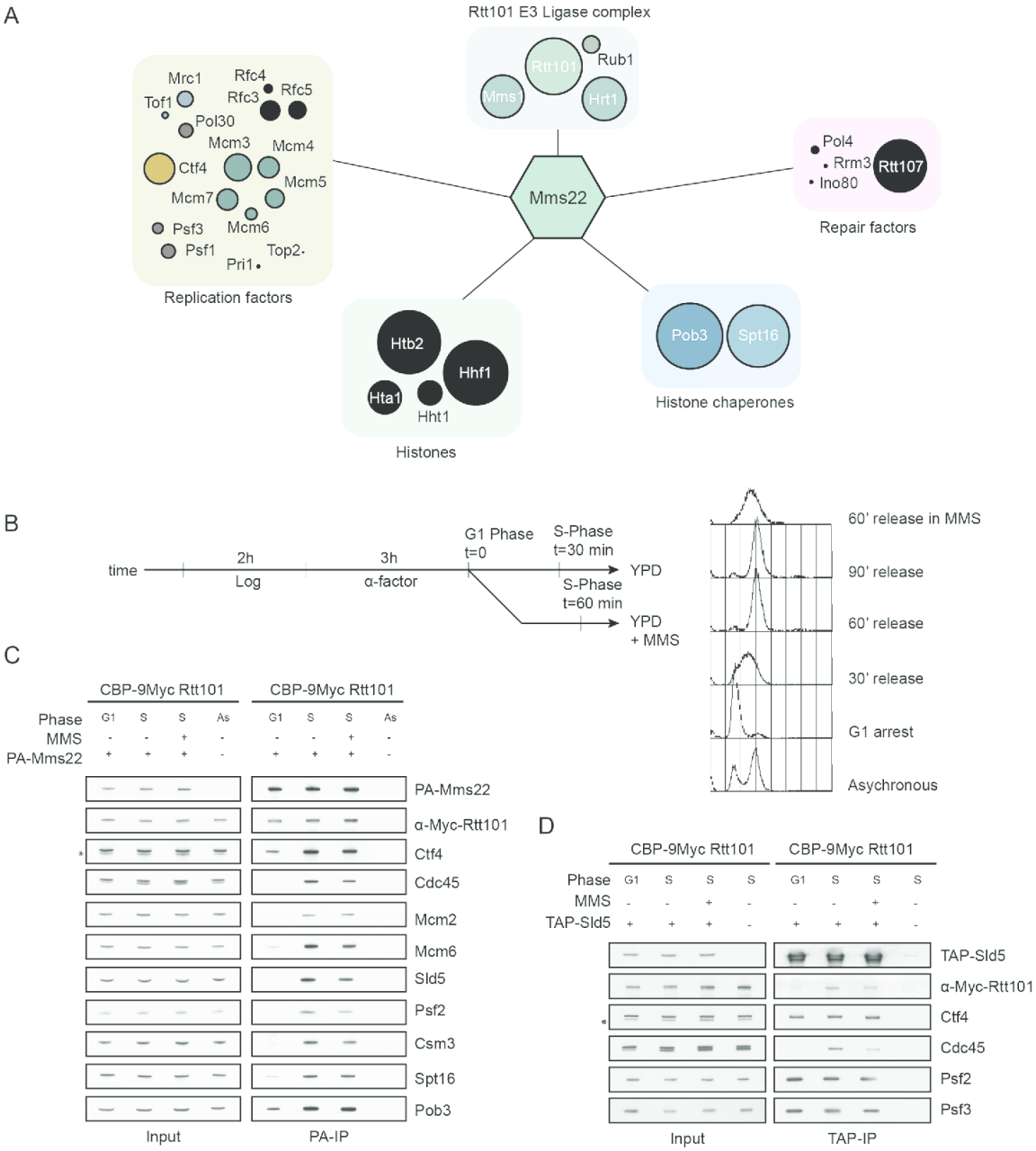

Fig 2. The substrate-specific adaptor Mms22 physically interacts with replisome components during S-phase. (A) The S-phase specific Mms22 interaction network identified by MS/MS. PA-tagged Mms22 was immunoprecipitated from cells synchronized in S-phase and associated proteins were identified by MS-analysis. The hits were grouped according to known functions and the ring diameter is proportional to the percent of coverage measured for the indicated proteins. (B) and (C) Mms22 physically interacts with components of the replisome during S-phase. Cells endogenously expressing CBP-9Myc-Rtt101 were transformed with PA-Mms22 and synchronized in S-phase by release from α-factor arrest as schematically outlined (B), and either treated or not

with 0.03% MMS to induce fork stalling. Visualizing the DNA content by flow cytometry monitored cell synchronization. PA-Mms22 was immunoprecipitated from the indicated cell extracts and associated proteins detected by immunoblotting using specific antibodies (C). The asterisk (*) indicates an unspecific band. (D) S-phase specific interaction of Rtt101 with replisome components. Cells endogenously expressing CBP-9Myc-Rtt101 and TAP-Sld5 were synchronized and treated as in (C). TAP-Sld5 was purified from the indicated extracts and interacting proteins visualized by immunoblotting with specific antibodies.

doi:10.1371/journal.pgen.1005843.g002

Mcm2, Cdc45 and Csm3 during S-phase in *ctf4Δ* cells (Fig 3B), while binding to Spt16 and Pob3 FACT complex components was not perturbed (Fig 3C). Mms22 interacts with Ctf4 both by two-hybrid [3,36] and co-immunoprecipitation analysis (Fig 2A and 2C), and requires the amino-terminal WD40 domain of Ctf4 (Figs 3D and S4; [3]). Together, these

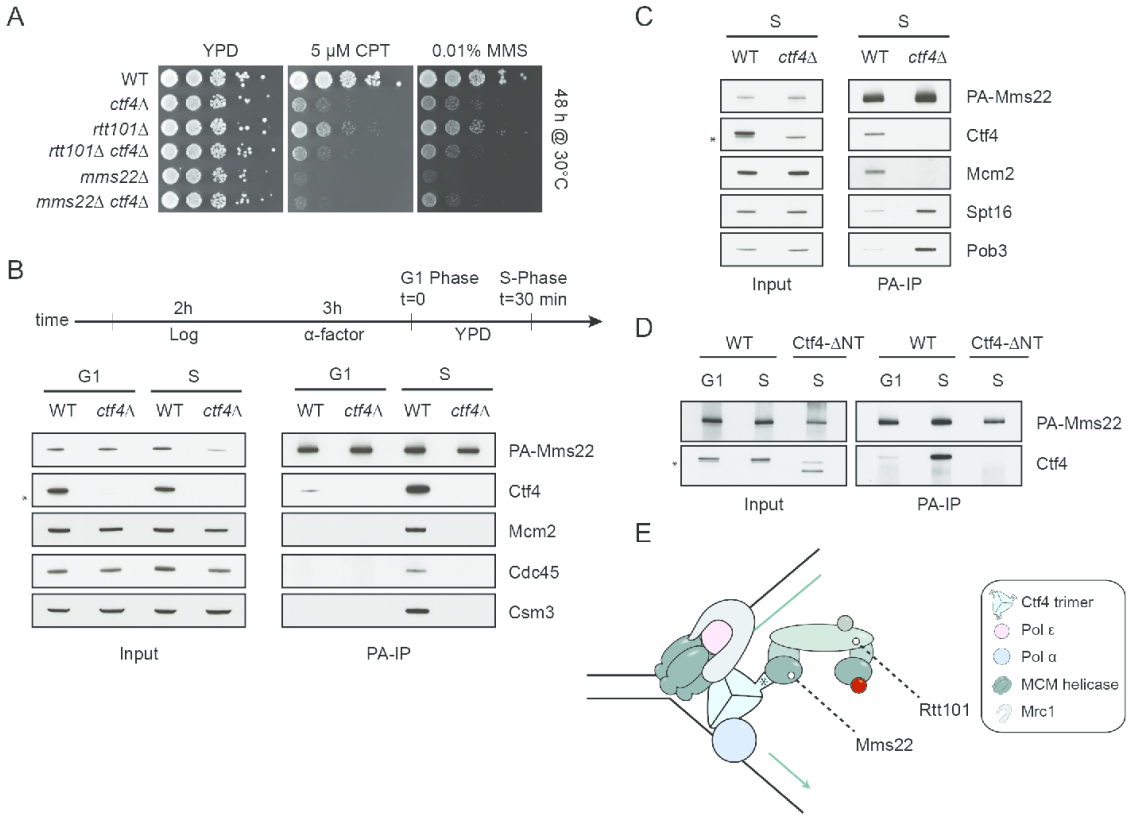

Fig 3. The WD40 domain of Ctf4 recruits the Rtt101^{Mms22} E3 ubiquitin ligase to the replisome progression complex. (A) *CTF4* is epistatic with *RTT101* and *MMS22*. Exponentially growing wild-type (WT), *ctf4Δ*, *rtt101Δ*, *mms22Δ*, *rtt101Δ ctf4Δ* and *mms22Δ ctf4Δ* cells were spotted in serial dilution on normal growth media (YPD) and media containing 5 μM CPT or 0.01% MMS. The plates were imaged after 48 hours incubation at 30°C. (B) and (C) Ctf4 tethers the Rtt101 E3 ligase to the replisome. Wild-type (WT) and *ctf4Δ* cells were transformed with a plasmid expressing PA-Mms22, arrested in α-factor (G1) or synchronously released into S-phase (S) (diagram). PA-Mms22 was purified from G1 or S-phase extracts and interacting replisome (B) or FACT (C) components were detected using specific antibodies. The asterisk (*) indicates an unspecific band. (D) The WD40 domain of Ctf4 is crucial for Mms22 interaction with the RPC. Wild-type (WT) and *ctf4-ΔNT* cells were synchronized as described in (B). PA-Mms22 was purified from extracts prepared from cells in G1 or S-phase and its interaction with Ctf4 was monitored by immunoblotting with specific antibodies. (E) Model of the Rtt101^{Mms22} E3 ubiquitin ligase interacting with the replisome. Ctf4 together with Mrc1 connects the DNA polymerases to the MCM helicase at replication forks. Mms22 interacts with the amino-terminal domain of Ctf4 (*), which is required to recruit the Rtt101^{Mms22} E3 ubiquitin ligase to active forks.

doi:10.1371/journal.pgen.1005843.g003

results suggest that the Rtt101^{Mms22} E3 ligase is tethered to active replisomes via the Ctf4 scaffold (Fig 3E).

The replicative functions of Mrc1 but not Tof1 or Csm3 are required to suppress toxicity in *rtt101Δ* and *mms22Δ* cells

To determine if the alleviated growth defect observed in *rtt101Δ mrc1Δ* strains is phenocopied by the removal of other components of the fork-protection complex (FPC), we tested whether deletion of either *TOF1*, *CSM3* alone or in combination would also rescue the sensitivity of *rtt101Δ* or *mms22Δ* cells to genotoxic agents. Neither the single nor double deletions of *CSM3* and *TOF1* were able to restore growth of *rtt101Δ* or *mms22Δ* cells on media containing MMS (Figs 4A and S5). These data suggest that Rtt101-Mms22 counteracts a function of Mrc1 at replication forks that is independent of its interactions with Tof1 and Csm3.

Since the replication and checkpoint functions of Mrc1 are genetically discernable, we set out to examine which functions of Mrc1 are causing lethality in the absence of Rtt101^{Mms22}. We analyzed the genetic interaction between *rtt101Δ* or *mms22Δ* mutants and the well-characterized checkpoint-deficient *MRC1-AQ* allele, coding for a mutant protein in which all Mec1-dependent phospho-serines (SQ) are mutated to alanine (AQ) [37]. Interestingly, when the checkpoint-defective Mrc1-AQ variant is the only source of Mrc1 in cells lacking the Rt101^{Mms22} E3 ubiquitin ligase, the lethal phenotype is comparable to *rtt101Δ* and *mms22Δ* single mutant cells when exposed to genotoxic stress (Fig 4B), unlike the complete deletion of *MRC1* (Figs 1C, 1E and S5). This result was surprising in light of recent data proposing that alleviation of the checkpoint-mediated late origin repression may rescue the sensitivity of *rtt101Δ* cells to MMS exposure [29]. To corroborate these results, we tested whether the requirement of Rtt101 to promote growth on MMS containing media could be bypassed by genetically de-repressing late origins in the *sld3-37A dbf4-4A* background [38]. In contrast to *rtt101Δ mrc1Δ* double mutants, *rtt101Δ sld3-37A dbf4-4A* cells were unable to rescue the sensitivity of *rtt101Δ* cells to MMS (Fig 4C), supporting the notion that Mrc1-dependent inhibition of late origin firing is not sufficient to explain the essential function of the Rtt101^{Mms22} complex in response to genotoxic stress. Conversely, the MMS-induced lethality of *rtt101Δ* or *mms22Δ* cells was suppressed by expressing an Mrc1 C-terminal truncation mutant (Mrc1$_{1-971}$) as the only copy of Mrc1 (Fig 4D). While this mutant has been reported to be checkpoint defective [24], the C-terminal domain of Mrc1 is known to directly interact with the C-terminal domain of Pol2 [13] and is important for the replication functions of Mrc1 [39]. To identify a *bonafide* separation-of-function Mrc1 allele, we thus constructed smaller C-terminal truncations of Mrc1. Strikingly, deletion of only the last C-terminal 18 amino acids (Mrc1$_{1-1078}$) was sufficient to confer a rescue of MMS sensitivity in both *rtt101Δ* and *mms22Δ* cells (Fig 4E, compare bottom two rows), while otherwise checkpoint defective cells expressing the Mrc1$_{1-1078}$ mutant protein were able to activate the replication checkpoint when challenged with replication stress (Fig 4F). Together, these results strongly suggest that loss of Mrc1's checkpoint function is not responsible for the genetic suppression of *rtt101Δ* or *mms22Δ* cells and implicates the Mrc1 replicative functions in the observed cell toxicity. Interestingly, the inability of *rtt101Δ* or *mms22Δ* cells to extinguish the DNA damage checkpoint following MMS recovery [28] was alleviated in *rtt101Δ mrc1Δ* or *mms22Δ mrc1Δ* strains (Fig 4G), and as a consequence *rtt101Δ mrc1Δ* double mutants proceeded into the next G1 phase four hours post-recovery whereas the *rtt101Δ* cells remained largely arrested at the G2/M border as expected (Fig 4H). Based on these data we conclude that Rtt101^{Mms22} specifically counteracts a replicative function of Mrc1 at stalled replisomes, thereby promoting replication fork repair/restart, which leads to an eventual checkpoint termination.

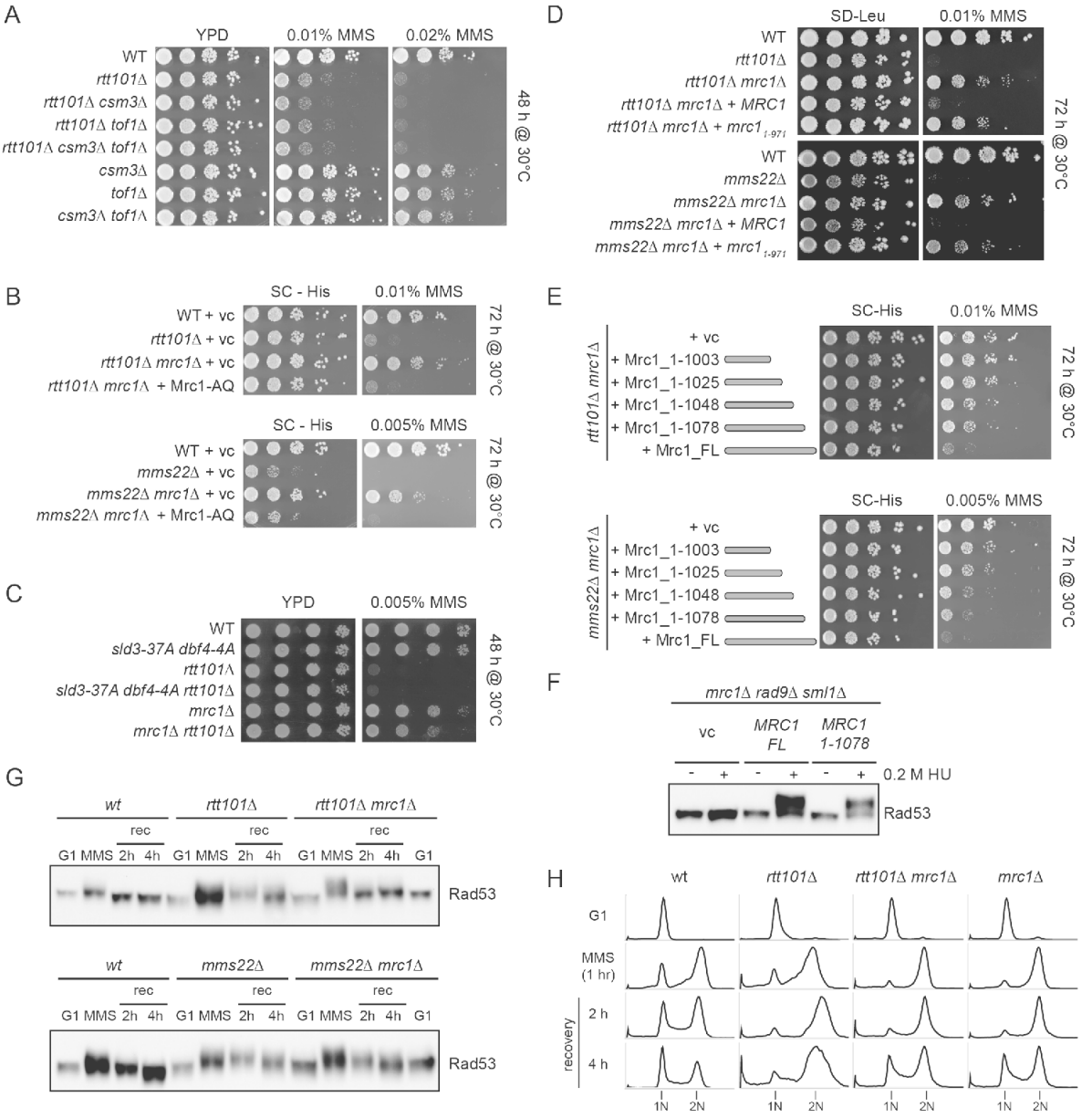

Fig 4. The replicative function of Mrc1 compensates for replication defects in cells lacking components of the Rtt101^{Mms22} E3 ubiquitin ligase. (A) Suppression of the growth phenotype of cells lacking components of the Rtt101^{Mms22} E3 ligase is specific to Mrc1. Serial dilution of wild-type (WT), *rtt101Δ*, *csm3Δ*, *csm3Δ rtt101Δ*, *tof1Δ*, *tof1Δ rtt101Δ*, *tof1Δ rtt101Δ csm3Δ* and *csm3Δ tof1Δ* cells were analyzed on normal growth media (YPD) with or without 0.01% and 0.02% MMS.(B) The checkpoint-defective Mrc1-AQ allele does not suppress the sensitivity of *mms22Δ* or *rtt101Δ* cells to MMS. Serial dilution of wild-type (WT), *rtt101Δ*, *mrc1Δ*, *mms22Δ*, *rtt101Δ mrc1Δ*, *mms22Δ mrc1Δ* strains were assayed on selective growth media (-His) with or without MMS. The lack of *MRC1* was complemented as indicated with plasmids expressing either vector control (vc) or Mrc1-AQ. Plates were imaged after 72 hours incubation at 30°C. (C) De-repressing late origins is not sufficient to suppress *rtt101Δ* MMS sensitivity. Strains with the indicated genotypes were serial diluted on the indicated media as described above. Plates were imaged after 48 hours incubation at 30°C. (D)-(F) C-terminal truncations of Mrc1 can provide a genetic

rescue of *rtt101Δ* and *mms22Δ* cells. (D and E) Cells expressing either a vector control (vc), wild-type (FL = full length) or the indicated Mrc1 truncation mutants were spotted on selective growth media (-His) with or without MMS. The black bars represent the c-terminally truncated Mrc1 proteins. Plates were imaged after 72 hours incubation at 30°C. (F) *mrc1Δ rad9Δ sml1Δ* cells were transformed with an empty control vector (vc), or plasmids encoding either wild-type ($MRC1_{FL}$) or the $MRC1_{1\text{-}1078}$ truncation allele and synchronously released into media with (+) or without (-) 0.2M hydroxyurea (HU). Rad53 phosphorylation was analyzed by immunoblotting of protein extracts with anti-Rad53 antibody. (G) and (H) The checkpoint defect of *rtt101Δ* and *mms22Δ* cells is alleviated by loss of *MRC1*. Cells were synchronized in G1 phase using α-factor and released into media containing 0.01% MMS for 60 min. Stalled forks were then allowed to restart in normal growth media (recovery) and the checkpoint status was monitored by Rad53 phosphorylation (G) and flow cytometry (H) at the indicated time points (in hours (h); rec = recovery).

doi:10.1371/journal.pgen.1005843.g004

MRC1 deletion compensates for homologous recombination defects in *mms22Δ* cells

Increasing evidence points towards a key HR function during replication fork restart at stalled replisomes [40]. Since Mrc1 is a known suppressor of HR [11], we hypothesized that its removal may promote restart of damaged replication forks in *rtt101Δ* and *mms22Δ* cells by an HR-dependent mechanism. To assess HR rates we used a previously described reporter system [41] that exploits a plasmid as a recombination substrate for both the single-strand invasion and annealing pathways, resulting in *CAN1* gene deletion (S6 Fig). In agreement with previous studies, HR levels were abolished in *rad52Δ* and reduced in *mms22Δ* strains [42], whereas *mrc1Δ* cells exhibited increased recombination rates compared to wild-type controls ([12] and Fig 5A). Interestingly, *mms22Δ mrc1Δ* double mutants showed a level of HR comparable to *mrc1Δ* cells, suggesting that in the absence of *MMS22*, Mrc1 may block recombination (Fig 5A). In contrast, *ctf4Δ mrc1Δ* double mutants are inviable ([3,43], S7 Fig), implying that Mrc1 and Ctf4 share a Mms22-independent essential function during DNA replication. The increased HR phenotype seems to be specific to Mrc1, as another mutant, *sgs1Δ*, with increased HR levels did not alleviate the genotoxic sensitivity (S8 Fig) or the low HR frequency [34] observed in *mms22Δ* strains. Since the increased HR level correlated positively with the observed genetic suppression in *mms22Δ mrc1Δ* cells, we tested whether HR was required for this suppression by deleting the *RAD52* gene, and thereby rendering cells HR defective. Indeed, the hyper-sensitivity of *rtt101Δ rad52Δ* and *mms1Δ rad52Δ* cells to MMS could no longer be rescued upon further deletion of *MRC1* (Figs 5B, top and S9), consistent with the notion that an intact HR machinery is required for suppression. A similar effect was also observed in cells lacking the substrate adaptor Mms22 (Fig 5B, bottom), but in this case a slight *mrc1Δ* rescue was still observed in the *rad52Δ* background. These data imply that in contrast to *rtt101Δ* and *mms1Δ*, deletion of *MRC1* in *mms22Δ* cells rescues MMS sensitivity, in part, in a *RAD52*-independent manner.

To corroborate these results, we released G1 synchronized cells endogenously expressing mCherry-tagged Rad52 (Rad52-mCherry) into media containing MMS and scored the ability of cells to form Rad52 foci, a proxy for active recombination [44]. As expected, the percentage of cells with Rad52 foci decreased in both *rtt101Δ* and *mms22Δ* cells, but strikingly, this defect was corrected by further deleting *MRC1* (Fig 5C and 5D). Together, these data indicate that HR upregulation induced by the loss of Mrc1 function may play a key role in the restart/repair of defective replication forks in cells lacking Rtt101^{Mms22} E3 ligase activity.

The stability of Mrc1 is not dependent on the Rtt101^{Mms22} E3 ubiquitin ligase

Available evidence suggests that SCF^{Dia2} targets phosphorylated Mrc1 for proteasomal degradation [22,24]. To test whether Mrc1 is degraded by a Rtt101^{Mms22}-dependent mechanism, we monitored Mrc1 stability in synchronized cells with MMS–induced replication stress (Fig 6A). Promoter shut-off by glucose addition to cells expressing galactose-inducible

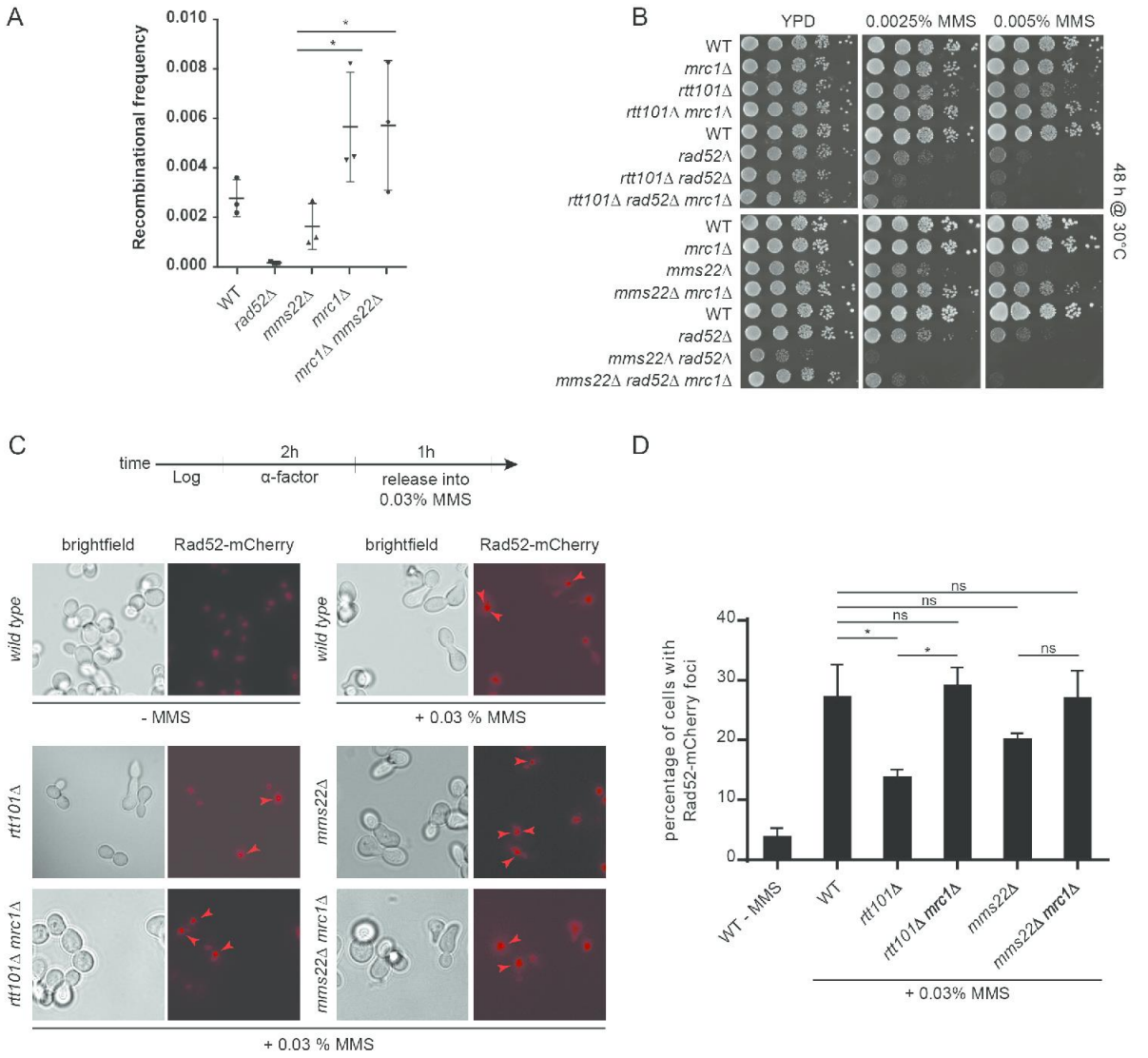

Fig 5. Mrc1 prevents Rad52-mediated HR in *mms22Δ* and *rtt101Δ* cells. (A) Deleting *MRC1* compensates for the HR defect of *mms22Δ* cells. Wild-type (WT) and the indicated mutant strains were transformed with a homologous recombination reporter plasmid (YCpHR), and the recombination frequency (%) was quantified from three independent experiments as schematically outlined in S6 Fig on plates containing 60 μg/ml canavanine. A one-way ANOVA analysis was used for the statistical analysis. * represents a significant difference with 95% confidence. Error bars indicate standard deviation. (B) The growth restoration of *rtt101Δ mrc1Δ* and *mms22Δ mrc1Δ* cells on MMS is *RAD52*-dependent. Serial dilution of wild-type (WT) or *mrc1Δ*, *rtt101Δ*, *rtt101Δ mrc1Δ*, *rtt101Δ mrc1Δ rad52Δ*, *mms22Δ*, *mms22Δ mrc1Δ*, *mms22Δ mrc1Δ rad52Δ* mutants were assayed on normal growth media and media containing 0.0025% or 0.005% MMS and imaged after 48 hours incubation at 30°C. (C) and (D) *rtt101Δ* and *mms22Δ* cells are defective in forming *RAD52* foci. Synchronized cells were released into the presence of MMS as depicted (top diagram) and cells with Rad52-mCherry foci were scored (C). The experiment was performed with two biological replicates, and for each genotype a minimum of 400 cells per replicate were counted (D). * represents a significant difference with 95% confidence intervals following a one-way ANOVA analysis. ns: not significant (below 95% confidence). Error bars indicate standard deviation.

doi:10.1371/journal.pgen.1005843.g005

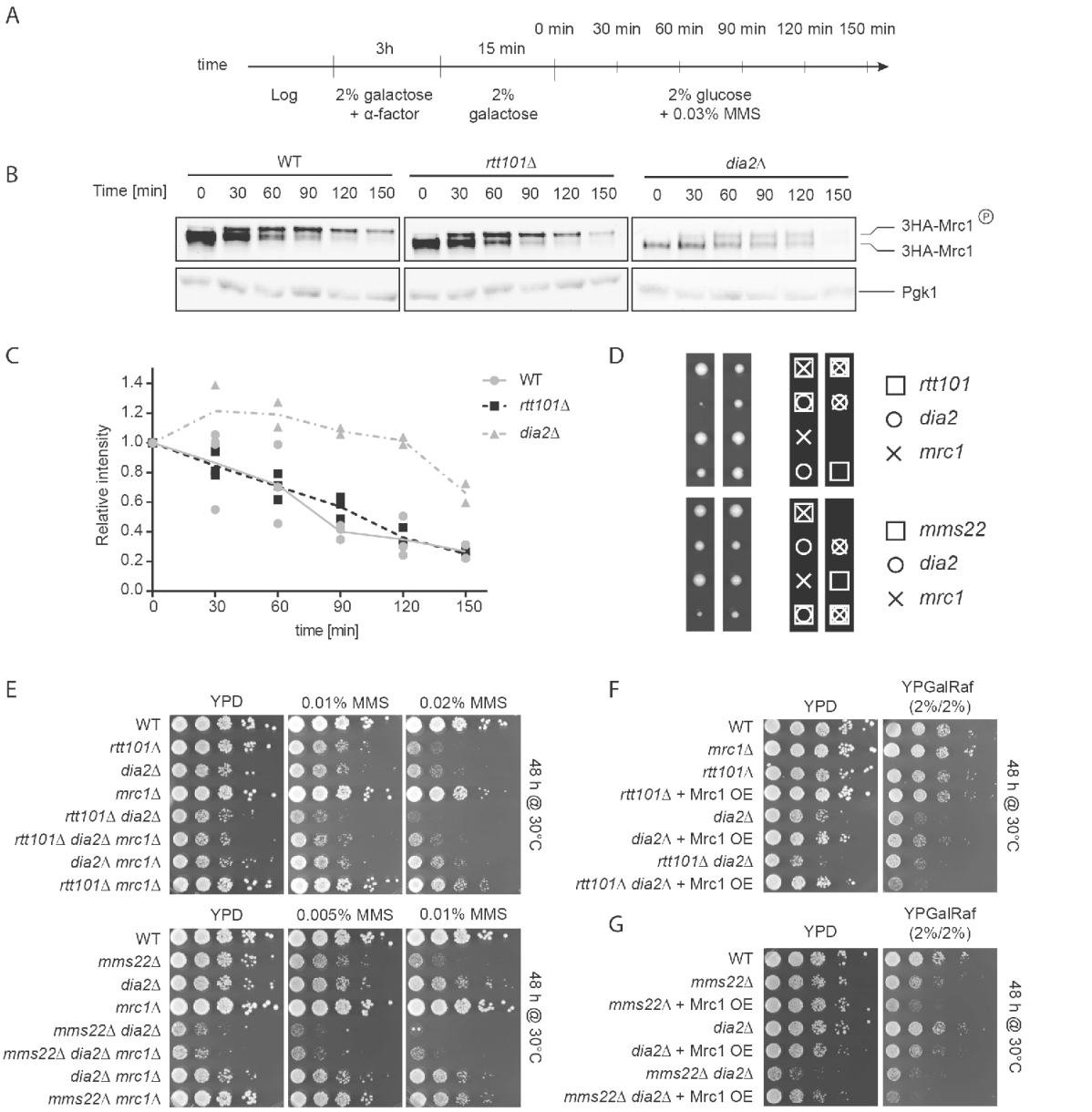

Fig 6. Rtt101^{Mms22} and SCF^{Dia2} counteract Mrc1 activity by distinct mechanisms. (A)–(C) Mrc1 stability is not altered in cells lacking *RTT101*. Wild-type (WT), *rtt101Δ* or *dia2*Δ cells expressing 3HA-tagged Mrc1 from the inducible *GAL1,10*-promoter were synchronized in G1 phase using α-factor in 2% galactose and released into S-phase in 2% galactose as outlined in (A). Subsequently, 0.03% MMS and 2% glucose was added to induce fork stalling and repress HA-Mrc1 expression, respectively. Samples were collected at the indicated time points (min) (A), quantified by anti-HA immunoblotting (B) and shown as scatter plots of individual biological replicates with their means (C). Immunoblotting for Pgk1 controls for equal loading. The position of phosphorylated (3HA-Mrc1-P) and unphosphorylated 3HA-Mrc1 is indicated. (D) *RTT101* and *MMS22* are synthetic-sick with *DIA2*. Tetrad analysis from sporulated heterozygote *rtt101Δ dia2Δ mrc1Δ* and *mms22Δ dia2Δ mrc1Δ* diploids. Boxes (□), crosses (X) and circles (O) indicate that the haploid cells lack *RTT101/MMS22*, *MRC1* or *DIA2*, respectively. Note that *rtt101Δ dia2Δ* and *mms22Δ dia2Δ* double mutants indicated by boxes and circles are barely viable.

(E) *rtt101Δ dia2Δ* and *mms22Δ dia2Δ* double mutants can be rescued by deletion of *MRC1*. Serial dilution of the indicated strains obtained from the tetrad dissections shown in (D) were assayed on normal growth media (YPD) and media containing 0.02%, 0.01% or 0.005% MMS. The plates were imaged after 48 hours of incubation at 30°C. (F) and (G) Overexpression of Mrc1 is lethal for *rtt101Δ dia2Δ* (F) and *mms22Δ dia2Δ* (G) double mutants. Serial dilution of wild-type (WT) and the indicated mutant strains overexpressing Mrc1 from the galactose-inducible *GAL1,10*-promoter were assayed on normal growth media containing 2% glucose (*GAL1,10*-promoter off), 2% galactose/2% raffinose (*GAL1,10*-promoter on). The plates were imaged after 48 hours of incubation at 30°C.

doi:10.1371/journal.pgen.1005843.g006

3HA-Mrc1 (Figs 6A–6C and S10) as well as cyclohexamide (CHX) chase experiments of endogenously tagged 3HA-Mrc1 (S10 Fig) showed that the degradation kinetics of phosphorylated and unphosphorylated Mrc1 in *rtt101Δ* or *mms22Δ* cells exposed to MMS were comparable to wild-type controls. These results were corroborated by quantitative mass spectrometry using selected reaction monitoring (SRM), which demonstrated that Mrc1 levels decreased with similar kinetics in wild-type, *rtt101Δ* and *mms22Δ* cells (S10 Fig). Surprisingly, deletion of *DIA2* had only slight effects on the half-life of Mrc1, and thus the role of SCF^{Dia2} in regulating Mrc1 stability remains to be further clarified [24,45]. Taken together, these data demonstrate that Rtt101^{Mms22} does not trigger degradation of the Mrc1 protein at stalled replication forks.

Tetrad analysis and plating assays revealed that the growth defects caused by loss of Rtt101 and Mms22 together with the loss of Dia2 function were additive, and double mutants were further impaired for growth in the presence and absence of MMS (Fig 6D and 6E). This indicates that the two E3 ligases may function independently and have non-overlapping roles during DNA replication. Interestingly, deletion of *MRC1* restored some of the growth defects of *mms22Δ dia2Δ* and *rtt101Δ dia2Δ* double mutants as shown by tetrad analysis (Fig 6D) as well as spotting assays on MMS containing media (Fig 6E). Conversely, overexpression of Mrc1 resulted in toxicity in *rtt101Δ dia2Δ* and *mms22Δ dia2Δ* double mutants even in the absence of exogenous genotoxic stress (Fig 6F and 6G). Together these results indicate that these two CRLs may genetically interact with Mrc1 function but likely by distinct mechanisms.

The Rtt101^{Mms22} E3 ligase may modulate the interaction of Mrc1 with the MCM helicase complex upon fork stalling

In addition to binding DNA polymerase ε [13], Mrc1 also interacts with the Mcm6 subunit of the MCM2-7 helicase [14]. In order to disrupt the binding of Mrc1 to Mcm6, we crossed the *mcm6-IL* allele [14] into *rtt101Δ*, *mms22Δ* and *mms1Δ* cells deleted for *MRC1*, and compared growth of the resulting single, double and triple mutants treated with DNA damaging agents (Fig 7A). Importantly, we observed that similar to deleting *MRC1* the presence of *mcm6-IL* was able to suppress the sensitivity of *rtt101Δ*, *mms22Δ* (albeit weakly) and *mms1Δ* cells to MMS (Fig 7B–7D), indicating that disrupting the association of Mrc1 with the CMG helicase is sufficient to restore growth of *rtt101Δ*, *mms1Δ*, and in part, *mms22Δ* mutants exposed to genotoxic stress. Importantly, deletion of *MRC1* in *rtt101Δ mcm6-IL or mms22Δ mcm6-IL* cells did not further improve growth on MMS containing media (Fig 7B and 7C), suggesting that these mutations affect the same molecular process. We did not observe a difference in the amount of chromatin bound Mrc1 when comparing wild-type to *rtt101Δ* and *mms22Δ* cells in the absence and presence of MMS, rendering it unlikely that Rtt101^{Mms22} promotes Mrc1 eviction from chromatin at sites of replication stress (S11 Fig). These genetic and biochemical results suggest that the Rtt101^{Mms22} E3 ligase counteracts a function of Mrc1 that is linked to the replicative helicase at stalled replication forks, and possibly modulates the interaction of Mrc1 with the MCM helicase complex upon fork stalling (Fig 7E).

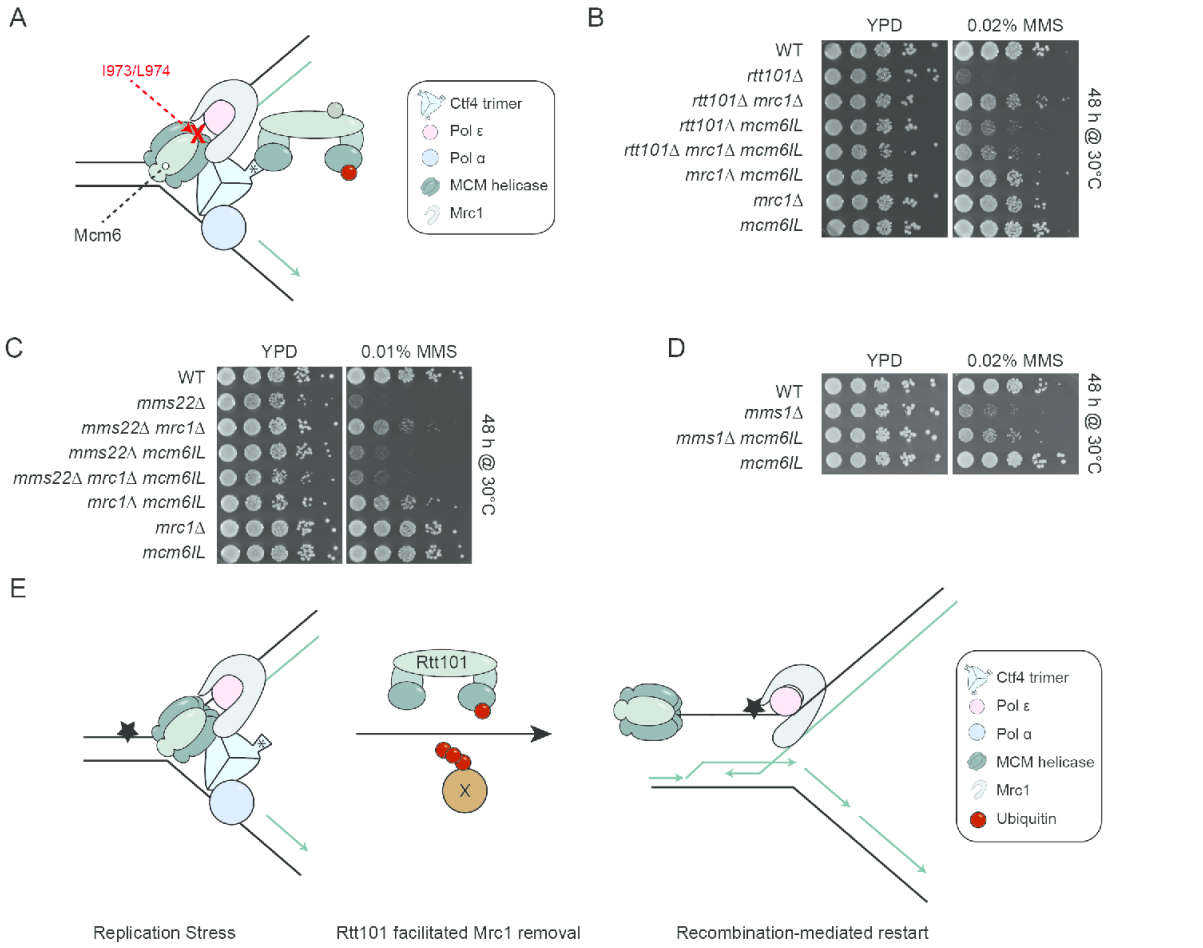

Fig 7. Altered regulation of replicative polymerases and the CMG may allow HR mediated fork restart in cells lacking Rtt101^{Mms22} activity. (A) *mcm6-IL* reduces its affinity to physically interact with Mrc1. Mutation of the indicated amino acids perturbs the interaction between Mcm6 and Mrc1 and is reported to promote uncoupling of the leading strand polymerase from the MCM replicative helicase [14]. The asterisk (*) indicates the WD40 domain of Ctf4. (B)-(D) The *mcm6-IL* allele rescues the genotoxic sensitivity of *rtt101Δ* (B), *mms1Δ* (C) or *mms22Δ* (D) mutants and is epistatic with *MRC1*. Cells with the indicated genotypes were spotted onto either YPD or YPD plates containing 0.02% or 0.01% MMS. Images were taken after 48 hours of incubation at 30°C. (E) Model of Rtt101^{Mms22}-facilitated removal of Mrc1 to allow HR-mediated repair/restart of stalled replication forks. The Rtt101^{Mms22} E3 ligase associates with replisomes by binding to Ctf4. When a replication fork encounters an obstacle (star), our data suggest that Rtt101^{Mms22} ubiquitylates a so far unidentified factor (X), which modulates the interaction between Mrc1 and the MCM helicase (Mcm6 is in light grey). This remodeling results in the Rad52-mediated repair/restart of the stressed replisome in order to by-pass the obstacle.

doi:10.1371/journal.pgen.1005843.g007

Discussion

In this study, we have employed genome-wide genetic screening together with a proteomics approach to gain insight into how the Rtt101^{Mms22} E3 ubiquitin ligase regulates stalled replication forks [28]. We demonstrate that Rtt101^{Mms22} is recruited to replisomes during S-phase by interacting with the N-terminal WD40 domain of Ctf4. Moreover, genetic analysis revealed that the introduction of the *mcm6-IL* allele, or deletion of either *MRC1* or the non-essential Pol

ε subunit, *DPB4*, can restore viability of *rtt101Δ*, *mms1Δ* and *mms22Δ* cells exposed to various genotoxic stress conditions. Together, our data suggest that the Rtt101^{Mms22} complex acts directly at replisomes to promote repair and restart of stalled replication forks by counteracting a replicative function of Mrc1, and hence promoting HR.

The Rtt101^{Mms22} complex counteracts Mrc1 to promote HR-dependent repair/restart of stalled replication forks in response to genotoxic stress

The tight association of DNA synthesis with the unwinding activities of the replicative helicase at replisomes is important for faithful DNA replication. Mrc1 represents a plausible candidate to reinforce this association as it physically interacts with both Pol2 as well as the MCM2-7 helicase. Indeed, altering this interaction may lead to exposed stretches of ssDNA, which are vulnerable to nicking and chemical modifications, and if extensive enough, may unleash the replication checkpoint following the association of sufficient replication protein A (RPA) molecules. In accordance, in the presence of MMS we observed more extensive Rad53 phosphorylation in the absence of MRC1 (Fig 4G). Previous studies have shown that *mrc1Δ* cells fail to inhibit late firing origins [6,46], an effect that could be used to bypass the adverse effects of stalled replication forks. Therefore, deletion of *MRC1* might conceivably alleviate the DNA damage sensitivity of *rtt101Δ* and *mms22Δ* cells by allowing the firing of additional origins and hence promoting the completion of replication [29]. In light of our results, however, this possibility seems unlikely given that the loss of Mrc1's checkpoint functions fails to rescue the defects associated with *rtt101Δ* and *mms22Δ* cells. Moreover, the requirement of the Rtt101^{Mms22} complex in genotoxic stress conditions could not be bypassed by genetically derepressing late origins using the *sld3-37A dbf4-4A* background [38]. Alternatively, our results suggest that Mrc1 deletion, and in turn replisome uncoupling, may promote HR-mediated fork restart at stalled replication forks [11]. In support of this idea, Rtt101, Mms1 and Mms22 have been demonstrated to stimulate HR, specifically upon exposure to genotoxic agents [42], and we found that deletion of *MRC1* rescued the reduced recombination rates in cells deleted for *MMS22*. Indeed, an intact HR machinery is required for *rtt101Δ mrc1Δ* and to a lesser extent *mms22Δ mrc1Δ* double mutants to grow in genotoxic stress conditions. Moreover, recombination foci visualized microscopically by Rad52-mCherry were decreased in both *rtt101Δ* and *mms22Δ* cells exposed to genotoxic drugs, but were restored by additionally deleting *MRC1*. We thus propose that the Rtt101^{Mms22} E3 ubiquitin ligase promotes HR-mediated repair and restart by counteracting a replicative function of Mrc1 at stalled replication forks. Surprisingly, this role of Mrc1 is not shared with the other subunits of the replisome progression complex Tof1 and Csm3, although they are thought to help stabilize Mrc1 at replication forks. However, Mrc1 also interacts with replisomes by a Tof1/Csm3-independent mechanism [47], perhaps through its interactions with Pol2 and Mcm6. It seems that this Mrc1 pool is sufficient to inhibit HR and may need to be counteracted by the Rtt101^{Mms22} E3 ligase upon fork stalling (Fig 7E).

The Rtt101^{Mms22} complex counteracts the replicative function of Mrc1 at stalled forks

In contrast to the S-phase checkpoint defective Mrc1-AQ mutant (Fig 4B), expression of a C-terminal truncation mutant of Mrc1 (Mrc1$_{1\text{-}971}$) was able to suppress phenotypes linked to both SCF^{Dia2} and Rtt101^{Mms22} E3 ligases ([24], Fig 4D). Importantly, we identified a Mrc1 separation-of-function mutant (Mrc1$_{1\text{-}1078}$), which is checkpoint-proficient but likely unable to perform the replicative function of Mrc1 that leads to toxicity when the Rtt101^{Mms22} E3 ligase is impaired. While the exact mechanism underlying this specific defect remains to be

elucidated, we propose that the C-terminus of Mrc1 may directly regulate replisome function by binding to either Pol2 or Mcm6. This model might also help explain the higher rate of HR (Fig 5A), as *mrc1Δ* strains leave more unreplicated single stranded DNA stretches at stalled replication forks [11] that require post-replicative HR.

Several mechanisms allow cells to restore stalled replication forks, underlining the importance of this process (reviewed in [19]). Based on our genetic and proteomic analysis, we propose that Rtt101^{Mms22}, presumably via a ubiquitylation event, counteracts a replicative function of Mrc1 in order to promote recombination at stalled DNA replication forks (Fig 7E). Since both the *mcm6-IL* allele as well as the deletion of *MRC1* may affect polymerase and helicase activities (Fig 7A), the Rtt101^{Mms22} complex may somehow regulate the activity of these factors at stalled forks. Indeed, our genetic analysis revealed that the requirement of the Rtt101^{Mms22} complex to inhibit the replicative-function of Mrc1 upon genotoxic stress is epistatic to loss of its binding to the MCM helicase, suggesting that the Rtt101^{Mms22} E3 ligase may directly or indirectly modulate the interaction of Mrc1 with the MCM complex. Although we did not observe a difference in the total amount of Mrc1 associated with chromatin following exposure to MMS (S11 Fig), it remains possible that regulation specifically occurs at a small subset of stalled replication forks. Interestingly, a previous study has reported decreased association of Pol ε and Mrc1 with replication forks in *mms1Δ* mutants [48], which may represent a compensatory response. Thus, while we cannot rigorously exclude that Rtt101^{Mms22} regulates Mrc1 via replisome association, we favor a model by which Rtt101^{Mms22}-dependent ubiquitination of Mrc1 or an unknown substrate leads to uncoupling of the MCM helicase at the stalled replicon, thereby promoting HR-dependent repair and restart of stalled replication forks (Fig 7E). However, we do not fully understand how Rtt101 or Mms22 interact with either the error prone TLS branch of bypass synthesis or with other means of replication fork restart (e.g. BIR and replication fork regression) [19]. Since Rad52 is synthetically-sick with Mms22 but not Rtt101 in unchallenged conditions (Fig 5B), it is conceivable that Mms22 may regulate either TLS or replication fork regression, as part of its Rtt101-independent functions. Future studies will be required to test these possibilities.

Material and Methods

Yeast strains, plasmids and growth conditions

Plasmids and yeast strains are listed in S3 and S4 Tables, respectively. Standard methods were used for yeast strain construction and molecular biology. Yeast cells were grown in rich medium (YPD; 1% yeast extract, 2% peptone, 2% glucose) or synthetic medium (SD; 0.17% yeast nitrogen base, 0.5% ammonium sulphate, 2% glucose, amino acids as required). Homologous recombination frequencies were measured as described [41]. For spotting assays, the indicated strains were grown overnight at 30°C, and the cultures were diluted to OD_{600} 0.5. Ten-fold serial dilutions were spotted using a pinning head (2 μl). The plates were incubated at 30°C and imaged using the ChemiDoc Touch Imaging System (Bio-Rad) after 2 and 3 days. For cell cycle synchronization, logarithmically growing cells were treated with 1:1000 α-factor solution (5 mg/ml + 0.1% BSA) at 24°C for 3 hours. G1 arrest was monitored by flow cytometry and microscopy (appearance of pear-shaped "shmoo" morphology of at least 95% of cells). Cells were then washed three times with YPD at room temperature and S-phase samples were collected 30 minutes after the release into fresh YPD medium.

SGA screening and hit validation

Synthetic Genetic Array (SGA) methodology was used as described [30], with the following modifications: the non-essential heterozygous diploid *S. cerevisiae* knockout collection (kindly

provided by M. Knop) was sporulated and crossed to a *rtt101*::*NAT can1*::*STE2pr-SpHis5* strain (Y7092, C. Boone). Diploids were selected by repinning on YPD plates containing 100 μg/ml nourseothricin and 250 μg/ml of the kanamycin analogue G418. After sporulation, haploid double mutants were selected by repinning on MATa selection plates (SD-his/arg/lys + canavanine + thiolysine) followed by a repinning on MATa selection plates containing 100 μg/ml nourseothricin and 250 μg/ml G418. Colonies were then re-pinned onto SD complete, SD + 0.01% MMS and SD + 5 μM CPT, and repinned twice onto the same media after 24 h incubation at 30°C. Pictures of the last repinning were taken after 24 h incubation at 30°C. The occurrence of suppressors, i.e. double mutants that showed increased resistance to either MMS or CPT, were scored manually, and validated by tetrad analysis from independent starter strains followed by duplicate spotting assays onto drug containing media.

DNA content quantifications using flow cytometry

Culture volumes of exponentially growing cells corresponding to 0.68 OD units were collected by centrifugation (3000 rpm for 5 min at RT), resuspended in 1 ml cold 70% ethanol and stored at 4°C. Cells were washed once in 1 ml H_2O (3000 rpm for 5 min at RT), resuspended in 0.5 ml 50 mM Tris-HCl (pH 8.0) and incubated with 10 μl RNase A (10 mg/ml) for 3 h at 37°C. After centrifugation (3000 rpm for 5 min at RT) cells were resuspended in 0.5 ml 50 mM Tris-HCl (pH 7.5) containing 1 mg/ml Proteinase K and incubated for 45 min at 50°C. Cells were spun down (3000 rpm for 5 min at RT) and resuspended in 0.5 ml 50 mM Tris-HCl (pH 7.5). 100 μl of cells were sonicated five times 15 sec at low intensity using the Bioruptor Twin XD10. 50 μl of cells were mixed with 1 ml 1 x SYTOX Green (Life Technologies) in 50 mM Tris-HCl (pH 7.5) to stain DNA. Cells were kept dark and analyzed immediately for DNA content using a BD FACSCanto II flow cytometer using the following filters and settings: FSC and SSC were detected with a 488 nm laser with detector settings of 318 V and 360 V, respectively. SYTOX Green was detected with a 502 nm longpass filter and 530/30 nm bandpass filter at 466 V. 20000 events per sample were analyzed in each run. Data collection and analysis was performed using BD FACSDiva software and FlowJo v10.0.6 (Miltenyi Biotec) software.

Yeast protein extraction, SDS-PAGE, western blotting and antibodies

2 OD_{600} units of exponentially growing cells were pelleted at 13'000 rpm for 2 min, and if necessary stored at -20°C. Cell pellets were resuspended in 150 μl of Solution 1 (0.97 M 2-mercaptoethanol, 1.8 M NaOH) and incubated on ice for 10 min. 150 μl of Solution 2 (50% TCA) were added, cells were incubated 10 min on ice and centrifuged at 13'000 rpm for 2 min at 4°C. Pellets were resuspended in 1 ml acetone, centrifuged at 13'000 rpm for 2 min at 4°C and the pellets resuspended in 100 μl urea buffer (120 mM Tris-HCl pH 6.8, 5% glycerol, 8 M urea, 143 mM 2-mercaptoethanol, 8% SDS, bromophenol blue indicator). Protein extracts were incubated 5 min at 55°C, centrifuged at 8'000 rpm for 30 sec, separated by SDS-PAGE and transferred onto nitrocellulose. Membranes were blocked with 5% milk and 1% BSA and incubated with appropriate antibodies: Rabbit peroxidase anti-peroxidase (1:10000), mouse monoclonal antibody against c-Myc (1:3000), HA (1:3000), Mcm2 (1:2000), Pgk1 (1:200000), Rad53 (1:16, EL7.E1, gift from M. Foiani), mouse polyclonal antibody against Orc6 (1:500, gift from H. Ulrich). Replisome antibodies are from sheep polyclonal antiserum: Ctf4 (1:2000), Cdc45 (1:1000), Mcm6 (1:1000), Sld5 (1:1000), Psf2 (1:250), Psf3 (1:3000), Csm3 (1:1000), Spt16 (1:3000), Pob3 (1:3000).

Acetate-salt based replisome affinity purifications

Cell harvesting was performed at 3000 rpm (Multifuge 3 5-R) for 3 min at RT. Samples were first washed with 20 mM Tris-acetate pH 9.0, then with lysis buffer (75 mM (or 100 mM in

Fig 2C and 2D) Tris-acetate pH 9.0, 50 mM KOAc, 10 mM MgOAc, 2 mM EDTA, 2 mM NaF, 2 mM β-glycerophosphate, 1× Roche protease inhibitor cocktail, 1× sigma inhibitors). The cell pellets' mass was weighted and re-suspended in 3 volumes of lysis buffer. The cell suspension was shock-frozen in liquid nitrogen as "droplets" and stored at -80°C. All cell manipulations and collection were performed at 4°C, if not specified otherwise. Equal weight of "droplets" was grinded with a cryogenic impact mill (Freezer-mill 6870 Large SamplePrep), using 5 min pre-cool followed by 6 cycles of 2 min milling at 12 CP and 2 min cooling down. Cells were thawed for 5 min at RT and 0.25 volume of glycerol mix (75 mM (or 100 mM in Fig 2C and 2D) Tris-acetate pH 9.0, 300 mM KOAc, 50 mM MgOAc, 2 mM EDTA, 0.5% NP40, 1 mM DTT, 2 mM NaF, 2 mM β-glycerophosphate, 1× Roche protease inhibitors, 1× yeast inhibitors) was added to the lysate. DNA was digested by 800 Units/ml DNA nuclease (Benzonase Novagen) at 4°C for 30 min, followed by 30 min centrifugation at 15'000 rpm (25'000g) at 4°C (Sorvall RC26 Plus, SS-34 rotor) and 60 min ultracentrifugation at 25'000 rpm (100'000g) at 4°C (Beckman Coulter Optima LE80K, SW-41 rotor) to remove insoluble material. From the resulting extract, 50 μl was used as whole cell extract (WCE) and the remaining was used for affinity-precipitation. 50 μl of WCE was dissolved in 100 μl 1.5×SDS-loading buffer (1× buffer: 50 mM Tris-Cl pH 6.8, 100 mM DTT, 2% SDS, 0.1% bromophenol blue, 10% glycerol) and boiled at 95°C for 5 min. 4 μl of sample was used to load on a Bis-Tris acrylamide gel. Washed IgG coupled dynabeads (M-270 Epoxy; 14302D, Life Technologies) were added to extracts for immuno-precipitation. Samples were incubated for 2 hours on a rotating platform at 4°C. Beads were washed 4 times at RT with 1 ml wash buffer (100 mM Tris-acetate pH 9.0, 100 mM potassium acetate, 10 mM magnesium acetate, 2 mM EDTA) and protein was eluted with 50 μl of 1× SDS-loading buffer.

Proteomics

In-gel trypsinization and protein identification. Acrylamide gel bands were minced into pieces, reduced in Farmer's solution (30 mM Potassium Ferricyanide (III), 30 mM sodiumthiosulfate) for 2 min and washed until recovering transparency. Gel slices were then incubated with 100 mM ammonium bicarbonate (ABC) for 20 min, washed with 50 mM ABC/50% acetonitrile (ACN), and rinsed with 100% ACN. Gel slices were subsequently dehydrated with 100% ACN for 20 min under gentle agitation and then rehydrated with 100 mM ABC containing 10 mM dithiothreitol (DTT) for 30 min at 56°C. Finally, gel slices were treated with 100 mM ABC containing 50 mM iodoacetamide (IAA) for 30 min at RT. After second dehydration with 100% ACN, the dried gel pieces were rehydrated with 0.02 μg/μl trypsin in 50 mM ABC and incubated 60 min on ice and then over night at 37°C. For the extraction, peptides were sonicated three times in 50% ACN containing 5% formic acid for 10 min at 4°C and dried in a vacuum centrifuge.

Peptide samples were subjected to a label-free, shotgun proteomic analysis on a 5600 TripleTOF (ABSciex, Concord, Canada) with a nano-electrospray ion source. For the chromatographic separation of the peptides, the instrument was coupled with an Eksigent Nano LC system (ABSciex, Foster City, CA, USA) and equipped with a 15-cm fused silica column (BGB Analytik, Böckten, Switzerland), packed in-house with Magic C18 AQ, 5 μm beads (Michrom Bioresources, Leonberg, Germany). Samples of ~3 μg each were loaded from an autosampler at 4°C and separated with a linear gradient of acetonitrile/water containing 0.1% formic acid from 5 to 35% acetonitrile in 120 min, with a flow rate of 300 nl/min. The mass spectrometer was operated in data-dependent acquisition mode, with the accumulation time for TOF scans set to 0.299995 s, and the mass range to 400–1250 Da. Peptides with 2–5 charges and signals exceeding 150 cps were selected for fragmentation. The product ion scan was performed with an accumulation

time of 0.149998 s, and a mass range of 170–1500 Da in a high sensitivity mode. The total cycle time was 3.35 s.

The collected spectra were searched against the *Saccharomyces cerevisiae* SGD protein database with Sorcerer-SEQUEST (Thermo Electron, San Jose, CA, USA). Trypsin was set as the digesting protease with the tolerance of two missed cleavages, one non-tryptic terminus and not allowing for cleavages of KP and RP peptide bonds. Protein identifications were statistically analyzed with ProteinProphet (v3.0) and filtered to a cutoff of 0.9 ProteinProphet probability, which in this case corresponds to a FDR<1%, calculated based on a target-decoy approach. The data was used to generate a protein identification list.

In-solution trypsinization and SRM analysis. Protein samples were dissolved to a final concentration of 1–3 mg/ml in corresponding lysis buffer (0.1 M NH_4HCO_3, 7 M Guanidinium) and sonicated for 5 min. Disulfide bonds were reduced in 12 mM DDT for 30 min at 32°C under agitation. Iodoacetamide (IAA) was then added to a final concentration of 40 mM and samples were incubated under agitation in the dark for 45 min at 25°C, to alkylate free cysteine residues. Samples were diluted to a final concentration of 0.5 M Guanidinium with freshly prepared 0.1 M NH_4HCO_3. Sequencing Grade Modified Trypsin (Promega) was added to an enzyme/substrate ratio of 1/50 (w/w) and the reaction mixture incubated at 37°C overnight. The digestion was stopped with formic acid to a final pH <3. The peptide mixtures were applied onto Sep-Pak tC18 cartridges (Waters), desalted according to the manufacturer instructions and eluted with 50% acetonitrile (ACN). Peptide samples were evaporated on a vacuum centrifuge to dryness and re-solubilized in 0.1% formic acid for LC-MS analysis. For the quality control of transitions and retention time estimation, samples were measured in SRM mode on a triple-quadrupole/ion-trap mass spectrometer (5500 QTrap, ABSciex, Concord, Canada) with a nano-electrospray ion source. The instrument was coupled to an Eksigent 1D-plus Nano liquid chromatography system with a 20 cm fused-silica column with 75 μm diameter packed with Magic C18 AQ 5 μm beads for on-line chromatographic separation of peptides. Approximately 1 μg of sample was separated with a linear gradient from 5% to 35% ACN in 30 min. The SRM measurements were conducted with Q1 and Q3 operated at unit resolution (0.7 m/z half-maximum peak width) with a dwell time of 20 ms and cycle time of < 3.0 s.

Data were analyzed with Skyline to define the best transitions, and 3–4 transitions per peptide were retained based on retention time and relative fragment-ion intensity for the final SRM assay. Five peptides were measured for Mrc1 (e.g APEQNHNNGK, CITLDLDSDSDEY GDDDMDSIK, IAINLGHYGDNIGEDTDK, SSAFFESMVEDIIEYK, SVELNLTDETR). For time-scheduled experiments a LC-SRM method was used for peptide measurements with 3 min window, 30 min gradient using the same MS parameters as for SRM assay validation. After data acquisition, the sum of the area corresponding to each selected transition was used to evaluate relative peptide abundances.

Fluorescence microscopy

At the indicated time points, cells expressing Rad52-mCherry (0.08 OD_{600} units) were pelleted at 3'000 rpm for 3 min, resuspended in 300 μl SD-Trp containing 0.03% MMS, and then transferred into one chamber of a Nunc Lab-Tek coverglass (Thermo Fisher Scientific) coated with 2 mg/ml Concanavalin A (Sigma Aldrich). Images were obtained on a Leica AF7000 widefield microscope using a 63x/1.4 oil objective. Brightfield and fluorescent images were taken along the z-axis, and Rad52-mCherry foci counted in all focal planes for at least 400–600 cells per strain (n = 2 biological replicates).

Chromatin association assay

G1-arrested cell cultures were split and released into YPD media containing DMSO solvent or 0.03% MMS. S-phase cells were collected after 30 min (untreated) or 1 hour (MMS-treated) at 30°C, stopped with 0.1% sodium azide and harvested at RT by centrifugation for 5 min at 4000 rpm. The pellet was resuspended in 1.5 ml pre-spheroplasting buffer (100 mM PIPES, pH 9.4, 10 mM DTT, 0.1% sodium azide), pelleted again after 10 min at room temperature, and resuspended in 1 ml spheroplasting buffer (50 mM potassium phosphate buffer, pH 7.5, 0.6 M sorbitol, 10 mM DTT, 0.2 mg/ml zymolyase (>200 units/mg)). After 1 h incubation at 30°C, spheroplasts were spun down at 4°C for 1 min at 2500 rpm, washed with 1 ml wash buffer (100 mM KCl, 50 mM HEPES-KOH, pH 7.5, 2.5 mM $MgCl_2$, 0.4 M sorbitol) and resuspended in 100 μl extraction buffer (100 mM KCl, 50 mM HEPES-KOH, pH 7.5, 2.5 mM $MgCl_2$, 1× Roche protease inhibitor cocktail). The suspension was split into three aliquots of 50 μl each (whole cell extract, soluble fraction, chromatin bound fraction), cells lysed by adding 0.25% Triton X-100 and 5 min incubation on ice, and the cell extract treated with 1 μl of a 1:50 dilution of benzonase (NEB). After 15 min incubation on ice, NuPAGE LDS sample buffer was added, the soluble fraction centrifuged at 4°C for 10 min at 14000 rpm, and the supernatant transferred to a new reaction tube. The chromatin bound fraction was underlayed with 30% sucrose solution and centrifuged at 4°C for 10 min at 14000 rpm. The supernatant was discarded and the pellet resuspended in 50 μl extraction buffer with 0.25% Triton X-100. This was repeated once, the resuspended final pellet treated at 4°C with 1 μl of a 1:50 dilution of benzonase, and the reaction stopped after 15 min by the addition NuPAGE LDS sample buffer. All samples were incubated for 10 min at 70°C, cleared by centrifugation for 10 min at 13000 rpm, and the samples analyzed by immunoblotting using 4–15% pre-cast polyacrylamide gels (Bio-Rad).

Supporting Information

S1 Fig. Exemplary plates from the synthetic genetic array (SGA) screening. Genotoxic conditions included MMS (0.01%) and CPT (5 μM). Plates were imaged after 72 hours at 30°C. The boxes highlight double mutants (pinned in quadruplicate) where genetic suppression was detected.
(TIF)

S2 Fig. Genotoxic sensitivity of the neddylation-deficient *RTT101-K791R* allele is alleviated in cells lacking *MRC1*. Serial dilution of *rtt101Δ* or *rtt101Δ mrc1Δ* cells transformed with plasmids containing either *RTT101* or *RTT101-K791R* were analyzed on selective growth media (SD-His) with or without 10 μM CPT or 0.01% MMS. The plates were imaged after 48 hours of incubation at 30°C (A). Expression of CBP-9Myc-tagged Rtt101 and Rtt101-K791R was monitored by immunoblotting with anti-myc antibodies (B). The slower migrating band marks neddylated, active Rtt101 (CBP-9Myc-Rtt101^{Nedd8}).
(TIF)

S3 Fig. Deletion of *MRC1* does not suppress the genotoxic sensitivity of cells lacking *RAD52* or *UBC13*. Serial dilution of wild-type (WT) or *rtt101Δ*, *mrc1Δ*, *mrc1Δ rtt101Δ*, *rad52Δ*, *mrc1Δ rad52Δ*, *ubc13Δ* and *mrc1Δ ubc13Δ* mutant strains were assayed on normal growth media (YPD) or media containing MMS (0.005%, 0.01%, 0.02%). The plates were imaged after 48 hours of incubation at 30°C.
(TIF)

S4 Fig. Domain structure of Ctf4. Schematic drawing of Ctf4, with its WD40, beta propeller and alfa-helical domains. The numbers indicate the amino-acids starting with the amino-terminal methionine. The amino-terminally truncated Ctf4-ΔNT mutant (encompassing amino acids 461–927) unable to interact with Mms22 is indicated below.
(TIF)

S5 Fig. Suppression of the growth phenotype of cells lacking components of the Rtt101^{Mms22} E3 ligase is specific to Mrc1. Serial dilution of wild-type (WT) or *mrc1Δ*, *tof1Δ*, *csm3Δ*, *mms22Δ*, *mms22Δ mrc1Δ*, *mms22Δ tof1Δ and mms22Δ csm3Δ* cells were analyzed on normal growth media (YPD) with or without 0.01% MMS. The plates were imaged after 48 hours of incubation at 30°C.
(TIF)

S6 Fig. Homologous recombination reporter assay. (A) Schematic representation of the YCpHR plasmid reporter [41] used in Fig 5A. (B) Cells transformed with the YCpHR reporter were grown for 5 hours in normal growth conditions (SD-Leu) and plated on either SD-Leu or SD–Leu + canavanine (CAN) media to assess the recombination frequency. CAN resistant colonies were quantified after 72 hours using a SegmentColonies Matlab script.
(TIF)

S7 Fig. *MRC1* cells are synthetic-lethal with *CTF4*. Tetrad analysis from sporulated heterozygote *ctf4Δ mrc1Δ* diploids. Crosses (X) and circles (O) indicate haploid cells lacking *MRC1* or *CTF4* respectively.
(TIF)

S8 Fig. Deletion of *MRC1* does not suppress the genotoxic sensitivity observed in cells lacking *SGS1*. Serial dilution of wild-type (WT) or *mms22Δ*, *mrc1Δ*, *mms22Δ mrc1Δ*, *sgs1Δ*, *mms22Δ sgs1Δ* mutants were analyzed on normal growth media (YPD) with or without 0.005% MMS or 5 μM CPT. The plates were imaged after 48 hours of incubation at 30°C.
(TIF)

S9 Fig. The growth restoration of *mms1Δ mrc1Δ* cells on MMS is *RAD52* dependent. Serial dilution of wild-type (WT) or *mrc1Δ*, *mms1Δ*, *mms1Δ mrc1Δ* and *mms1Δ mrc1Δ rad52Δ* mutants were assayed on normal growth media and media containing 0.0025% or 0.005% MMS. The plates were imaged after 48 hours of incubation at 30°C.
(TIF)

S10 Fig. Mrc1 stability is not altered in cells lacking *RTT101* or *MMS22*. *mms22Δ* cells expressing 3HA-tagged Mrc1 from the inducible *GAL1,10*-promoter were synchronized in G1 phase using α-factor in 2% galactose and released into S-phase in 2% galactose as outlined in Fig 6A. Subsequently, 0.03% MMS and 2% glucose was added to induce fork stalling and repress HA-Mrc1 expression, respectively. Samples were collected at the indicated time points (min) and HA-Mrc1 levels monitored by anti-HA immunoblotting (A). Immunoblotting for Pgk1 controls for equal loading. The position of phosphorylated (3HA-Mrc1-P) and unphosphorylated 3HA-Mrc1 is indicated. In an independent approach, wild-type (WT), *mms22Δ* and *rtt101Δ* cells expressing 3HA-tagged Mrc1 were synchronized in G1 phase using α-factor in YPD and released into S-phase in YPD + 0.03% MMS as outlined in (B). After 40 min, cells were released in normal growth media containing 200 μg/ml cycloheximide (CHX) and 3HA-Mrc1 was detected at the indicated times by immunoblotting with HA-antibodies (C). The position of phosphorylated (3HA-Mrc1-P) and non-modified (3HA-Mrc1) is marked. Mrc1 protein levels were quantified and normalized from two independent experiments. In addition, endogenous, untagged Mrc1 levels in wild-type (WT), *rtt101Δ* and *mms22Δ* were

independently quantified by selective-reaction-monitoring (SRM) by measuring transitions corresponding to 5 independent Mrc1 peptides (**D**). Relative intensities are indicated with standard deviations from five independent peptide measurements. Note that Mrc1 is degraded after release from genotoxic stress by a Rtt101^{Mms22}-independent mechanism.
(TIF)

S11 Fig. Chromatin association of Mrc1 is not altered in *rtt101Δ* or *mms22Δ* cells both in the absence and presence of damage. Mrc1-myc expressing strains were synchronized in G1 phase using α-factor and released into medium with (+) or without (-) 0.03% MMS. S-phase samples were collected and the chromatin-bound proteins were separated from the soluble fraction (for detailed experimental procedure see Materials and Methods section). The presence of Mrc1-myc as well as chromatin-associated Orc6 and the soluble Pgk1 controls were detected by immunoblotting in whole cell extract (WCE), the chromatin-associated fraction (pellet = P) and the soluble fraction (supernatant = Sup).
(TIF)

S1 Table. List of candidates identified in the SGA screen.
(XLSX)

S2 Table. List of Mms22 interactors. PA-tagged Mms22 was immunoprecipitated from cells synchronized in S-phase and associated proteins were identified by LC-MS/MS. The percentage (%) coverage of each associated protein is indicated.
(XLSX)

S3 Table. List of plasmids used in this study.
(XLSX)

S4 Table. List of yeast strains used in this study.
(XLSX)

Acknowledgments

We thank N. Osheroff (Vanderbilt University, USA) for the recombination reporter plasmids, D. Koepp (University of Minnesota, USA) for the Mrc1 alleles, M. Knop (University of Heidelberg, Germany) for sharing the heterozygous diploid deletion library, K. Shirahige (University of Tokyo, Japan) for the *mcm6-IL* allele, P. Zegerman (University of Cambridge, UK) for the *sld3-37A dbf4-4A* strain, M. Foiani (IFOM, Italy) and H. Ulrich (Institute of Molecular Biology, Germany) for antibodies, and the IMB microscopy and media core facilities for technical support. We are grateful to members of the Labib, Luke and Peter laboratories for helpful discussions, H. Sharifian and S. Pelet for the colony quantification script and R. Dechant and A. Smith for critical reading of the manuscript.

Author Contributions

Conceived and designed the experiments: WP BL KL MP. Performed the experiments: RB VK CWZ LK MD MM RS AM. Analyzed the data: RB VK AM. Contributed reagents/materials/analysis tools: MP BL KL PP. Wrote the paper: RB VK BL MP.

References

1. Hodgson B, Calzada A, Labib K (2007) Mrc1 and Tof1 regulate DNA replication forks in different ways during normal S phase. Mol Biol Cell 18: 3894–3902. doi: 10.1091/mbc.E07-05-0500 PMID: 17652453

2. Gambus A, Jones RC, Sanchez-Diaz A, Kanemaki M, van Deursen F, et al. (2006) GINS maintains association of Cdc45 with MCM in replisome progression complexes at eukaryotic DNA replication forks. Nat Cell Biol 8: 358–366. doi: 10.1038/ncb1382 PMID: 16531994
3. Gambus A, van Deursen F, Polychronopoulos D, Foltman M, Jones RC, et al. (2009) A key role for Ctf4 in coupling the MCM2-7 helicase to DNA polymerase alpha within the eukaryotic replisome. EMBO J 28: 2992–3004. doi: 10.1038/emboj.2009.226 PMID: 19661920
4. Tanaka H, Katou Y, Yagura M, Saitoh K, Itoh T, et al. (2009) Ctf4 coordinates the progression of helicase and DNA polymerase alpha. Genes Cells 14: 807–820. doi: 10.1111/j.1365-2443.2009.01310.x PMID: 19496828
5. Simon AC, Zhou JC, Perera RL, van Deursen F, Evrin C, et al. (2014) A Ctf4 trimer couples the CMG helicase to DNA polymerase α in the eukaryotic replisome. Nature 510: 293–297. doi: 10.1038/nature13234 PMID: 24805245
6. Tourrière H, Versini G, Cordón-Preciado V, Alabert C, Pasero P (2005) Mrc1 and Tof1 promote replication fork progression and recovery independently of Rad53. Mol Cell 19: 699–706. doi: 10.1016/j.molcel.2005.07.028 PMID: 16137625
7. Szyjka SJ, Viggiani CJ, Aparicio OM (2005) Mrc1 Is Required for Normal Progression of Replication Forks throughout Chromatin in S. cerevisiae. Mol Cell 19: 691–697. doi: 10.1016/j.molcel.2005.06.037 PMID: 16137624
8. Mohanty BK, Bairwa NK, Bastia D (2006) The Tof1p-Csm3p protein complex counteracts the Rrm3p helicase to control replication termination of Saccharomyces cerevisiae. Proc Natl Acad Sci USA 103: 897–902. doi: 10.1073/pnas.0506540103 PMID: 16418273
9. Calzada A, Hodgson B, Kanemaki M, Bueno A, Labib K (2005) Molecular anatomy and regulation of a stable replisome at a paused eukaryotic DNA replication fork. Genes Dev 19: 1905–1919. doi: 10.1101/gad.337205 PMID: 16103218
10. Razidlo DF, Lahue RS (2008) Mrc1, Tof1 and Csm3 inhibit CAG· CTG repeat instability by at least two mechanisms. DNA Repair (Amst) 7: 633–640.
11. Alabert C, Bianco JN, Pasero P (2009) Differential regulation of homologous recombination at DNA breaks and replication forks by the Mrc1 branch of the S-phase checkpoint. EMBO J 28: 1131–1141. doi: 10.1038/emboj.2009.75 PMID: 19322196
12. Xu H, Boone C, Klein HL (2004) Mrc1 is required for sister chromatid cohesion to aid in recombination repair of spontaneous damage. Mol Cell Biol 24: 7082–7090. doi: 10.1128/MCB.24.16.7082-7090.2004 PMID: 15282308
13. Lou H, Komata M, Katou Y, Guan Z, Reis CC, et al. (2008) Mrc1 and DNA Polymerase ε Function Together in Linking DNA Replication and the S Phase Checkpoint. Mol Cell 32: 106–117. doi: 10.1016/j.molcel.2008.08.020 PMID: 18851837
14. Komata M, Bando M, Araki H, Shirahige K (2009) The direct binding of Mrc1, a checkpoint mediator, to Mcm6, a replication helicase, is essential for the replication checkpoint against methyl methanesulfonate-induced stress. Mol Cell Biol 29: 5008–5019. doi: 10.1128/MCB.01934-08 PMID: 19620285
15. Alcasabas AA, Osborn AJ, Bachant J, Hu F, Werler PJ, et al. (2001) Mrc1 transduces signals of DNA replication stress to activate Rad53. Nat Cell Biol 3: 958–965. doi: 10.1038/ncb1101-958 PMID: 11715016
16. Katou Y, Kanoh Y, Bando M, Noguchi H, Tanaka H, et al. (2003) S-phase checkpoint proteins Tof1 and Mrc1 form a stable replication-pausing complex. Nature 424: 1078–1083. doi: 10.1038/nature01900 PMID: 12944972
17. Nedelcheva MN, Roguev A, Dolapchiev LB, Shevchenko A, Taskov HB, et al. (2005) Uncoupling of unwinding from DNA synthesis implies regulation of MCM helicase by Tof1/Mrc1/Csm3 checkpoint complex. J Mol Biol 347: 509–521. doi: 10.1016/j.jmb.2005.01.041 PMID: 15755447
18. Luciano P, Dehé P-M, Audebert S, Géli V, Corda Y (2015) Replisome Function During Replicative Stress Is Modulated by Histone H3 Lysine 56 Acetylation Through Ctf4. Genetics: genetics.114.173856. doi: 10.1534/genetics.114.173856
19. Yeeles JTP, Poli J, Marians KJ, Pasero P (n.d.) Rescuing Stalled or Damaged Replication Forks. cshperspectivescshlporg.
20. Li J-M, Jin J (2012) CRL Ubiquitin Ligases and DNA Damage Response. Front Oncol 2: 29. doi: 10.3389/fonc.2012.00029 PMID: 22655267
21. Maric M, Maculins T, de Piccoli G, Labib K (2014) Cdc48 and a ubiquitin ligase drive disassembly of the CMG helicase at the end of DNA replication. Science 346: 1253596. doi: 10.1126/science.1253596 PMID: 25342810
22. Mimura S, Komata M, Kishi T, Shirahige K, Kamura T (2009) SCF(Dia2) regulates DNA replication forks during S-phase in budding yeast. EMBO J 28: 3693–3705. doi: 10.1038/emboj.2009.320 PMID: 19910927

23. Morohashi H, Maculins T, Labib K (2009) The amino-terminal TPR domain of Dia2 tethers SCF(Dia2) to the replisome progression complex. Curr Biol 19: 1943–1949. doi: 10.1016/j.cub.2009.09.062 PMID: 19913425

24. Fong CM, Arumugam A, Koepp DM (2013) The Saccharomyces cerevisiae F-box protein Dia2 is a mediator of S-phase checkpoint recovery from DNA damage. Genetics 193: 483–499. doi: 10.1534/genetics.112.146373 PMID: 23172854

25. Han J, Zhang H, Zhang H, Wang Z, Zhou H, et al. (2013) A Cul4 E3 Ubiquitin Ligase Regulates Histone Hand-Off during Nucleosome Assembly. Cell 155: 817–829. doi: 10.1016/j.cell.2013.10.014 PMID: 24209620

26. Zaidi IW, Rabut G, Poveda A, Scheel H, Malmström J, et al. (2008) Rtt101 and Mms1 in budding yeast form a CUL4(DDB1)-like ubiquitin ligase that promotes replication through damaged DNA. EMBO Rep 9: 1034–1040. doi: 10.1038/embor.2008.155 PMID: 18704118

27. Han J, Li Q, McCullough L, Kettelkamp C, Formosa T, et al. (2010) Ubiquitylation of FACT by the cullin-E3 ligase Rtt101 connects FACT to DNA replication. Genes Dev 24: 1485–1490. doi: 10.1101/gad.1887310 PMID: 20634314

28. Luke B, Versini G, Jaquenoud M, Zaidi IW, Kurz T, et al. (2006) The cullin Rtt101p promotes replication fork progression through damaged DNA and natural pause sites. Curr Biol 16: 786–792. doi: 10.1016/j.cub.2006.02.071 PMID: 16631586

29. Hang LE, Peng J, Tan W, Szakal B, Menolfi D, et al. (2015) Rtt107 Is a Multi-functional Scaffold Supporting Replication Progression with Partner SUMO and Ubiquitin Ligases. Mol Cell 60: 268–279. doi: 10.1016/j.molcel.2015.08.023 PMID: 26439300

30. Tong AH, Evangelista M, Parsons AB, Xu H, Bader GD, et al. (2001) Systematic genetic analysis with ordered arrays of yeast deletion mutants. Science 294: 2364–2368. doi: 10.1126/science.1065810 PMID: 11743205

31. Michel JJ, McCarville JF, Xiong Y (2003) A role for Saccharomyces cerevisiae Cul8 ubiquitin ligase in proper anaphase progression. J Biol Chem 278: 22828–22837. doi: 10.1074/jbc.M210358200 PMID: 12676951

32. Rabut G, Le Dez G, Verma R, Makhnevych T, Knebel A, et al. (2011) The TFIIH subunit Tfb3 regulates cullin neddylation. Mol Cell 43: 488–495. doi: 10.1016/j.molcel.2011.05.032 PMID: 21816351

33. Hoege C, Pfander B, Moldovan G-L, Pyrowolakis G, Jentsch S (2002) RAD6-dependent DNA repair is linked to modification of PCNA by ubiquitin and SUMO. Nature 419: 135–141. doi: 10.1038/nature00991 PMID: 12226657

34. Endo H, Kawashima S, Sato L, Lai MS, Enomoto T, et al. (2010) Chromatin dynamics mediated by histone modifiers and histone chaperones in postreplicative recombination. Genes Cells 15: 945–958. doi: 10.1111/j.1365-2443.2010.01435.x PMID: 20718939

35. Pintard L, Willems A, Peter M (2004) Cullin-based ubiquitin ligases: Cul3-BTB complexes join the family. EMBO J 23: 1681–1687. doi: 10.1038/sj.emboj.7600186 PMID: 15071497

36. Mimura S, Yamaguchi T, Ishii S, Noro E, Katsura T, et al. (2010) Cul8/Rtt101 forms a variety of protein complexes that regulate DNA damage response and transcriptional silencing. Journal of Biological Chemistry 285: 9858–9867. doi: 10.1074/jbc.M109.082107 PMID: 20139071

37. Osborn AJ, Elledge SJ (2003) Mrc1 is a replication fork component whose phosphorylation in response to DNA replication stress activates Rad53. Genes Dev 17: 1755–1767. doi: 10.1101/gad.1098303 PMID: 12865299

38. Zegerman P, Diffley JFX (2010) Checkpoint-dependent inhibition of DNA replication initiation by Sld3 and Dbf4 phosphorylation. Nature 467: 474–478. doi: 10.1038/nature09373 PMID: 20835227

39. Naylor ML, Li J-M, Osborn AJ, Elledge SJ (2009) Mrc1 phosphorylation in response to DNA replication stress is required for Mec1 accumulation at the stalled fork. Proceedings of the National Academy of Sciences 106: 12765–12770. doi: 10.1073/pnas.0904623106

40. Costes A, Lambert SAE (2012) Homologous recombination as a replication fork escort: fork-protection and recovery. Biomolecules 3: 39–71. doi: 10.3390/biom3010039 PMID: 24970156

41. Sabourin M, Nitiss JL, Nitiss KC, Tatebayashi K, Ikeda H, et al. (2003) Yeast recombination pathways triggered by topoisomerase II-mediated DNA breaks. Nucleic Acids Res 31: 4373–4384. PMID: 12888496

42. Duro E, Vaisica JA, Brown GW, Rouse J (2008) Budding yeast Mms22 and Mms1 regulate homologous recombination induced by replisome blockage. DNA Repair (Amst) 7: 811–818. doi: 10.1016/j.dnarep.2008.01.007

43. Warren CD, Eckley DM, Lee MS, Hanna JS, Hughes A, et al. (2004) S-phase checkpoint genes safeguard high-fidelity sister chromatid cohesion. Mol Biol Cell 15: 1724–1735. doi: 10.1091/mbc.E03-09-0637 PMID: 14742710

44. Thorpe PH, Alvaro D, Lisby M, Rothstein R (2011) Bringing Rad52 foci into focus. J Cell Biol 194: 665–667. doi: 10.1083/jcb.201108095 PMID: 21893595

45. Maculins T, Nkosi PJ, Nishikawa H, Labib K (2015) Tethering of SCF(Dia2) to the Replisome Promotes Efficient Ubiquitylation and Disassembly of the CMG Helicase. Curr Biol 25: 2254–2259. doi: 10.1016/j.cub.2015.07.012 PMID: 26255844

46. Crabbé L, Thomas A, Pantesco V, De Vos J, Pasero P, et al. (2010) Analysis of replication profiles reveals key role of RFC-Ctf18 in yeast replication stress response. Nat Struct Mol Biol 17: 1391–1397. doi: 10.1038/nsmb.1932 PMID: 20972444

47. Bando M, Katou Y, Komata M, Tanaka H, Itoh T, et al. (2009) Csm3, Tof1, and Mrc1 form a heterotrimeric mediator complex that associates with DNA replication forks. Journal of Biological Chemistry 284: 34355–34365. doi: 10.1074/jbc.M109.065730 PMID: 19819872

48. Vaisica JA, Baryshnikova A, Costanzo M, Boone C, Brown GW (2011) Mms1 and Mms22 stabilize the replisome during replication stress. Mol Biol Cell 22: 2396–2408. doi: 10.1091/mbc.E10-10-0848 PMID: 21593207

8 Acknowledgements

First of all, I would like to thank my supervisor Brian Luke for giving me the chance to shift my scientific focus back from Physics to Biology, for being encouraging and motivating even when results were negative or experiments inconclusive and for being understanding when the responsibilities of being a parent clashed with those of a PhD student.

I would like to thank Professor Dr. Christine Clayton for evaluating my thesis and for her advice during my TAC meetings.

I would like to thank Professor Dr. Michael Knop for his encouragement and ideas during my TAC meetings and for allocating the Singer ROTOR HDA robot as well as the yeast knockout collection of his laboratory.

Next, I would like to thank Martina Dees and Vanessa Kellner for great team work on the Rtt101 project. Thank you both for your enthusiasm, for generously sharing your data and your ideas and for the perfect coordination of strains, plasmids, samples and experiments! Vanessa, I am very curious to see, where you will take this project (or where the project will take you)!

My sincere thanks go to all members of the Luke-lab: Sarah, Heiko, André, Julia, Tina, René, Rebecca, Katharina, Arianna and Marco: thank you all for your support, your good humour and a great working atmosphere!

Finally, I would like to thank my parents, especially my mother, for her support and for stepping in when combining a PhD thesis with founding a family was more work than I could manage on my own.

Last, but most of all, I would like to thank my husband, Tom, who went with me through all the ups and downs of my thesis (and more than 20 senescence curves). You kept calm and cheered me up and looked after Robert and did whatever else was necessary to help me combine my PhD thesis with family life.